Energy Flow and Thermal Comfort in Buildings

Energy Flow and Thermal Comfort in Buildings

Comparison of Radiant and Air-based Heating & Cooling Systems

Revised Version

PhD Thesis
Defended in public at Aalborg University
31 March 2014

Jérôme Le Dréau

Department of Civil Engineering,
The Faculty of Engineering and Science,
Aalborg University, Aalborg, Denmark

River Publishers

ISBN 978-87-93237-23-0 (e-book)

Published, sold and distributed by:
River Publishers
Niels Jernes Vej 10
9220 Aalborg Ø
Denmark

Tel.: +45369953197
www.riverpublishers.com

Publications

Thesis title	Energy flow and thermal comfort in buildings - Comparison of radiant and air-based heating & cooling systems
PhD student	Jérôme Le Dréau
Supervisors	Per Heiselberg (Professor) Rasmus Lund Jensen (Associate Professor)

List of papers

- Paper 1: Le Dréau J., Heiselberg P. “Potential use of radiant walls to transfer energy between two building zones”. Proceedings of ISHVAC. Vol. 1 Tsinghua University Press, 2011. p. 120-126.
- Paper 2: Le Dréau J., Heiselberg P. “Comparison of the thermal performances of radiative and convective terminals: A conceptual approach”. PLEA 2012 Lima Peru - Opportunities, Limits & Needs: Towards an environmentally responsible architecture. 2012.
- Paper 3: Le Dréau J., Heiselberg P. “Sensitivity analysis of the thermal performance of radiative and convective terminals”. Energy and Buildings 82, 2014. p. 482-491.
- Paper 4: Le Dréau J., Heiselberg P., Jensen R.L. “A full-scale experimental set-up for assessing the energy performance of radiant wall and active chilled beam for cooling buildings”. Building Simulation: An International Journal, 2014.
- Paper 5: Le Dréau J., Heiselberg P., Jensen R.L. "Experimental investigation of convective heat transfer during night cooling with different ventilation systems and surface emissivities”. Energy and Buildings 61, 2013. p. 308-317.
- Paper 6: Le Dréau J., Heiselberg P., Jensen R.L. “Experimental investigation of the influence of the air jet trajectory on convective heat transfer with air-based and radiant cooling systems”. Journal of Building Performance Simulation, 2014.

The thesis is based on the published scientific papers listed above. Parts of the papers are used directly or indirectly in the extended summary of the thesis.

Abstract

Heating and cooling terminals can be classified in two main categories: convective terminals (e.g air conditioning, active chilled beam, fan coil) and radiant terminals. The two terminals have different modes of heat transfer: the first one is mainly based on convection, whereas the second one is based on both radiation and convection. Radiant terminals have the advantage of making use of low grade sources (i.e. low temperature heating and high temperature cooling), thus decreasing the primary energy use of buildings. But there is a lack of knowledge on the heat transfer from the terminal towards the space and on the parameters influencing the effectiveness of terminals. Therefore, the comfort conditions and energy need of four types of terminals (active chilled beam, radiant floor, wall and ceiling) have been compared for a typical office room, both numerically and experimentally. This thesis addressed mainly the cooling case.

From the steady-state numerical analysis and the full-scale experiments, it has been observed that the difference between the two types of terminals is mainly due to changes in the ventilation losses (or gains). At low air-change rates (below 0.5 ACH), radiant and air-based terminals have similar energy needs. For higher air change rate, the energy need of radiant terminals is lower than that of air-based terminals due to the higher air temperature. At 2 ACH, the energy savings of a radiant wall can be estimated to around 10 % compared to the active chilled beam (in terms of delivered energy). The asymmetry between air and radiant temperature, the air temperature gradient and the possible short-circuit between inlet and outlet all play a role equally important in decreasing the cooling need of the radiant wall compared to the active chilled beam. The higher the air change rate and the warmer the outdoor air, the larger the savings achieved with a radiant cooling terminals. Therefore, radiant terminals have a large potential of energy savings for buildings with high ventilation rates (e.g. shop, train station, industrial storage). Among radiant terminals, only small differences have been observed for the geometry considered. Only if the occupants are assumed to be sitting, the large view factor with the floor can lead to a reduction of the energy need for floor cooling systems.
These conclusions are valid for multi-storey and/or highly insulated buildings ($R > 5$ $m^2.K/W$). In case of single-storey building with a low level of insulation, the effectiveness of radiant terminals is lower due to the larger back losses, and an air-based terminal might be more energy-efficient than a radiant terminal (in terms of delivered energy).

Regarding comfort, a similar global level has been observed for the radiant and air-based terminals in both numerical and experimental investigations. But the different terminals did not achieve the same uniformity in space. The active chilled beam theoretically achieves the most uniform comfort conditions (when disregarding the risk of draught), followed by the radiant ceiling. The least uniform conditions were obtained with the cooled floor due to large differences between the sitting and standing positions. Local comfort conditions (radiant asymmetry, vertical air temperature gradient, risk of draught) have also been evaluated both theoretically and numerically, and no discomfort has been observed for normal cooling needs.

Besides this comparative study of different terminals, the relation between cooling system and internal convective flow has also been investigated experimentally. The comparison with existing models pointed out the specificity of existing correlations and the limitation of their range of application. Because of differences in the air jet trajectory, existing correlations tend to overestimate the convective flow, especially at the ceiling. Two approaches have thus been tested to better account for the air flow pattern in the definition of convective heat transfer coefficients (CHTCs). In a first method, local values of air velocity have been used to evaluate convection at the ceiling. An alternative approach consists in including a modified Archimedes number in the definition of CHTCs. Both methods improved the modelling of CHTCs with an error around ± 15-17 %. Before implementing these correlations in BES tools, further validations are needed for other types and positions of inlet and other room geometries.

Dansk resumé

Varme- og køleanlæg kan inddeles i to hovedkategorier: konvektive systemer (fx. aircondition, aktiv kølebaffel, fan-coils) og stråle køling/varme systemer. De to systemer har forskellige former for varmeoverførsel; den første er hovedsageligt baseret på konvektion, mens den anden er baseret på både stråling og konvektion. Strålevarmesystemer har den fordel at kunne gøre brug af lav kilder (dvs. opvarmning ved lave temperature og køling ved høje temperaturer) og dermed reducere bygningers primære energiforbrug. Der er imidlertid en mangel på viden om varmeoverførsel fra terminalen mod rummet og på de parametre, der påvirker anlæggenes ydelse. Derfor er der foretaget en sammenligning af komfortbetingelserne og energiforbruget for fire typer anlæg (aktiv kølebaflen, strålende gulv, væg og loft) for et typisk kontorlokale, både numerisk og eksperimentelt.

Fra den stationære numerisk analyse og fuldskalaforsøgene er det observeret, at forskellen mellem de to typer anlæg primært skyldes ændringer ventilationstab. Ved lave ventilationstilskud (under 0,5 ACH), har stråle- og luftbaserede systemer samme energibehov. Ved højere ventilationstilskud er strålevarmesystemers energiforbrug lavere end de luftbaserede systemers på grund af den højere lufttemperatur. Ved 2 ACH kan en strålevægs energibesparelser vurderes til ca. 10 % sammenlignet med den aktive kølebaflen (med hensyn til leveret energi). Asymmetrien mellem luft og strålingstemperatur, lufttemperaturgradienten og den mulige kortslutning mellem indløb og udløb spiller en lige så vigtig rolle ved reduceringen af strålevæggens kølebehov sammenlignet med den aktive kølebaflen. Jo højere et luftskifte og jo højere, jo større er de opnåede besparelser med en strålekølesystem. Derfor har strålekølesystemet et stort potentiale for energibesparelser i bygninger med et højt ventilationskifte (fx butikker, togstation, industriel opbevaring). Blandt strålesystemer er der kun observeret små forskelle i den påtænkte geometri. Kun hvis beboerne antages at sidde ned, kan den store vinkelforhold med gulvet føre til en reduktion af energibehovet for gulvkølesystemer.

Disse konklusioner gælder for fler-etagers eller højisolerede bygninger ($R > 5$ m^2.K/W). Når det drejer sig om en enetagers bygning med et lavt isoleringsniveau, er strålesystemers effektivitet lavere på grund af de større klimaskærmstab, og et luftbaseret system kan være mere energieffektivt end et stråleanlæg (med hensyn til leveret energi).

Et tilsvarende globalt komfort niveau er blevet observeret for stråle- og luftbaserede systemer i både numeriske og eksperimentelle undersøgelser, men de forskellige anlæg opnåede ikke den samme ensartethed i rummet. Den aktive kølebaflen opnår teoretisk de mest ensartede komfortbetingelser (når der ses bort fra risikoen for træk) efterfulgt af kølelofter. De mindst ensartede betingelser blev opnået med det afkølede gulv, på grund af store forskelle mellem siddende og stående stilling. Lokale komfortbetingelser (strålingstemperaturasymetrien, lufttemperaturgradient, risiko for træk) er også blevet evalueret både teoretisk og numerisk, og der er ikke observeret ubehag ved normal kølekapacitet.

Udover denne sammenlignende undersøgelse af forskellige anlæg, er sammenhængen mellem kølesystemer og interne konvektionsstrømme også blevet undersøgt eksperimentelt. Sammenligningen med eksisterende modeller påpegede specificiteten af eksisterende sammenhænge og begrænsningen i deres anvendelsesområder. På grund af forskelle i indblæsning stråle, har eksisterende korrelationer en tendens til at overvurdere konvektionsstrømningen, især ved loftet. To fremgangsmåder er således blevet testet for bedre at kunne forklare strømingsformer i definitionen af konvektion koefficienter. Ved den første fremgangsmåde blev lokale værdier af lufthastigheden anvendt til at evaluere konvektion ved loftet. En alternativ fremgangsmåde består i at inkludere et modificeret Archimedes tal i definitionen af konvektion koefficienter. Begge fremgangsmåder forbedrede modelleringen af konvektion koefficienter med en afvigelse på ± 15-17% . Før implementeringen af disse sammenhænge i BES-værktøjer er der er behov for yderligere valideringer for andre typer og placeringer af indløb og andre rum geometrier.

Nomenclature

A	surface area (m²)
ACR	air change rate (ACH or h^{-1})
BES	Building Energy Simulation
$CHTC$	Convective heat transfer coefficient
C_p	heat capacity (J/kg.K)
C_m	heat capacity (J/K)
D_h	hydraulic diameter (m)
E	energy (Wh/m²)
ΔE_{i-j}	energy difference $(E_i - E_j)/E_j$ (%)
F_{i-j}	view factors from surface i to surface j (-)
F_{p-i}	view factors from the plane to the surface i (-)
g	total solar energy transmittance (-)
H	height of the surface (m)
h	convective heat transfer coefficient (W/m².K)
I_{cl}	thermal insulation from the skin surface to the outer clothing surface (clo)
I_T	thermal insulation from the body surface to the environment, including all clothing, enclosed air layers and boundary air layer (clo)
M	metabolic rate (met)
$\dot{m}$	mass flow (kg/s)
PPD	Predicted Percentage Dissatisfied (%)
PD	Percentage Dissatisfied (%)
Q	heat flow (W)
q	heat flux (W/m²)
R	thermal resistance (m².K/W)
RH	relative humidity (%)
T	temperature (°C)
t	time (s)
ΔT_{i-j}	temperature difference $T_i - T_j$ (K)
U	U-value of a construction element (W/m².K)
V	volume (m³)
$\dot{V}$	volume flow (m³/s)

Greek symbols

α	solar absorptance (-)
ε_T	temperature efficiency (-)
μ	mean value
η	heat/cold recovery of the heat exchanger (-), if bypassed $\eta = 0$
ρ	density (kg/m³)
ρ^*	solar reflectivity (-)
σ	standard deviation

Subscripts

cond	conduction
conv	convection
ext	external
i	sub-surface i
LW	long-wave radiation
pr	plane radiant
rad	radiation
SW	short-wave radiation

Table of content

Preface

The present doctoral thesis “Comparison of radiant and air-based heating & cooling systems” has been carried out by Jérôme Le Dréau at the Department of Civil Engineering, at Aalborg University, under the supervision of Professor Per Heiselberg and the co-supervision of Associate Professor Rasmus Lund Jensen. The thesis is based on the submitted or published scientific papers in conferences and peer-reviewed journals. This work has been sponsored by the Danish Agency for Science, Technology and Innovation (Danish International DSF project nbr. 09-71598) and involved colaboration with universities in China.

Firstly, I would like to thank Professor Per Heiselberg for his continuous support and guidance over the three years. The implication in different national and international projects has been fruitful for the development of this work. I also would like to thank Associate Professor Rasmus Lund Jensen for sharing his knowledge and experience in building physics. His expertise has been extremely useful for these three years, especially for setting and analysing the experiments. I also had a great support from Benoit Pedel, Hicham Johra and the technicians during these months of experiments.

I also would like to thank my friends and colleagues from the Department of Civil Engineering for the nice and friendly environment. I will always keep in mind the talks, the jokes (good and bad) and the coffees/beers shared together. I also would like to thank my friends and family, for supporting and visiting me during these three years. Finally I am very grateful to Carmen, for her patience and kindness during these last months. Merci!

Aalborg, 2013

Introduction

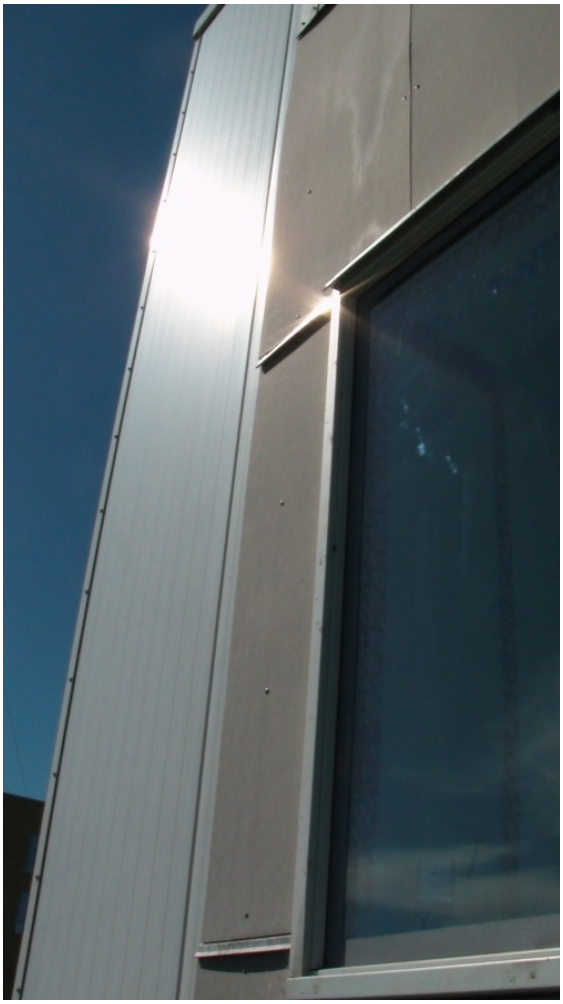

In the European Union, buildings are responsible for 40 % of energy use and for 36 % of CO_2 emissions. The energy performance of buildings is the key to achieve the EU Climate and Energy objectives, namely the reduction of 20 % of the greenhouse gases emissions and 20 % energy savings by 2020 (based on the level of 2005) [1]. In low energy buildings, the extended thermal insulation and enhanced air tightness remove the need for high temperature heating. Highly varying heat loads due to solar radiation and building occupation determine the needs for heating and cooling [2]. Low temperature heating and high temperature cooling can thus be used to increase the energy effectiveness of buildings [3]. Different terminals (or emitters) exist to maintain thermal comfort. The objective of this thesis is to compare the energy performance and the comfort level achieved by different types of terminals.

In this first part, general information about the different types of terminals and the comfort evaluation will be introduced. A literature review will also be performed in order to give an overview of the current knowledge in this field.

1. Types of terminals

A person exchanges heat with the environment in different ways: radiation to surrounding surfaces, convection to the ambient air, conduction, evaporation and respiration. Thermal comfort is usually achieved by a combination of these different modes of heat transfer.
Similarly to humans, terminals (or emitters) exchange heat in different manners. They are classified in two main categories: air-based (or convective) and radiant terminals. With air-based terminals, the indoor temperature is maintained within a certain range by controlling the air temperature, whereas radiant terminals control the surface(s) temperature through a water-based, an air-based or an electric system.

Air-based terminals have been widely used both for heating and cooling purposes, despite their high initial cost, high energy use and often unacceptable indoor climate. When buildings are cooled down with such a system, occupants sometimes complain about the noise or the draught [4]. Switzerland and the state of Hamburg in Germany have even restricted the installation of full air-conditioning in buildings [5]. Air-based systems can be either centralized or decentralized. Typical centralized air-based systems are all-air systems, such as Variable Air Volume (VAV) and Constant Air Volume (CAV). Typical decentralized air-based systems are fan coil units or active chilled beams.

Radiant technology is an alternative to air-based systems. Contrary to convective terminals, which transfer heat mainly by convection, radiant terminals transfer heat partly by radiation to (or from) the neighbouring surfaces, and partly by convection to (or from) the indoor air [6]. The first radiant heating systems was developed in Asia, where “kangs” were used to heat up beds back to the 11th century B.C. [7]. Starting from the 3rd century B.C., ancient Europe developed an underfloor heating system called “hypocaustum” [8]. The first radiant cooling system was installed in the Bank of England after the First World War [8]. During the 1970s, the use of floor heating systems became very popular, especially in the residential sector. In the 1990s, European offices had been increasingly equipped with cooled ceilings because of longer overheated periods during summer time [9]. In 2004, a cooled radiant floor was installed in a humid climate, in Bangkok airport [10]. More recently radiant walls have been introduced to the market.

The radiant terminals can be classified according to the activated surface: floor, wall, and ceiling. The radiant interaction between the terminal and the occupant(s) will differ with the surface and the shape of the room. In Table 1, the view factors between the occupant and different room surfaces are given. It can be observed that the view factor between the occupant and the floor is usually larger than for other surfaces. In industrial rooms, the view factors between the walls and the person are relatively small compared to other surfaces.

Table 1: View factors F_{p-i} between occupant and room surfaces for two different rooms [3]

Surface	Office room		Industrial room	
	Seated	Standing	Seated	Standing
Floor	0.32	0.24	0.48	0.48
Ceiling	0.12	0.12	0.22	0.22
Front wall	0.03	0.04	0.03	0.03
Window	0.06	0.06	-	-
Back wall	0.09	0.1	0.03	0.03
Side wall 1	0.19	0.22	0.12	0.12
Side wall 2	0.19	0.22	0.12	0.12

Other than a classification according to the surface activated, a distinction can be made based on the level of interaction between the terminal and the building structure [3] (Figure 1):

- *Panels* are mounted on a structure independent from the building construction (e.g. ceiling panels). Radiant ceiling panels are usually installed by means of hangers holding a structure, on which the pipes are fitted. The pipes are generally made of steel or copper.
- *Embedded surface systems* are insulated from the main building structure (e.g. radiant floor, wall, ceiling). The separating layer of insulation has the dual purpose of minimizing the thermal coupling with the main building structure and of decreasing the heat exchange at the backside. This type of system has been increasingly used in Europe because no additional work is required on the structure and occupants cannot see the terminal unit. Different systems are available on the market: pipes embedded in the screed or concrete ("wet" systems), pipes embedded in the insulation layer ("dry" systems), pipes connected to a wooden floor, capillary systems, etc.
- *Systems embedded in the building structure* (e.g. in slabs, walls). The purpose of Thermally Active Building Systems (TABS) is to desynchronise the conditioning plants and the heat load, by making use of the heat storage capacity of the building structure. TABS can take advantage of the cheaper price of electricity at night by shifting the loads to night-time. This type of system has a cooling capacity limited to around 40 W/m^2.

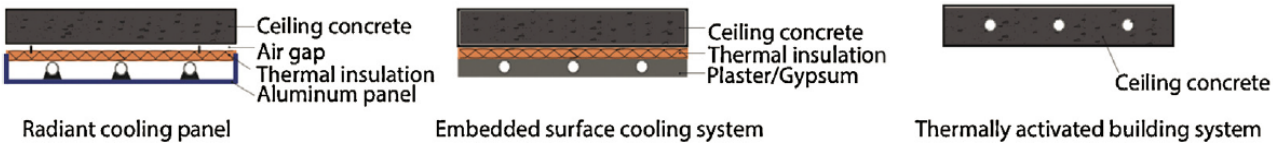

Figure 1: Schematic of three types of radiant terminals [11].

For some terminals, the classification into radiant or convective terminal can be difficult. Therefore, the limit of 50 % of radiation emitted toward the conditioned space has been set to distinguish a radiant from a convective terminal [3].

The type of terminal affects both the heat transfer in the space and the energy efficiency of the production systems. In fact, the terminal influences the water temperature needed in the primary circuit. In order to achieve efficient energy production and make use of renewable energy sources (e.g. ground water, outdoor air), the temperature difference between the space and the water should be reduced [3]. The concept of low temperature heating (25–40°C) and high temperature cooling systems (13–20°C) has been an active research topic for the past 20 years and several IEA projects have addressed this issue: Annex 28 (Low Energy Cooling Systems), Annex 37 (Low Exergy Systems for Heating and Cooling), Annex 44 (Integrating

Environmentally Responsive Elements in Buildings), Annex 49 (Low Exergy Systems for High-Performance Buildings and Communities) and Annex 59 (High Temperature Cooling and Low Temperature Heating in Buildings). New types of terminals, such as thermo-active building systems [12] or active chilled beams [13], have been developed to promote the use of low temperature heating and high temperature cooling systems. A classification of the different types of terminals is given in Figure 2. Radiant terminals are often classified as a low temperature heating and high temperature cooling system. The large surface of exchange for radiant terminals allows the use of a source temperature close to the room temperature. Moreover, they are an efficient way of transporting energy due to the high heat capacity of water [4].

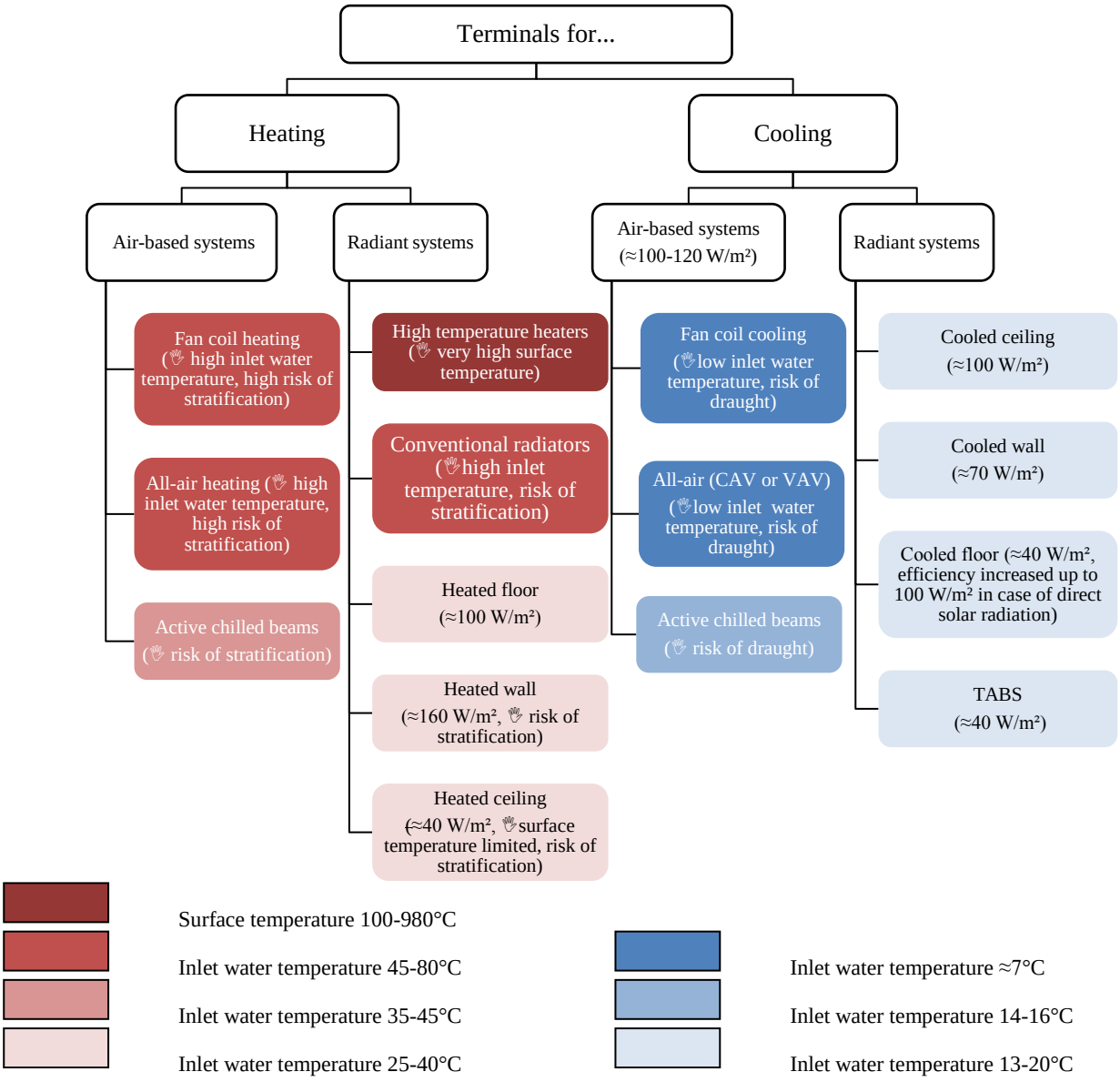

Figure 2: General characteristics of terminals (the maximum capacity is given between parentheses).

The ambient air, the geothermal energy, the ground-water or the lake water can be used as sources for both low temperature heating and high temperature cooling. Other sources available for low temperature heating systems are: condensing and low temperature boilers, waste heat, solar energy, etc.

2. Modelling the interaction between the terminal and the space

Radiant and air-based terminals have an influence on the three modes of heat transfer: conduction, convection and radiation. The purpose of this chapter is to give an overview of the existing techniques to model these modes of heat transfer when establishing the room/space heat balance.

In most BES tools, the conductive heat transfer through the building construction is evaluated assuming a one-dimensional heat flow and homogenous surface temperature. Conduction under dynamic conditions is calculated using numerical methods, such as Finite Volume Method (FVM), Finite Element Method (FEM) or transfer functions.
When modelling an air-based terminal, the non-uniformity of the surface temperature due to the inlet jet can cause inaccuracy in the conduction calculation.
For a radiant terminal, the correct modelling of the conductive flow is more difficult due to the two-dimensional heat transfer at the pipe level. The conductive flow at the activated surface is mainly influenced by the type of pipe (diameter, wall thickness and material), the pipe spacing, the water flow (water velocity) and the resistance of the additional conducting layer [3]. Different calculation methods have been developed to model the conductive flow from the pipe level to the surface with the objective of either calculating the heating/cooling capacity of the radiant systems or of simulating their dynamic behaviour in BES tools:

- Glück [14] has developed an analytical solution of the thermal field due to the presence of pipes embedded in an infinitely long slab under steady-state conditions. However the consequent analytical solution is very complex and cannot be widely applied [15].
- Most of the models are based on a one-dimensional RC transformation, similar to the technique described in EN 15377-1 [16]. The principle of this calculation method is to determine an equivalent resistance between the heating or cooling medium to the fictive core (or heat conduction layer) at the position of the pipes. Koschenz and Lehmann [17] have developed the calculation procedure for TABS and this model has been extended for other systems by De Carli, Koschenz, Olesen and Scarpa in the standard EN 15377-1. Weber and Jóhannesson [18] have proposed an optimisation of the RC model in order to better account for the dynamic behaviour. Scarpa et al. [15] and Ren and Wright [19] have developed and validated the RC model for different geometries of radiant systems. It has to be noted that the accuracy of these RC models is greatly affected by the determination the thermal properties of the different RC components [20].
- Other methods have been developed such as the conduction transfer function method from Strand and Pedersen [21], the response factors technique from De Carli et al. [22] or the universal single power function of EN 1264-2 [23]. More detailed models, which are evaluating the conductive heat transfer based on two-dimensional calculations (FEM, FVM), are also available [24].

The zone heat balance is affected by two types of radiative exchange: short-wave radiation, also called solar radiation, and long-wave radiation. Due to the different temperatures of the emitting bodies, these two types of radiation have different spectrums of emission. Solar radiation comes from a body heated at 5800 K, and 75 % of the flux is emitted at a wavelength lower than 1 μm. On the contrary, long-wave radiation is emitted by objects at ambient temperature and is concentrated in the infrared region (around a few micrometres wavelength). For example, a black body heated at 300 K has a peak emission at 10 μm. The material properties change with the type of radiation considered, i.e. the type of spectrum.
The correct calculation of the long-wave radiative exchange is especially important when studying radiant terminals. More than 50% of the energy of such a terminal is emitted through radiation. The main difficulty for calculating radiation in an enclosure arises from the treatment of the multiple reflections. Different calculation methods exist, starting from simplified methods fitted for BES tools to the exact method (the radiosity method) [25]. The radiosity method is not always used in building simulations due to the long computational time when the surface temperatures are not known. Table 2 gives the resulting radiative heat flux at the ceiling obtained with different models (based on experimental data from a test-room).

Table 2: Differences between calculation methods for evaluating the radiative heat flux at the ceiling (experimental room of dimension 2.64 m × 3.17 m × 2.93 m equipped with low-emissivity flooring [26]).

	Simplified CIBSE [27]	2-surfaces interaction, infinite reflection [28]	2- and 3-surfaces interaction, infinite reflection [29]	Radiosity method (exact solution) [30]
$q_{rad\ Ceiling}$ (W/m^2)	9.8	5.7	7.8	8.7
$\Delta q_{Radiosity\ method}$ (%)	12.3%	-34.8%	-10.5%	-

While conduction and radiation have been thoroughly examined and can be accurately modelled in BES tools, this is not yet the case for convection [31]. Most BES tools employ the so-called well-mixed assumption, which treats the room air as uniform [32]. The convective heat flux is then calculated as follows:

$$q_{conv} = h_{conv} \cdot \Delta T_{Surface-Reference} \qquad (1)$$

The coefficient h_{conv} defines the intensity of the convective heat transfer at the surface and is highly dependent on the type of flow. The convective heat transfer coefficient (CHTC) is expressed as a function of a reference temperature ($T_{Reference}$), which changes with the type of flow [31]. Convective flow in building can be classified in three categories:

- *natural convection* is driven by buoyancy forces resulting from surface-to-air temperature differences. CHTC are usually expressed as a function of the temperature difference between the surface and the room air ($\Delta T_{Surface-Room\ air}$) and $q_{conv} = h_{natural} \cdot \Delta T_{Surface-Room\ air}$. Under perfect mixing conditions, the mean air temperature is equal to the exhaust temperature. Nevertheless, the mean room air temperature is not a proper reference when the temperature is not homogenous (e.g. stratification). Therefore, the near wall (local) air temperature is sometimes used, in combination with advanced airflow modelling techniques (zonal, CFD).
- *forced convection* is generally caused by an external force, i.e. a fan or the wind. CHTCs are usually expressed as a function of the air change rate (ACR) and $q_{conv} = h_{forced} \cdot \Delta T_{Surface-Inlet}$, with $\Delta T_{Surface-Inlet}$ temperature difference between the surface and the inlet air.
- *mixed convection* occurs when both mechanical and buoyancy forces are important. In such a case, one technique commonly used to derive CHTCs is Churchill and Usagi's method [33], which interpolates two independent variables between limiting solutions: $h_{mixed}^n = h_{natural}^n + h_{forced}^n$ with n blending coefficient. Different values have been chosen for n depending on the cases: Beausoleil-Morrison [34] and Novoselac [35] defined this blending coefficient to 3, whereas the value $n = 3.2$ was used by Neiswanger et al. [36] and Awbi et al. [37]. Novoselac et al. [38] used $n = 6$ for displacement ventilation because it showed better agreement with experimental results.

The type of terminal greatly influences the convective heat transfer and is crucial for accurately modelling the asymmetry between the air and the surfaces. Therefore, a large part of this thesis (Part III) will focus on validating existing correlations and developing new calculation methods to model convective heat transfer with the different types of terminals.

3. Thermal comfort: definitions and limits

Before comparing the different types of heating and cooling terminals, the heat exchange between the human body and the surrounding environment needs to be detailed.

When assessing thermal environment, both global and local thermal comfort must be taken into consideration. The global comfort can be assessed by the Predicted Percentage Dissatisfied (PPD) developed by Fanger [39] or based on the operative temperature (T_{op}).

The PPD is an index that predicts the percentage of a large group of people likely to feel thermally dissatisfied for the body as a whole, i.e. either too warm or too cool [40]. This index is based on a steady-state heat balance of the body that accounts for internal heat production and losses through respiration, evaporation, convection and radiation. The results of Fanger are widely used to assess comfort in buildings and constitute the basis of the international standard ISO 7730 [40].

The PPD index is applicable to a wide range of clothing and activity levels. In office buildings, these parameters vary within a defined range, and the comfort limits can be expressed in terms of an operative temperature range (Table 3).

Table 3: Global thermal comfort criteria for typical spaces with sedentary activity in mechanically ventilated or air conditioned buildings (category II - normal level of expectation) [41].

PPD	Operative temperature range	
	Winter (I_{cl} = 1.0 clo / M = 1.2 met / 40% RH)	Summer (I_{cl} = 0.5 clo / M = 1.2 met / 60% RH)
< 10 %	20 – 24 °C	23 – 26 °C

For a person sitting, the operative temperature is evaluated at a height of 0.6 meter, whereas 1.1 meter is the reference height for a person standing. For relative air velocity below 0.2 m/s and asymmetry between radiant and air temperature below 4 K, the operative temperature is defined as the mean value of the radiant and the air temperature [42]. The air temperature is evaluated at a precise location and should account for the inhomogeneity of the air distribution (e.g. temperature gradient). The mean radiant temperature (T_{rad}) is evaluated by Equation 2 for a person sitting and by Equation 3 for a person standing (orientation not fixed [42]). The factors used in the calculation of the radiant temperature correspond to the projected area factors of a person sitting or standing in the six directions.

$$T_{rad} = 0.13\,(T_{pr\,[up]} + T_{pr\,[down]}) + 0.185\,(T_{pr\,[right]} + T_{pr\,[left]} + T_{pr\,[front]} + T_{pr\,[back]}) \quad (2)$$

$$T_{rad} = 0.06\,(T_{pr\,[up]} + T_{pr\,[down]}) + 0.220\,(T_{pr\,[right]} + T_{pr\,[left]} + T_{pr\,[front]} + T_{pr\,[back]}) \quad (3)$$

where $T_{pr}^4 = \sum_i T_i^4 F_{p-i}$

Besides the global comfort parameters, local comfort also needs to be evaluated: vertical air temperature difference, radiant temperature asymmetry and draught rate (Table 4). In terms of radiant asymmetry, the tighter requirement is for the heated ceiling, where the maximum allowed asymmetry is equal to 5 K.

Table 4: Local thermal comfort limits (category II - normal level of expectation) [40].

Draught rate	Vertical air temperature difference between head and ankles	Radiant asymmetry			
		Vertical (warm ceiling)	Vertical (cold ceiling)	Horizontal (warm wall)	Horizontal (cold wall)
< 20 %	< 5 K	< 5 K	< 14 K	< 23 K	< 10 K

Considering the radiant asymmetry limits and some restrictions on the surface temperature, limits for maximum and minimum surface temperatures can be derived (Table 5).

Table 5: Maximum and minimum surface temperatures (category II - normal level of expectation) [40].

Surface	Minimum surface temperature	Maximum surface temperature
Wall	≈ 17°C **	40°C ***
Floor	19°C ***	29°C ***
Ceiling	≈17°C **	≈ 27°C *
** Radiant asymmetry / ** Risk of condensation / *** Contact discomfort*		

4. Comparison of the performance of terminals

The purpose of this chapter is to review the different studies, which have compared the influence of terminals on the energy use and also the interaction with the air distribution in the room. Most of the publications are based on numerical comparison of different terminals. Only a few experimental comparisons are available due to the difficulty of carrying out measurements on the same set-up with different heating or cooling systems.

4.1. Heating

When comparing the energy effectiveness of radiant and air-based systems, the conclusion differs from publication to publication. The large scattering in the energy savings can be explained by differences in the level of insulation (the first studies were performed in the 1970s [9, 43]), by the sources considered, the type of ventilation and also the surface activated (e.g. close to the window, at the floor level or at the ceiling). Some studies have been disregarded due to improper modelling of radiant systems and/or improper reference temperature (e.g. the air temperature instead of the operative temperature). But recent publications tend to prove the better effectiveness of radiant systems compared to air-based systems, mainly due to the lower water temperature required by radiant heating systems [44-47].

Some studies have explained in detail the effect of radiant terminals on the heat balance and mentioned the positive effect of a lower air temperature to decrease the ventilation losses [44-46, 48, 49]. Hannay et al. [50] compared experimentally different types of heating systems and observed that the air temperature is 1 K higher with a warm air heater than with a radiator. Howell and Suranarayana [51, 52] performed steady-state simulations of a typical office building (9 m × 9 m × 2.75 m) relatively well insulated: $U_{floor/ceiling}$ = 0.4 W/m^2.K, U_{walls} = 0.4 W/m^2.K and U_{window} = 3.3 W/m^2.K. They analysed the parameters influencing the efficiency of radiant terminals compared to an air-based heater: room height, emissivity of surfaces, air change rate, level of insulation, convection coefficient, etc. They concluded that the air change rate was the parameter influencing the energy effectiveness of radiant heating terminals the most compared to air-based terminals and proposed a correction on the ASHRAE design calculation procedure (Figure 3). At 4 ACH, the design method assuming similar surface and air temperature overestimate the sizing of radiant systems by 15 %. They also pointed out the influence of an air temperature gradient in the efficiency of warm-air heating. Heat recovery on the ventilation losses was not included in the simulations. Inard et al. [53] developed a zonal model to compare the performance of localised and distributed heat sources and observed up to 10 % energy savings for a heated floor compared to an electrical convector. Based on CFD calculations, Myhren and Holmberg [44] calculated that the annual energy savings with a radiant heating terminal could be around 7 % due to the lower air temperature.

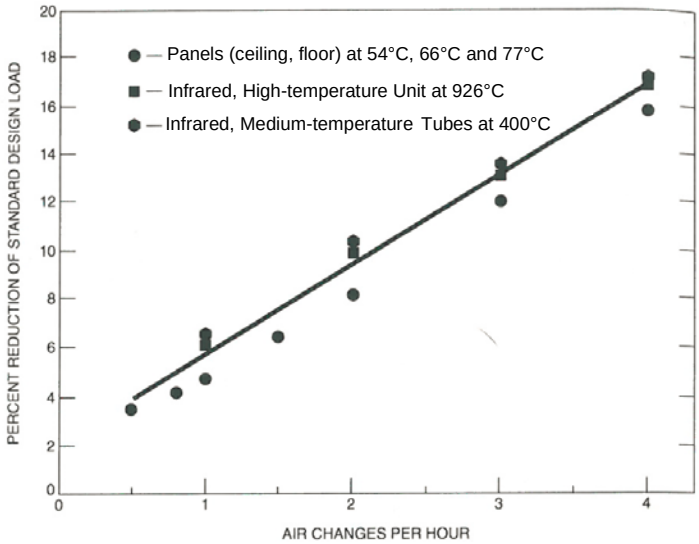

Figure 3: Reduction of the heating load compared to the ASHRAE design load calculation as a function of the air change rate when using radiant systems [45].

Recently, some publications have proposed optimisation of the layout of radiant terminals based on BES tools or combined BES and CFD tools [44, 54]. These studies concluded that the energy use could be reduced by placing the panels further from the cold sources, but this layout would result in a less homogenous level of comfort in the room.

Detailed studies of the airflow and the comfort level have also been performed. The air temperature gradient in the room is driven by both the type of terminal and the room conditions: window temperature, inlet/outlet locations, inlet temperature and air change rate [44, 48-50, 55]. It has been observed that the air temperature gradient is higher with terminals such as warmed air, convector or radiant ceiling. Some researchers provided values of temperature efficiency (Equation 4) for different configurations [48, 55]. For example, the temperature efficiency of an air-based heating terminal varies between 0.7 and 1 depending on the inlet/outlet positions and the air change rate, whereas radiant floor associated with mixing ventilation has an efficiency equal to 1.

$$\varepsilon_t = \frac{T_{exhaust} - T_{supply}}{T_{occupied\ zone} - T_{supply}} \qquad (4)$$

Radiant floor is able to provide a homogenous comfort level in the room with a low temperature gradient. Nevertheless, some studies pointed out the higher risk of draught at the inlet level [44] and the weakness of the floor heating to control the down-draught from cold vertical surfaces [56]. If the risk of draught close to the window is too high, the floor heating system can be designed to provide a higher heating capacity at specific locations by adapting the piping layout [46]. When radiant floor is combined with displacement ventilation, the air temperature is no more homogenous. Causone et al. [48] provided typical temperature gradient obtained with such a terminal (Figure 4).

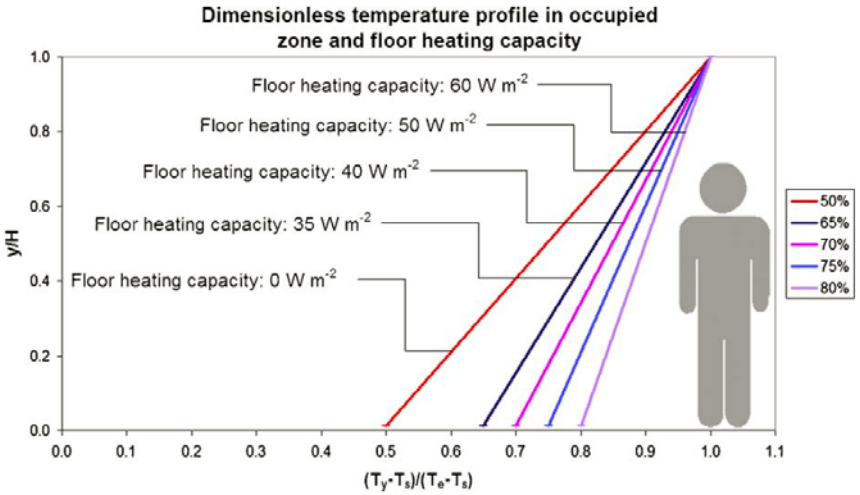

Figure 4: Air temperature gradient in a room heated by a radiant floor and using displacement ventilation [48].

The influence of the terminal on the air and temperature distribution is already included in several standards, but it is not clear how these values have been chosen. In the British guide CIBSE [27], the fabric losses are corrected directly (Figure 5). In the French building regulation (RT 2005), an additional equivalent internal temperature is accounted for depending on the type of emitter and the height of the room [57]. In the German standard DIN 18599, the heat emitted is corrected by a factor η_{str} to account for stratification [57].

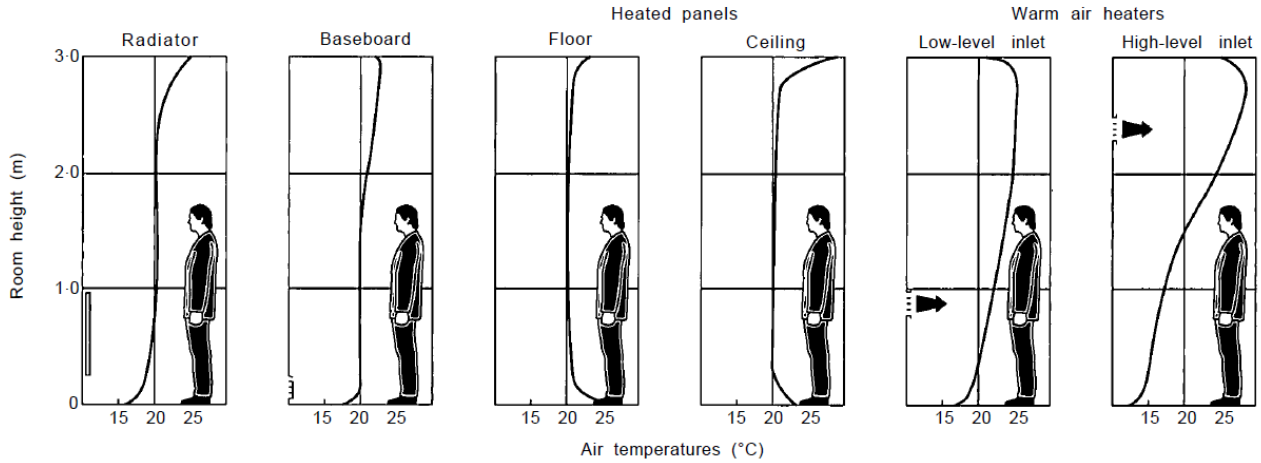

Figure 5: Profile of air temperature with different types of terminals [27].

Finally, radiant heating systems have a positive influence on the air quality perception due to the lower air temperature [46].

4.2. Cooling

In addition to terminals for heating, cooling systems have raised interest in the past twenty years due to the increased level of insulation and air-tightness of buildings and the higher expectation for thermal comfort. Most of the studies have been performed by comparing all-air systems (mainly VAV) and cooled ceiling, both under steady-state and dynamic conditions. The CAV systems are usually not included in the comparisons because they have a lower effectiveness than VAV systems due to the high fan and load operation, which decreases the total efficiency of the production system [58, 59]. Fan coil units are also rarely included in the simulations due to the low water temperature required [59-61]. The different comparisons have been performed by evaluating the energy (delivered or primary), the cost and sometimes the comfort achieved with the different systems. Nevertheless, it has to be noted that the comfort evaluation with all-air systems is usually quite limited, as the risk of draught due to the high air change rate is rarely evaluated. This drawback of all-air systems is often source of complaints from occupants [4, 62].

Most of the studies comparing cooling systems conclude that the primary energy use of cooled ceiling is lower than that of VAV systems [60, 62-66]. The primary energy savings oscillate in the range 10–60 % depending on the climate, the source considered, the area of radiant terminals and the efficiency of the different components. Most of the energy savings are achieved by the reduced energy use in the air handling process (e.g. fans), which is much greater than the increased pump energy to operate the cooled ceiling (Figure 6). The large scattering in the energy savings given in the different publications is mainly due to the sources considered to cool down the building [60]. Some researchers did not include free-cooling possibilities on the water-side (e.g. pre-cooling during night-time, cooling towers or other low exergy sources) in their studies. But the climate dependency of energy savings has been pointed out by several researchers [60, 66, 67]. The radiant systems operating in dry climates achieve higher savings than the ones in humid climates. Hot and dry climates showed the largest potential for energy savings due to the large portion of sensible heat [67]. The use of radiant terminals in hot and humid climates such as Japan [62], USA [66, 67] and south Asia [10, 64] is also beneficial. But the risk of condensation at the activated surface

usually leads to longer fan operation and thus decreases the system effectiveness. In cold and dry climates, free cooling sources are available for both VAV and radiant systems. VAV systems benefit directly from the low outdoor air temperature and radiant systems benefit from different high-temperature sources. The ground temperature (which is often around 10°C) can be used directly to cool down the building through a heat exchanger [68]. Evaporative cooling techniques can also provide cold water to the radiant ceiling without using any heat pumps [64, 66]. Some studies have also included radiant floor cooling [60, 68] and similar savings have been observed. For example, the reduction of energy use associated with the use of a radiant floor has been estimated to 30 % for the airport in Bangkok, Thailand [10]. These numerical results have been confirmed by field measurements [62, 69].

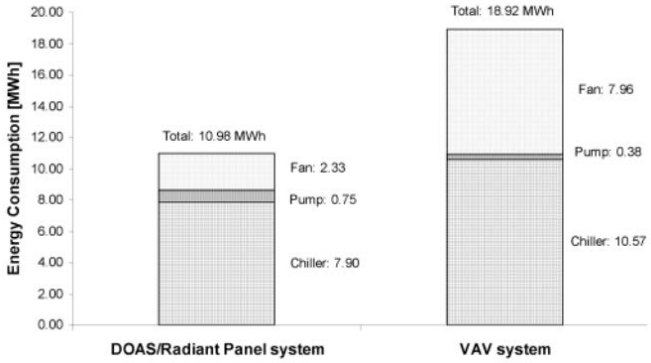

Figure 6: Example of yearly total energy use comparison for Pennsylvania, USA [65].

Because of the low energy effectiveness of classic air-based systems (e.g. high fan use and low temperature required), a new type of convective terminal was developed in the mid-1990s: the active chilled beam (also known as induction diffuser). This type of terminal has the dual function of providing fresh air and cooling down the room air. Contrary to VAV systems, the air flow rate is kept to its minimum level. Contrary to fan-coil units, no additional fan is needed to blow the indoor air over the cooling coil. The supplied fresh air passing through nozzles induces an additional airflow from the conditioned space through the cooling coil and down the conditioned space [13]. The mixing ratio can be as high as 6:1 (discharge air to primary air) and can result in draught in the occupied zone if not properly designed [70, 71]. Active chilled beams use higher chilled water temperature than convectional air-based systems (13–17°C vs. 4–7°C) and less fan energy, resulting in energy savings up to 10–20 % per year compared to a VAV system [13]. Besides the effect of the source used for cooling, two other parameters influence the energy savings: the design of the primary air system and the static pressure of the ducts [70, 72, 73]. Livchak and Lowell [73] showed that active chilled beams would perform poorly if the primary air supply was oversized. Alexander and O'Rourke [70] observed that decreasing the pressure at the nozzle level lowered its cooling capacity, resulting in a lower efficiency. Active chilled beam are not recommended for buildings with high indoor latent loads, such as restaurants, sport facilities, theatres, hospitals [13, 70].

In addition to the primary energy use, some studies compared the energy delivered to the space. Differences in the heat balance were noted in several publications. The variation of the conductive flux through the outer walls was pointed out by Imanari et al. [62] and Feng et al. [11]. Variation of the air temperature was also observed. But the effect of these parameters on the energy need has only been investigated for specific cases and the conclusions are uncertain. Some studies showed a higher demand [11], a lower demand [74] or a similar demand [60, 64] for radiant terminals.

When studying the space heat balance, researchers have focussed on comparing the dynamic behaviour of radiant terminals and have questioned the effect of the thermal mass on the performance of radiant terminals compared to air-based terminals. Fabrizio et al. [60] observed that the radiant ceiling could achieve savings compared to the cooled floor due to its lower thermal inertia, which allows a finest thermostatic control. Stetiu [67] observed a more stable environment with a cooled ceiling compared to a VAV system.

In case of high radiant heat load, radiant floors have the advantage of removing this heat load directly and thus avoid an increase of the air temperature. Niu et al. [58], Feng at al. [11] and Causone et al. [75] observed both numerically and experimentally an increase of the cooling power under high direct solar radiation, but different control strategies have been proposed. Niu et al. [58] and Feng at al. [11] considered decreasing the water temperature and by so increasing the size of the cooling system. Causone et al. [75] suggested another approach, which consisted of increasing the water flow rate. An alternative approach could be to keep both the flow and the inlet temperature constant and use the construction thermal mass to store the heat between the surface and the pipes. It would result in a slightly higher surface temperature, but it would still limit the increase of the air temperature. It has to be noted that the numerical studies did not mention nor evaluate the effect of the type of convective flow. This parameter has probably a large impact on the charge and discharge of the thermal mass.

Most of the BES tools disregard the interaction between the ventilation system and the terminals. The interaction has mainly been studied to assess the comfort and air quality with different ventilation systems. The effect on the energy need has, therefore, never been clearly addressed, but many publications discuss the air temperature gradient under different cooling loads. Most of the research focussed on displacement ventilation due to the high risk of discomfort when associated with other cooling systems.

When combining cooled ceiling with displacement ventilation, the characterisation of the air temperature gradient is relatively difficult due to the conflicting air flow from the two systems. The air temperature gradient, which can be as high as 3 K between ankle and head, is function of the cooling ratio between the radiant and displacement system, the air change rate, the radiant surface temperature and also the heat load position [76-78]. Keblawi et al. [79] and Schiavon et al. [80] have proposed simplified correlations characterising the air temperature gradient as a function of these different parameters.

Large vertical air temperature gradients have also been observed when associating floor cooling with mixing or displacement ventilation (Figure 7). With mixing ventilation, Tomasi et al. [56] observed that the air temperature gradient exceeded the comfort range in the case of high heat load and warm inlet air temperature (inlet located at the ceiling). Additionally, a risk of short-circuit was noticed when both supply and extract air terminals were located at high level. With displacement ventilation, the risk of exceeding the comfort range is even higher due to the high stratification created by the two systems [48]. Cooled floor has, therefore, a large impact on the vertical air temperature gradient and influences both the comfort level and the energy efficiency.

One study evaluated the potential of cooled wall. Kim et al. [74] combined measurements and CFD calculation to characterise the air flow in an office. With a panel surface temperature of 5°C, an air temperature gradient of 6 K between the floor and the ceiling (2-meter high) was observed.

Few studies characterise the air distribution of air-based cooling systems. Mumma and Lee [81] proposed a calculation method to include the effect of short-circuit paths between supply and return for VAV systems, but did not quantify its effect.

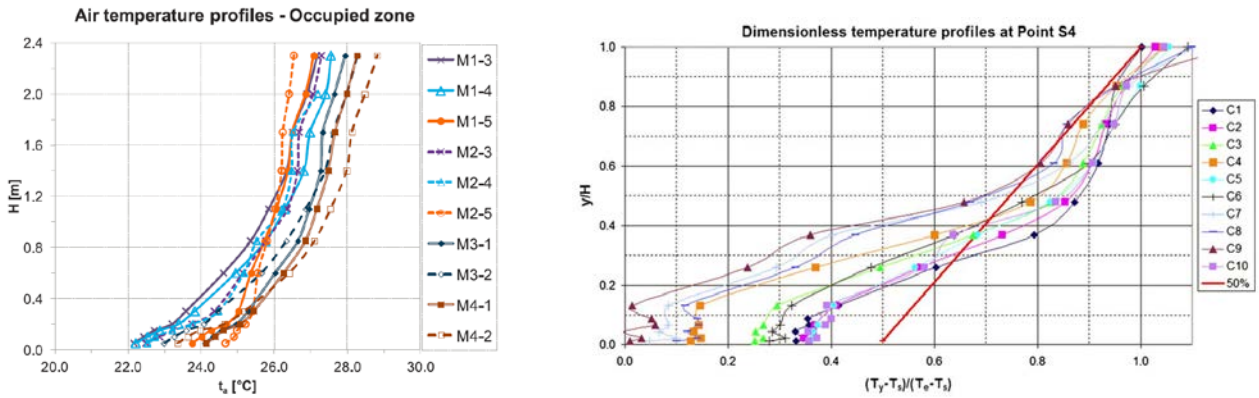

Figure 7: Air temperature gradient with a cooled radiant floor
combined with mixing ventilation (on the left [56]) and displacement ventilation (on the right [48])

An additional effect of the ventilation system is to modify the convective flow in the room. Increasing convection on a cold surface leads to an increase of the surface temperature and a decrease of the air temperature. These two effects have thus an opposite influence on the operative temperature and needs to be assessed for specific cases. Jeong and Mumma [82] evaluated the effect of increasing air velocity close to a cooled ceiling. It was observed that the total cooling capacity did not vary much for local air velocity below 2 m/s. The influence of increasing the air velocity (up to 4 m/s) close to a vertical cold surface has been investigated by Venko et al. [83]. The enhanced convective heat transfer at the surface decreases the need for mechanical cooling system. But the conclusions of this study have to be taken with caution, as the energy requirement for keeping a constant surface wall temperature (17.5°C) has not been accounted in the evaluation.

Furthermore, Fang et al. [84] highlighted the "strong and significant impact of temperature and humidity on the perception of air quality". The higher air temperature of radiant cooling systems can be a disadvantage, as the perceived air quality decreases with increasing enthalpy [42]. Nevertheless, this effect is relatively small: at constant air moisture content, the percentage dissatisfied increases by only a few percentage point (Figure 8).

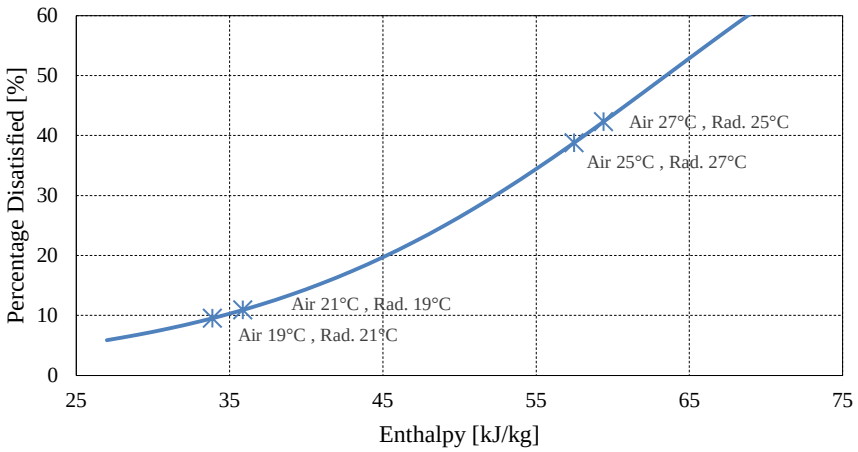

Figure 8: Perception of clean air during whole-body exposure of persons to different levels of indoor air enthalpy [84]. The dots indicate values calculated for specific heating/cooling terminals (at constant moisture content of 5.9 g/kg and 12.8 g/kg respectively).

The investment cost of different cooling solutions has been evaluated by Kalz and Pfafferott [85] for a typical office building:

- fan coil: 85 €/m²
- radiant cooling ceiling panel: 138 €/m²
- thermoactive building system: 117 €/m²

In the 1990s, different overall cost analyses were performed in Germany and USA [86, 87]. The studies showed that reducing the ventilation flow rate had a positive influence on the first cost of radiant systems. For a cooling load higher than 40 W/m^2, the first cost of a radiant system was lower than that of a VAV system (considering a fresh air change rate of around 2 ACH). Nevertheless, no economical comparison of air-based and radiant systems with updated prices has been found in the literature. The cost of radiant systems might have changed in the past ten years due to the increased use of this technology.

5. Objectives of the thesis

The objective of this thesis is to compare the comfort condition and energy need of radiant and air-based terminals. The study will focus on terminals for cooling, but the energy effectiveness of different emitters during the heating season will also be briefly addressed. The cooling case has been selected because more cooling systems are being installed in offices due to the higher level of insulation, larger glazed area and increased internal heat gains in modern offices. In the European Union, the cooled area in non-residential buildings has increased by 45 % between 2000 and 2010, resulting in a total energy use of 95 TWh for the EU-15 members [88]. In Denmark, an increase of the cooled area by 45 % is expected between 2010 and 2020. This situation already creates serious supply difficulties during peak load periods, especially in southern European countries such as Spain or Italy [89].
The type of radiant terminal considered in this study is embedded surface terminal, which has a minimised thermal coupling with the building structure (Figure 1). In order to quantify the influence of view factors on the effectiveness of radiant terminals, all three surfaces (floor, wall and ceiling) will be considered for conditioning the space [3]. Different types of air-based terminals will also be simulated, but only the active chilled beam will be tested experimentally. This terminal has been preferred to VAV and fan coil units for its minimised fan usage. This type of cooling system is commonly used in offices in Nordic countries.

Instead of being focussed on the primary energy use, the thesis has the objective to explain in detail the heat transfer within the space and evaluate the parameters influencing the heat exchange between the terminal and the occupant. As stated by Djunaedy et al. [90] and Feng et al. [11], "no research can be found that fundamentally studies the differences of the heat transfer process in zones conditioned by an air and a radiant system". The interest of better understanding the heat transfer within the space is to identify the advantages and drawbacks of radiant and air-based terminals. Most of the publications performed yearly dynamic simulations, which do not highlight the sensitivity of one specific parameter on the heating or cooling need. Steady-state analysis with wide parameter variations will be performed. Some examples of parameters studied are the air change rate, the type of convective flow and the air temperature gradient. This work will focus on energy-efficient buildings with a relatively high level of insulation ($R > 5\ m^2.K/W$). This insulation level has been chosen in accordance to the Danish building regulation [91] and is higher than the minimum values specified in EN 1264-4 (Table 6). Nevertheless, the influence of the level of insulation and the limitations of this work will be addressed in the numerical analysis.
Humidity control will not be considered, as this study focusses on the heat transfer inside the space. The problem of humidification or dehumidification has to be treated in the plant, before the air enters the space.

Table 6: Minimum thermal resistance below the pipes of heating/cooling systems according to EN 1264-4 [92].

	Heated room below or adjacent	Unheated or intermittent heated room (below, adjacent) or directly on the ground	External air below or adjacent		
			External design temperature $\theta_d \geq 0℃$	External design temperature $0℃ > \theta_d \geq -5℃$	External design temperature $-5℃ > \theta_d \geq -15℃$
Heat conduction resistance $R_{\lambda\ ins}$	0.75	1.25	1.25	1.50	2.00

The different terminals will be compared by maintain the operative temperature constant at a reference point of the space. The global and local comfort parameters will then be evaluated numerically and experimentally.

Besides this comparative study of different cooling terminals, the objective is also to improve the modelling of terminals with BES or design tools. This task consists in identifying the parameters that need to be considered and also in improving the heat transfer modelling. As convection characterises the level of interaction between the air flow and the building structure, it needs to be precisely defined for the different terminals. Therefore, studies will be performed to evaluate the accuracy of existing correlations and to propose other approaches when needed.

This study will be based on both simulations and full-scale experiments. Experiments are useful to validate the numerical simulations and also obtain more details about the comfort level.

Part I

Numerical investigation of the performance of terminals

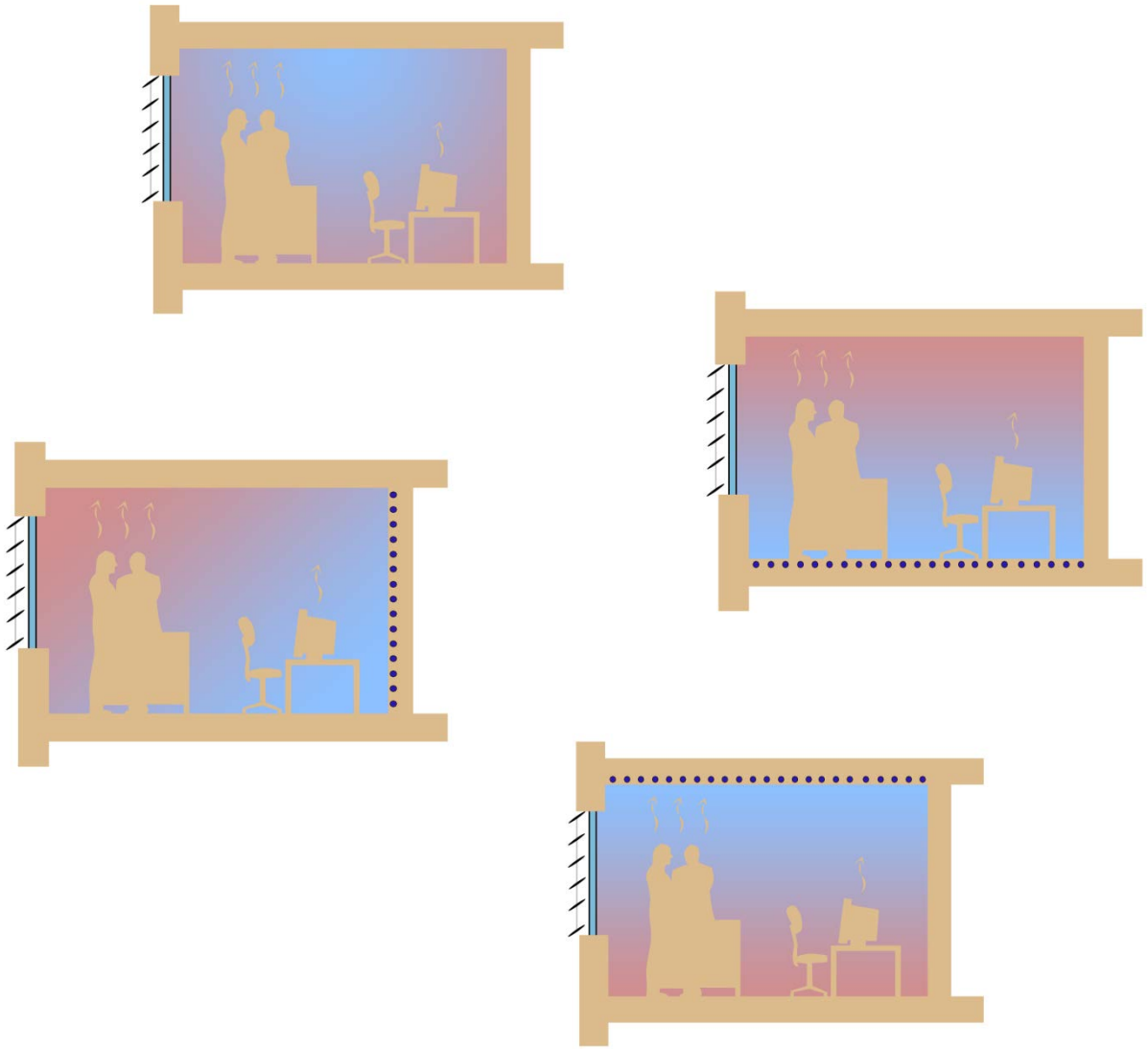

The objective of this chapter is to numerically assess the performance of different terminals. First, the problem and the different parameters involved will be introduced by performing a simplified evaluation. Then the model developed will be described and, finally, the simulation results will be presented and discussed.

Before evaluating the heat balance of the different terminals, it is useful to give the definition an "ideal" terminal. An "ideal" terminal is a terminal, which achieves homogenous temperature in the zone, meaning that the air temperature is equal to the radiant temperature.
During the heating season, radiant terminals achieve a higher surface temperature and a lower air temperature than an ideal terminal. The conduction losses thus increase, whereas the ventilation losses decrease. During the cooling season, the radiant terminals achieve a lower surface temperature and a higher air temperature. Therefore, in both heating and cooling cases, the conductive heat transfer tends to increase the energy need of a radiant terminal, whereas the ventilation heat transfer has the opposite effect. For convective systems, the ventilation heat transfer tends to increase the energy need, whereas the conductive heat transfer has the opposite effect.

Equation 5 gives an *approximation* of the difference in energy need between a "real" and an "ideal" terminal for achieving the same operative temperature. This equation has been developed assuming uniform surface and air temperature, similar level of insulation for all surfaces and making the hypothesis that the operative temperature is equal to the average of air and radiant temperature.

$$Q_{"real" terminal} - Q_{"ideal" terminal} = \left((1-\eta) \cdot \dot{m} \cdot C_{p\,air} - \frac{1}{R_{ext.} + \sum_i R_i} \cdot A \right) \cdot \left(\frac{T_{air} - T_{radiant}}{2} \right) \qquad (5)$$

This equation shows that the air change rate, the insulation level and the asymmetry between radiant and air temperature are the parameters influencing the energy effectiveness of radiant terminals the most compared to convective terminals. The influence of these last two parameters is shown in Figure 9 for a typical office room. The right side corresponds to the case of a radiant terminal during the cooling season ($T_{air} > T_{radiant}$), whereas the left side is related to the winter season ($T_{air} < T_{radiant}$). The heating and cooling needs of radiant terminals is thus lower than that of ideal terminals in the case of a well-insulated building (hatchings).
From Equation 5, it can also be observed that radiant terminals are more energy-efficient than air-based terminals at high ventilation rates. Similar results were observed by Howell and Suranarayana [51, 52] and Olesen [46] for heating systems.

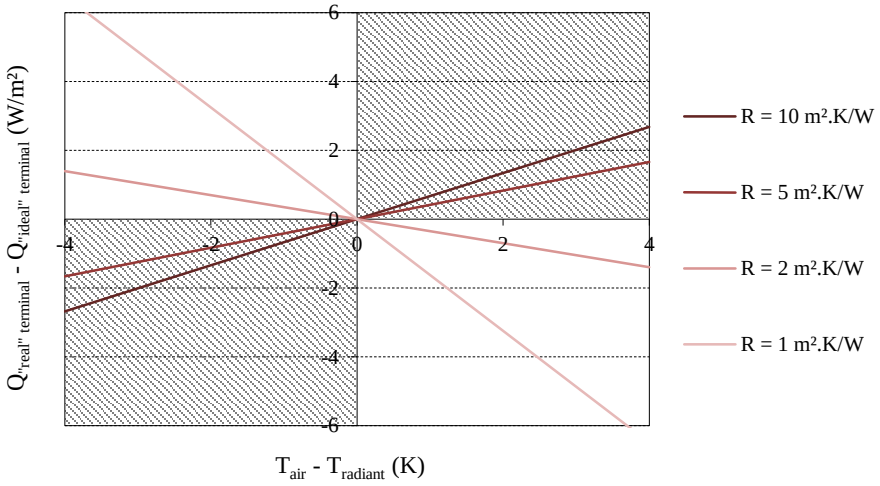

Figure 9: Difference of energy need between a real and an ideal terminal for different asymmetry levels (2 ACH and no heat recovery).

But equation 5 cannot be used directly to evaluate the performance of terminals because the calculation of conduction is too simplified, assuming that the conduction losses can be directly calculated from the radiant temperature. This assumption can lead to a large error, especially when evaluating radiant terminals. The average surface temperature can be quite different from the radiant temperature in the case of a panel placed close to the occupant. Moreover, this equation does not account for the possible differences in the insulation level of surfaces (e.g. at the back of the radiant terminal). Finally, this equation can be used only if the asymmetry between the air and the radiant temperature is known. This parameter is relatively difficult to evaluate with basic calculation tools.
This simplified calculation shows the importance of performing a detailed heat balance for each surfaces of the room/zone. Advanced modelling of the convective and radiative heat exchange is necessary to estimate the energy use and to correctly evaluate the asymmetry between air and radiant temperature.

1. Presentation of the case study

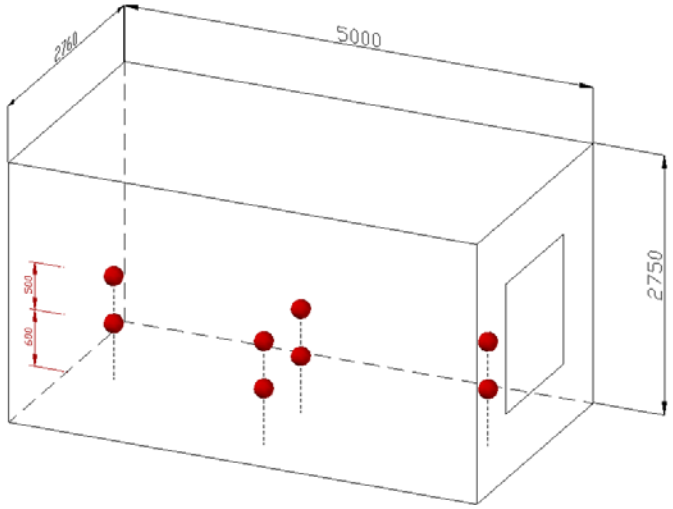

Figure 10: Geometry of the room (internal dimension in mm).
The red dots indicate the different positions of the occupant chosen for the sensitivity analysis.

An office room located in Europe has been chosen as the case to study the influence of the type of terminal on the energy need for cooling. The internal dimensions of the room have been chosen similar to the PASSYS test cell [93]: 5 m × 2.76 m × 2.75 m (length × width × height), resulting in a floor area of 13.8 m². One quarter of the south façade is equipped of a double glazing with a low-emissivity coating and a g-value of 0.6. The thermal characteristics of the building components are given in Table 7; the insulation level of the floor and the roof is relatively high, in order to model the case of a multi-storey building. Internal heat loads are equal to 20 W/m^2 [94].

Four terminals have been selected: active chilled beam, radiant floor, radiant wall and radiant ceiling. The performance of the three radiant terminals can be compared to each other, as the activated areas are similar. All four types of terminals are associated with a ventilation system (Dedicated Outdoor Air System) in order to ensure an acceptable indoor air quality. This system is not equipped with heat recovery. The inlet is assumed to be located at the ceiling, either in the middle or close to a side wall. The inlet temperature is varying depending on the type of terminal. For radiant terminals, the inlet air is equal to the outdoor air temperature (no preheating or precooling). For the active chilled beam, the supply of fresh air and the heating/cooling unit are combined together. Therefore, the inlet air temperature is modified as a function of the heating/cooling power. The outlet is assumed to be located in the upper part of the room.

Table 7: Thermal properties of the construction elements.

Surface	R (m^2.K/W)
Wall	6.66
Window	0.71
Floor	10.0
Roof	10.0

2. Model description

The analysis is performed under steady-state conditions. In order to model the heat transfer in the room, the space is discretized in a total of 62 nodes: 61 nodes correspond to the sub-surface temperatures (Equations 7) and one node to the mean room air temperature (Equations 6). Even though the air temperature is modelled by only one node, it is possible to model an air temperature gradient in order to account for more complex air distribution. The 62 unknowns are determined by simultaneously solving the heat balance at the construction and at the air-node level. As the objective is to achieve an operative temperature of 26°C, the heat absorbed by the terminal ($Q_{rad\ terminal}$ or $Q_{conv\ terminal}$) is changed iteratively until convergence is achieved (i.e. 26±0.005 °C).

Heat balance at the air node:

$$0 = \sum_i A_i h_{conv\,i}\,\Delta T_{Surface\,i-Reference} + Q_{ventilation} + Q_{conv\,internal\,sources} + Q_{conv\,terminal} \qquad (6)$$

Heat balance at each sub-surface (61 in total):

$$Q_{cond\,i} + Q_{rad\,SW\,i} + Q_{rad\,internal\,sources\,i} + Q_{rad\,terminal\,i} = A_i\,h_{conv\,i}\,\Delta T_{Surface\,i-Reference} + Q_{rad\,LW\,i} \qquad (7)$$

The part of solar radiation transmitted through the glazing ($Q_{rad\,SW}$) is distributed over the room surfaces using the method proposed in BESTEST [95]. Long-wave radiative exchange between surfaces ($Q_{rad\,LW}$) has been modelled assuming diffuse grey surfaces. The non-linearity of the radiative exchange implies the use of iterative techniques to solve the radiosity equations. The method proposed by Blomberg [96] has been chosen for its robustness and its short execution time. This technique linearizes the radiosity equations around a reference temperature, and an additional term (called excess radiation temperature) is then used to obtain the exact solution. The use of this model implies several iterations before convergence is reached (assessed by a change in the surface temperature smaller than 10^{-10} %).

3. Performance during the heating season

In order to observe the heating requirement of the different terminals, the operative temperature has been set to 21°C, and the influence of different parameters on the energy performance and on local comfort has been observed. Heat recovery is not considered, and internal heat load is set to 0 W/m^2.

It can be observed that, at low air change rates, the convective terminal is slightly more energy-efficient, but the differences between the four terminals are rather small (Figure 11). When increasing the air change rate, radiant terminals show significant energy savings. They are taking advantage of the high portion of radiative exchange and are thus not greatly influenced by the air temperature and the air change rate. At 3 ACH, the energy need for a radiant terminal is around 10 % lower than for a convective terminal. No significant difference can be observed between the three radiant terminals. Similar results were obtained by Howell and Suranarayana [51, 52].

If the air temperature gradient between the floor and the ceiling is equal to 4 K (≈ 1.5 K/m), the heating need of the terminals increases by 10 % at 3 ACH.

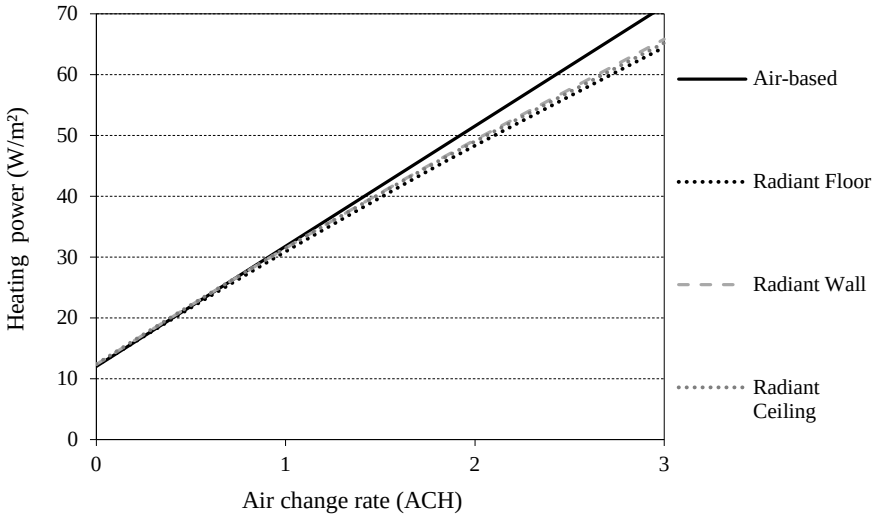

Figure 11: Heating need of the terminals depending on the air change rate and terminal type ($T_{outdoor}$ = 0°C).

Even though all terminals achieve the same level of global comfort, the local comfort conditions are not identical. Local parameters are changing only in the case of radiant terminal. When increasing the air change rate, a higher asymmetry between the air and the radiant temperature can be observed. The air temperature is decreasing, whereas the radiant temperature is increasing (Figure 12). At 3 ACH, this asymmetry can be up to 5 K. The radiant floor has the lowest surface temperature due to its high convective heat transfer, whereas the ceiling has the highest one. The local comfort criteria are respected in all cases, except for the radiant ceiling. At air change rate higher than 2.5 ACH (i.e. heating power higher than 50 W/m^2), the vertical radiant asymmetry is larger than 5 K.

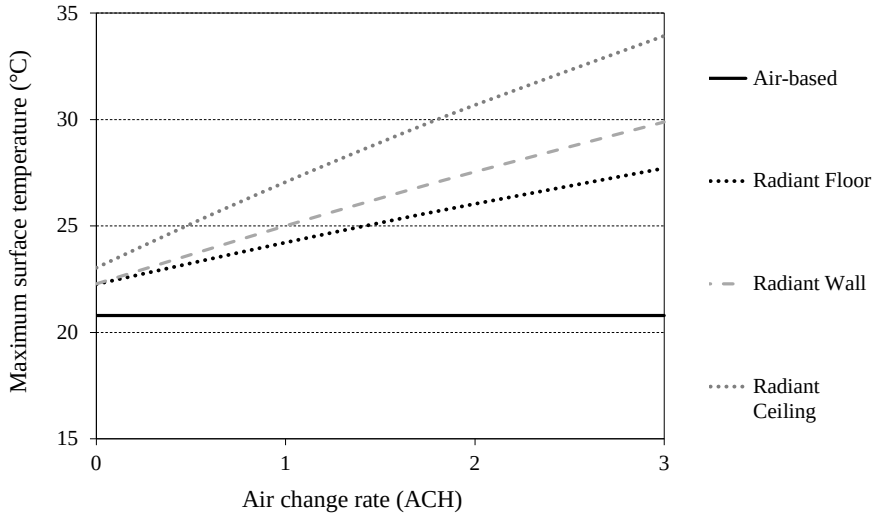

Figure 12: Maximum surface temperature depending on the air change rate and terminal type ($T_{outdoor}$ = 0°C).

For further information, the reader can refer to Paper 2:
"Comparison of the thermal performances of radiative and convective terminals: A conceptual approach"

4. Performance during the cooling season

Similarly to the heating case, steady-state simulations of the different terminals have been performed under various boundary conditions and the energy need for cooling has been compared. The main objective is to identify the case(s) in which the different technologies achieve the best performance in maintaining a constant operative temperature of 26°C. Heat recovery is not considered. In a first part, the parameters influencing the performance of terminals the most have been identified through a sensitivity analysis, and then a detailed analysis of these parameters has been performed.

4.1. Sensitivity analysis

Parameters such as the amount of solar radiation, the level of insulation and the internal heat loads are primary factors for determining the cooling need. The first stage of the building design consists in optimising these parameters, e.g. by changing the orientation of the building or the type of solar shading. Once the cooling load has been determined (around 40 W/m² in this case), it is of interest to study the parameters influencing the cooling performance of the different types of terminals. A list of eight different factors has been defined. These parameters are related to the weather (outdoor temperature, part of direct to total solar radiation), the type of ventilation system (air change rate, air temperature gradient, convective flow in the room), the room properties (emissivity and absorptivity of the internal surfaces) and the position of the person/sensor in the room.
Using the Morris Elementary Effect Method, the influence of these different parameters has been analysed for the four types of terminals. It is a one-at-a-time method, in which the impact of changing the value of each of the chosen factor is evaluated in turn [97]. This method combines the advantages of local and global methods, but it does not quantify the difference between the factors.

*Table 8: Definition of the variation range for the selected parameters (base case indicated by **bold characters**).*

		Variation range
Weather	Outdoor temperature (°C)	18 ; 20 ; **23** ; 26 ; 30
	Part of direct to total radiation (-)	0 ; 0.2 ; **0.4** ; 0.6 ; 0.8 ; 1
Ventilation	Air change rate (ACH)	0 ; 0.5 ; 1 ; **1.5** ; 2 ; 2.5 ; 3
	Air temperature gradient (K)	**0** ; 4
	Type of convective flow	Constant coefficients, **Alamdari & Hammond**, Mixed Fisher, Mixed Fisher & Pedersen
Others	Emissivity of the internal surfaces (-)	0.2 ; 0.5 ; **0.85**
	Absorptivity of the internal surfaces (-)	0.2 ; 0.4 ; **0.6** ; 0.8
	Position of the person/sensor in the room	**Sitting in the middle of the room** + 7 other positions (Figure 10)

The results of the sensitivity analysis for the four terminals are presented in Figure 13. The air change rate and the outdoor temperature are the parameters that have the highest effect on the cooling power. Moreover, both of them have a high standard deviation, which indicates that these factors are interacting with other factors or have a non-linear behaviour. The air temperature stratification has a relatively high influence on the cooling need. For active chilled beam and radiant floor, the correlation used for expressing the convective heat transfer coefficient is the fourth most influencing parameter. The absorptivity and part of direct to total solar radiation have a small influence on the cooling power. The influence of the position of the sensor can only be observed for a radiant wall. Finally, the surface emissivity plays a minor role in the definition of the cooling power.

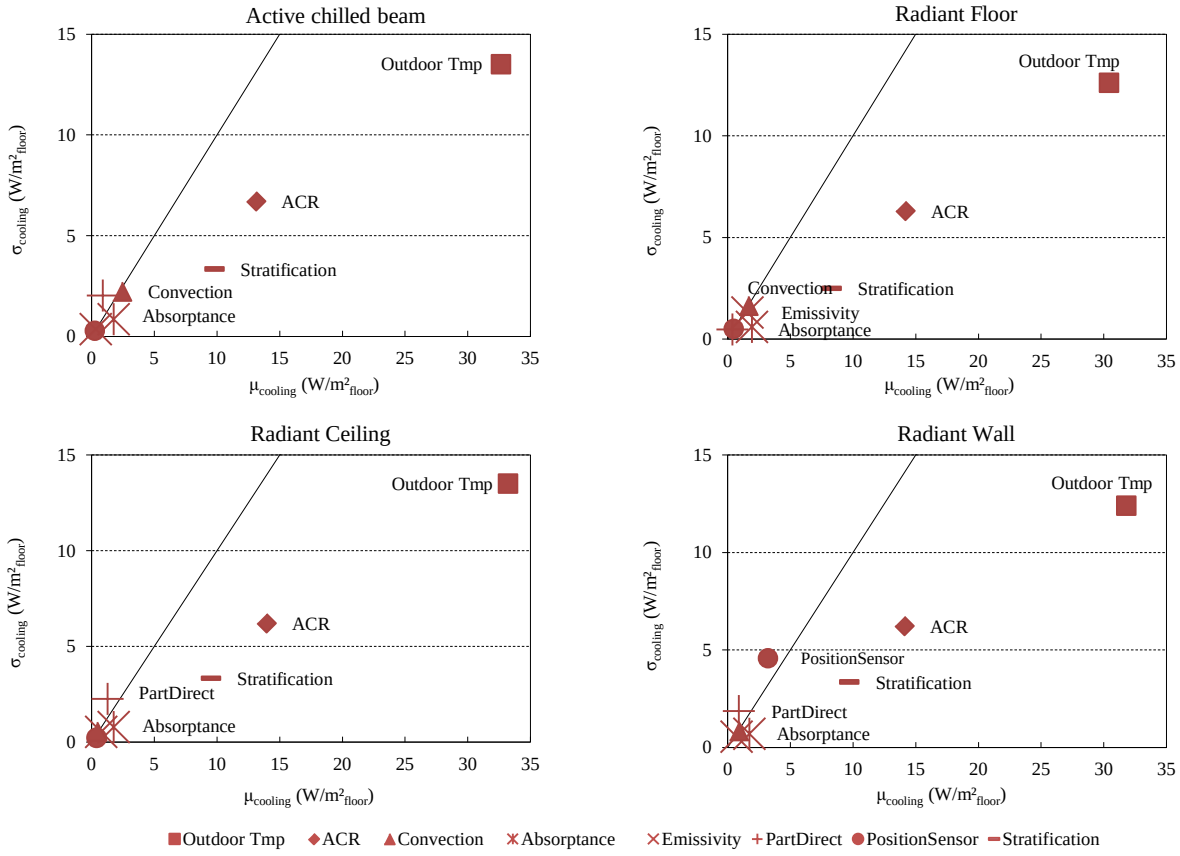

Figure 13: Estimated mean (μ) and standard deviation (σ) of the elementary effects of input factors on the energy need for cooling.

4.2. Analysis of the influencing parameters

The ventilation characteristics (i.e. outdoor temperature and air change rate) are the parameters that have the highest effect on the cooling power required to maintain a constant operative temperature (Figure 14). At low air change rates (lower than 0.5 ACH), the performances of the different terminals are similar. But differences between the terminals can be observed at higher air change rates (Figure 14 on the left). In this case, the outdoor air temperature plays an important role. In fact, radiant terminals benefit from the free cooling of the ventilation and save energy when the ambient air is warm (Figure 14 on the right).
Among radiant terminals, the cooled floor shows the best performance despite the low convective heat transfer coefficient. This is due to the large view factor between the person sitting and the floor (the view factors to the floor, wall and ceiling are respectively 0.35, 0.20 and 0.12). If the person is standing, the performance of radiant floor becomes closer to the other radiant terminals (the view factors to the floor, wall and ceiling become respectively 0.22, 0.24 and 0.15).

The effectiveness of terminals can be improved by achieving a temperature gradient in the room (Figure 15). In fact, the outlet temperature increases and it leads to energy savings. At 3 ACH and with a temperature gradient of 4K, the required power decreases by 30 % for a radiant wall. The restriction comes from the possibility to create such a temperature gradient. Displacement ventilation associated with radiant floor or radiant wall can probably achieve such temperature gradients, but it is less likely with a radiant ceiling or an active chilled beam.

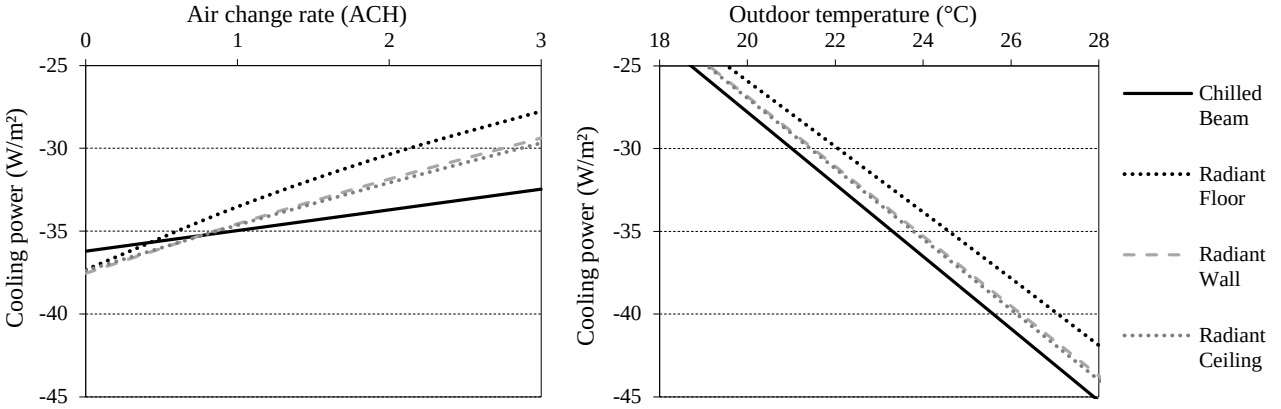

Figure 14: Cooling need of different terminals depending on the air change rate (on the left, with $T_{outdoor}$ = 23°C) and on the outdoor temperature (on the right, with ACR = 1.5 ACH).

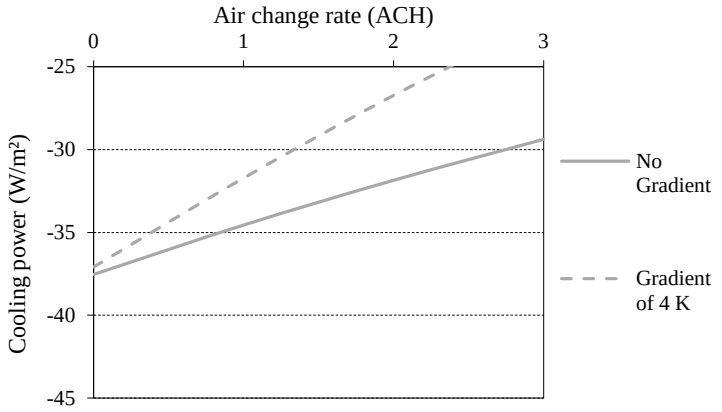

Figure 15: Influence of a temperature gradient on the cooling need of a radiant wall ($T_{outdoor}$ = 23°C).

It has also been observed that the efficiency of the active chilled beam is highly dependant of the type of convective flow in the room, i.e. on the design of the cooling terminal (Figure 16). Four convection models have been tested. Two of them (models 1 and 2) assume natural convection, meaning that the flow is driven by buoyancy forces resulting from surface-to-air temperature differences. The last two models assume mixed convection, which means that both mechanical and buoyancy forces can be important. The efficiency of air-based terminals improves with forced convection due to the lower ceiling temperature. This means that a terminal, which combines cooling by radiation and by convection, is more efficient and robust than a terminal, which is based only on one mode of heat transfer. The convective heat transfer with air-based cooling systems will be detailled in Part III (page 45).

At high air change rate, the radiant floor is also affected by the type of convective flow because of the relatively large temperature difference between the air and the surfaces (Figure 17).

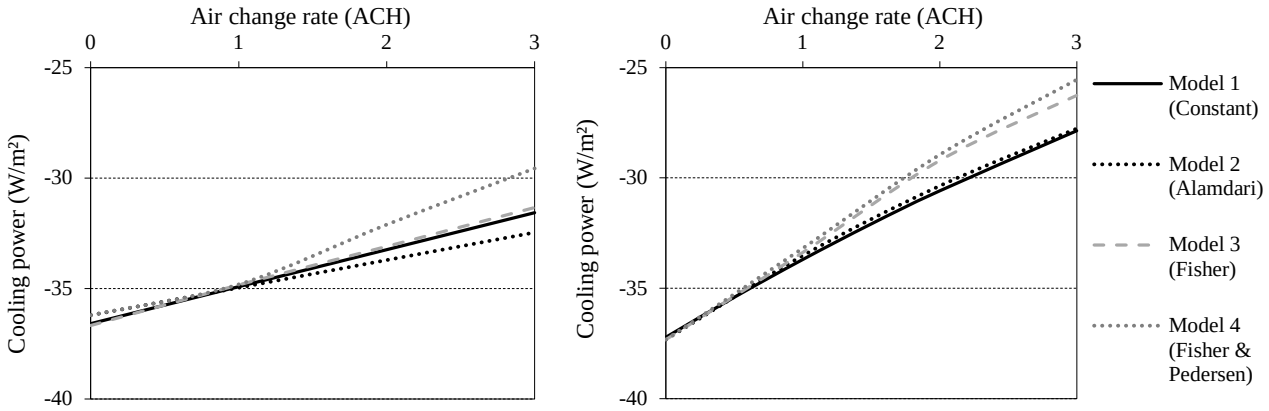

Figure 16: Influence of the model for convection on the cooling need of the active chilled beam (on the left) and the radiant floor (on the right).

Differences have also been observed in the terminal heat balance. The convective part varies greatly according to the type of terminal. For floor cooling, it represents only 7 % of the heat exchange, whereas it represents around 30–40 % for the other radiant terminals. These variations of the ratio convection/radiation are affecting the surface temperatures and, therefore, the asymmetry between air and radiant temperature (Figure 17).

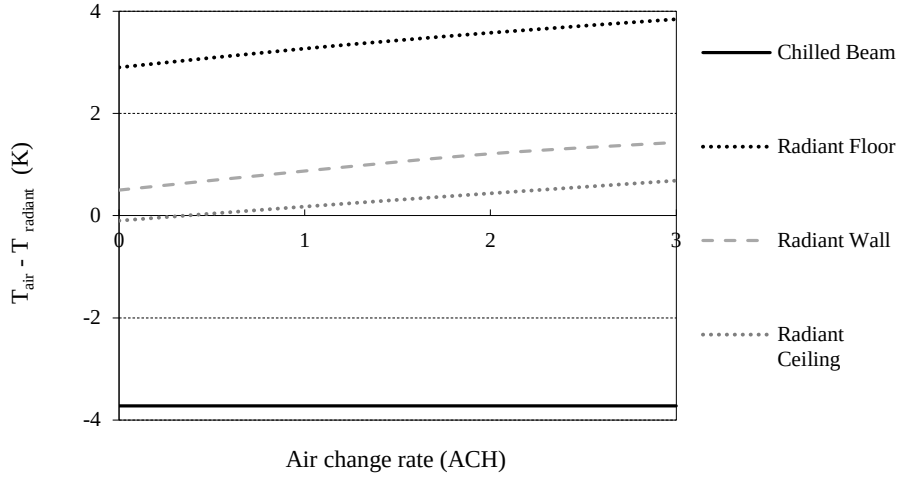

Figure 17: Difference between air and radiant temperature depending on the air change rate ($T_{outdoor}$ = 30°C).

Other than the investigation on the effect of different parameters on the cooling need, the comfort level has been evaluated. In order to account for warm conditions, the level of comfort has been investigated using the parameters of the base case, but with higher outdoor temperature (30°C).
The Predicted Percentage of Dissatisfied (PPD) for both sitting and standing persons has been calculated for 242 positions in the occupied zone (60 cm away from the walls). The average, minimum and maximum values and standard deviations are presented in Table 9. The active chilled beam theoretically achieves the most uniform environment. Nevertheless, it has to be noted that this evaluation does not account for the possible high air velocity in the room (over 0.08 m/s); this can both be a drawback (risk of draught) but also an advantage (compensate for high operative temperature). The cooled ceiling is the radiant terminal that achieves the most uniform environment, i.e. with a small standard deviation. On the contrary, radiant floor has the highest PPD. One reason is the relatively large variation of comfort between the sitting and the standing position, as mentioned before. The other reason is the air temperature, which is higher than that of other terminals. At equivalent operative temperature, the PPD increases for higher air temperature. In fact higher air temperature leads to lower losses through convection and respiration and thereby increasing the

PPD. It has to be noted that this index has been developed with persons exposed to a uniform environment [39] and the absolute value might not be accurate under asymmetric environment.

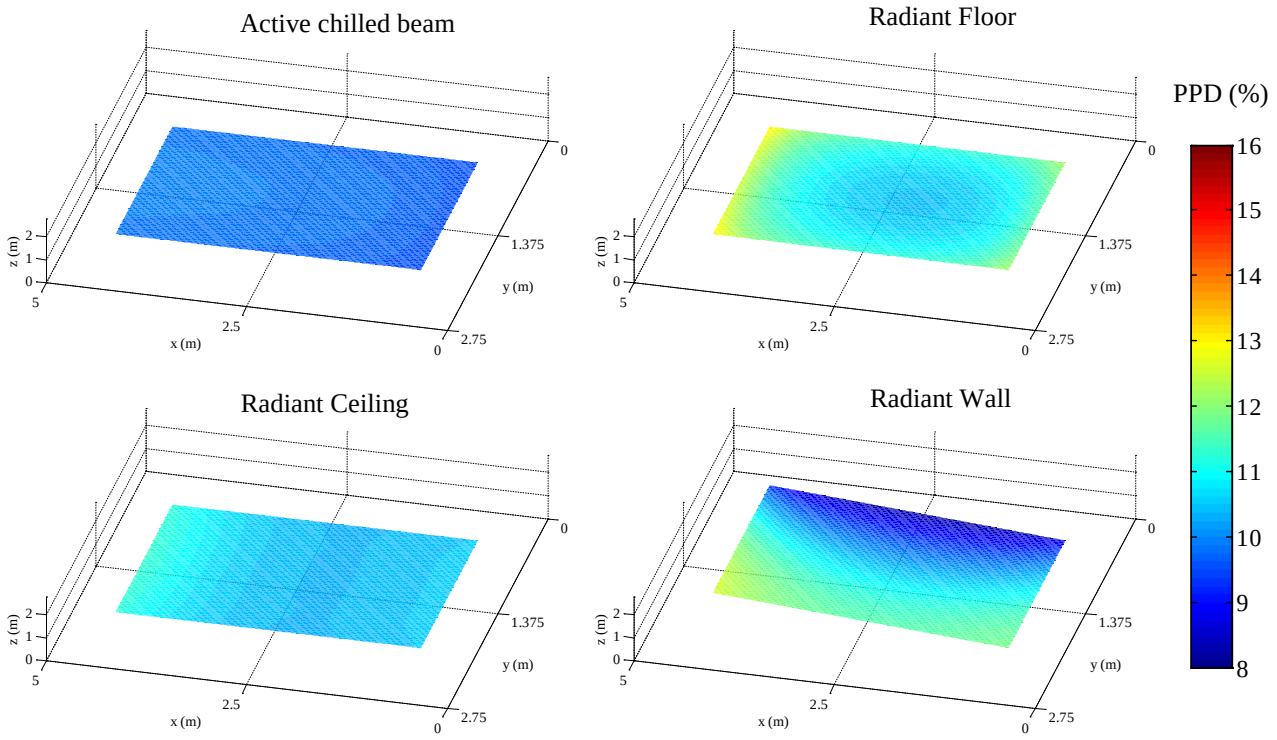

Figure 18: Predicted Percentage Dissatisfied (PPD) over the occupied zone for persons sitting ($T_{outdoor}$ = 30°C).

Table 9: Comparison of the Predicted Percentage of Dissatisfied (PPD) over the occupied zone for persons sitting and standing ($T_{outdoor}$ = 30°C).

	Minimum PPD (%)	Mean PPD (%)	Maximum PPD (%)	Standard deviation PPD (%)
Active chilled beam	9.24	9.65	9.93	0.17
Radiant Floor	10.46	12.64	15.96	1.55
Radiant Wall	7.30	10.06	12.63	1.26
Radiant Ceiling	9.54	10.23	11.30	0.47

Figure 17 and Figure 18 also show the importance of the choice and location of the sensor, which controls the terminal. The measurement of the operative temperature is relatively complex, and sometimes only the radiant or the air temperature is measured. With a radiant wall or ceiling, the difference will be rather small, whereas this difference is larger in case of a radiant floor or air-based cooling system (Figure 17). The location of the sensor close to the occupied zone is also important, especially for the radiant wall and floor (Figure 18).

When using radiant walls to cool down a building, the cold natural convective flows from the panels can create discomfort due to the down-draught. Correlations between surface temperature and air velocity have been developed by Heiselberg [98] to estimate the risk of draught from cold vertical surfaces. The percentage of dissatisfied persons (PD) increases with the cooling power from the panel and reaches 15 % for a cooling power of 70 W/m² (Figure 19): this value is below 20%, the limit of category II [40]. The risk of down-draught from the radiant wall is, therefore, not the factor limiting the cooling capacity of radiant walls.

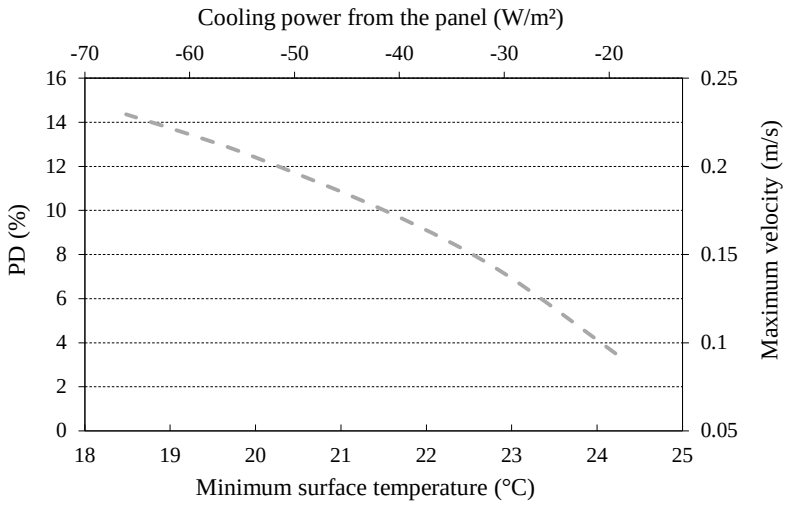

Figure 19: Percentage Dissatisfied due to the down-draught from the cooled wall.

For further information, the reader can refer to Paper 3:
"Sensitivity analysis of the thermal performance of radiative and convective terminals"

5. Possibility of transferring heat between buildings zones

The last part of the numerical analysis discusses an application of terminals to transfer heat within the building. South-facing rooms of office buildings are frequently overheated during daytime because of high solar heat gains. In low energy buildings, this load can be used as a heat source for the north-facing room, which is usually colder because it is unaffected by the direct solar radiation (Figure 20). This kind of system is, therefore, taking advantage of the asymmetry of the building loads, instead of considering it as a disturbance. During the winter season, the transfer of energy aims at heating the north-facing room, whereas this energy shifting has the purpose of cooling the south-facing room during the summer season. In addition to having a better indoor climate, the energy need for heating and cooling decreases when using this type of system.

Karlsson [99] has studied the possibility of transferring excess heat between two rooms via a floor heating system. The building located in Sweden had a highly glazed facade (56%) but no shading was applied. When running the system, the heating need decreased by 2.8% during the months of March and April. Another way of transferring energy between rooms with different heat loads is to use a surface system composed of capillary tubes, embedded at the inner surface of walls. Müller et al. [100] have performed experimental studies on different configurations of capillary mats (floor, walls, ceiling) to transfer energy between two rooms. The experiments showed that up to 70 % of the load difference (34 W/m^2) can be compensated by transferring the energy.

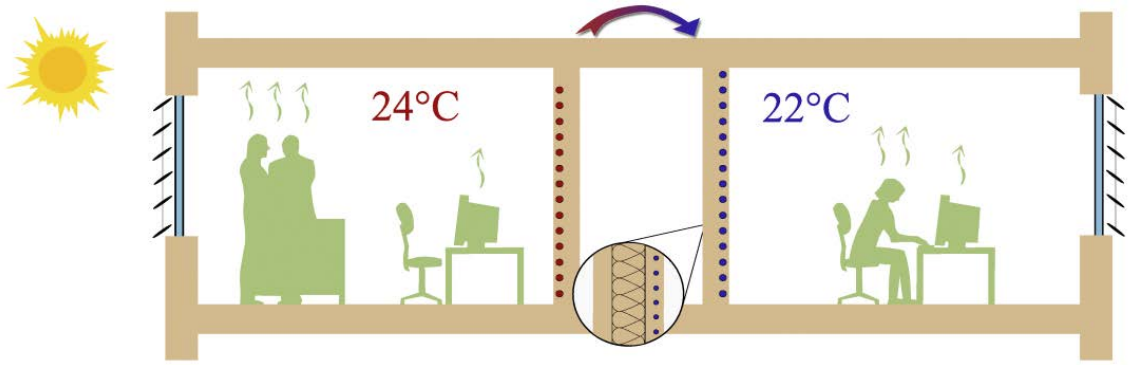

Figure 20: The concept of interzonal heat transfer applied to an office building.

By means of dynamic simulations [101], the possibility of shifting the energy demand between two office rooms with different thermal loads has been studied. Two types of office buildings located in Denmark have been simulated: one with a predominant cooling demand and the other one with a predominant heating demand. The efficiency of the system is mainly influenced by the solar shadings, which have to be set carefully in order to optimize both the energy use and the interzonal heat transfer. By transferring heat from one zone to another, the energy need of the building decreases and an improvement in the indoor climate can be observed due to the thermal homogenisation of the zones. Nevertheless, the energy savings reached with this system are not sufficient enough for the two types of buildings studied: the decrease in the heating and cooling need was always lower than 5 % (Figure 21). A comparison with a direct air exchange has also been performed, but it did not show better results. This can be explained by the fact that the surface temperature is higher than the air temperature for a low energy building. Therefore, if heat is absorbed at the wall level, a relatively high temperature is transferred leading to higher efficiency.

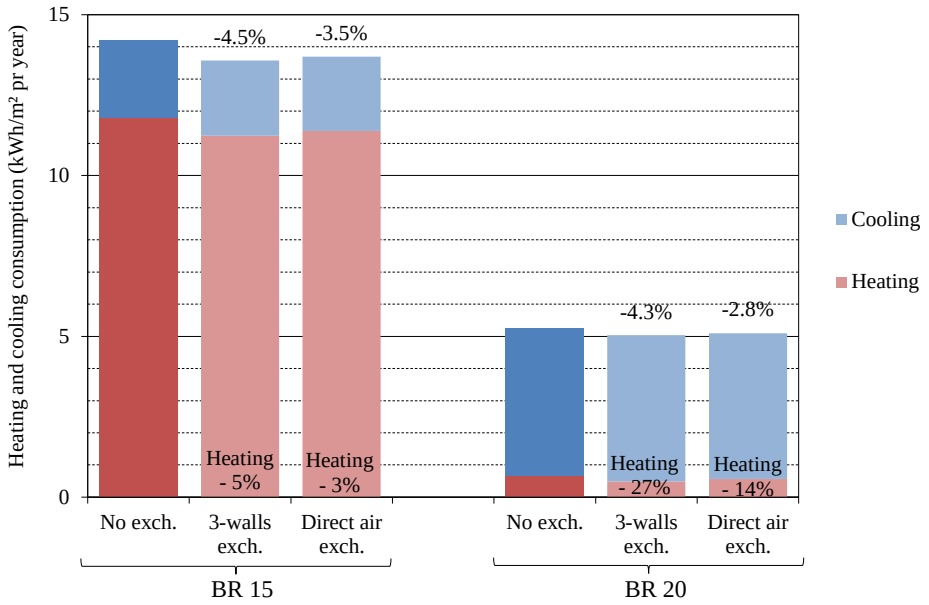

Figure 21: Comparison of different buildings and techniques to exchange heat.

For further information, the reader can refer to Paper 1:
"Potential use of radiant walls to transfer energy between two building zones"

6. Conclusion

Different heating and cooling strategies have been applied to a typical office room in order to evaluate the influence of the terminal type on the heating and cooling power required to achieve a fixed operative temperature. The thermal performances of four terminals (active chilled beam, radiant floor, radiant wall and radiant ceiling) have been compared for different boundary conditions. The objective of this steady-state analysis is to identify the advantages and drawbacks of the different technologies and assess their robustness.

During the heating season, the air change rate should be minimised in order to decrease the ventilation heat losses. For air change rates below 1 ACH, the four types of terminals have a similar effectiveness. Only at high air change rates, radiant terminals perform better than air-based terminals. In fact, the air temperature is lower with radiant heating systems, thus decreasing the ventilation losses and the heating need. It has to be noted that the heated ceiling has a limited capacity due to the constraint on the radiant asymmetry.

Most of the simulations have been performed for the cooling case. The most influencing parameters have been identified by performing a sensitivity analysis. It has been observed that the interaction between the ventilation system and the terminal (e.g. outdoor temperature, air change rate, air temperature stratification) play an important role in the zone heat balance. For low air change rates (lower than 0.5 ACH), the performances of the different terminals are similar. But differences between the terminals can be observed at higher air change rates. The air temperature is warmer with radiant cooling terminals, resulting in higher air temperature, thus increasing the ventilation losses and decreasing the cooling need. The higher the air change rate and the warmer the outdoor air, the larger the savings achieved with a radiant cooling system. Therefore, radiant cooling terminals have a large potential of energy savings for buildings with high ventilation rates (e.g. shops, train station, industrial storage). It also means that studies, which have disregarded the ventilation system in their simulations (e.g. [11]), will overestimate the energy need of radiant terminals compared to air-based terminals. The positive effect of a vertical air temperature gradient has also been observed. At 1 ACH, the cooling need of the terminal is decreasing by 10 % if a temperature gradient of 4 K is achieved between the floor and the ceiling. Such a temperature gradient can be achieved by a cooled floor or wall or by using displacement ventilation.
Among radiant cooling terminals, the cooled floor achieves the lowest energy need for cooling due to the large view factor between a sitting person and the activated surface. When considering people standing, the three terminals have a similar effectiveness.

Additionally, the variation of comfort with the different terminals has been evaluated. The radiant ceiling achieves the most uniform comfort conditions in the space, whereas the least uniform conditions are obtained with the cooled floor. The active chilled beam achieves uniform comfort conditions in theory, but further simulations (e.g. CFD simulations) are needed to validate these results to account for the non-uniform air distribution and the draught risk. Finally, it has been observed that the cooling power from a radiant wall is not limited by the risk of down-draught from the cold surface.

These simulations have been performed for a highly insulated room, which corresponds to the Danish building regulation. Would the conclusions change with the level of insulation of the building? Two additional simulations have been performed to assess the effect of changing the insulation level either at the façade (Figure 22) or for the entire room (Figure 23). From Figure 22, it can be observed that changing the level of insulation at the façade affects the cooling need of all terminals, but it does not change the relative difference between radiant and convective terminals. Simulations with a thermal resistance decreased by a factor 4 have also been performed and similar results were obtained. In Figure 23, the insulation level of all construction parts has been decreased, and a large effect can be observed on the relative difference between terminals. When decreasing the thermal resistance of the construction, the back losses of radiant terminals

increase and air-based terminals become more advantageous. Therefore, the conclusions are valid for well-insulated buildings (R > 5 m^2.K/W) and also for multi-storey buildings. For single-storey buildings with a low level of insulation, an air-based terminal might save energy compared to radiant terminals due to the lower conduction losses. In this case, the calculation has to be performed for the specific building characteristics.

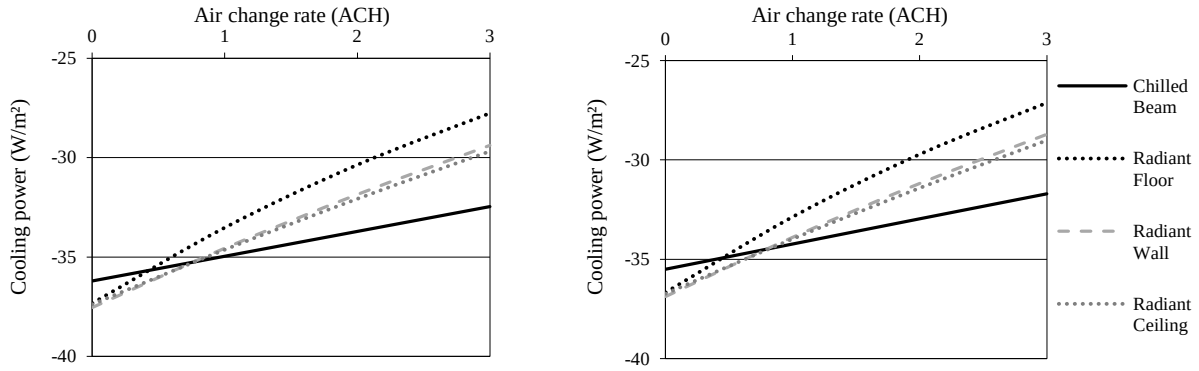

Figure 22: Cooling need of different terminals depending on the air change rate with the original insulation level (on the left) and with the R-value of the facade decreased by a factor 2 (on the right).

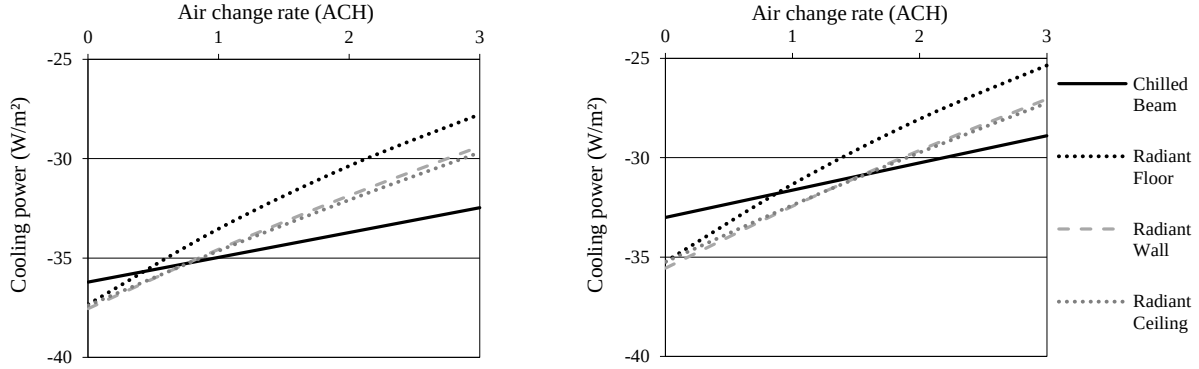

Figure 23: Cooling need of different terminals depending on the air change rate with the original insulation level (on the left) and with the R-value of all surfaces decreased by a factor 2 (on the right).

Part II

Experimental investigation of the performance of active chilled beam and radiant wall for cooling buildings

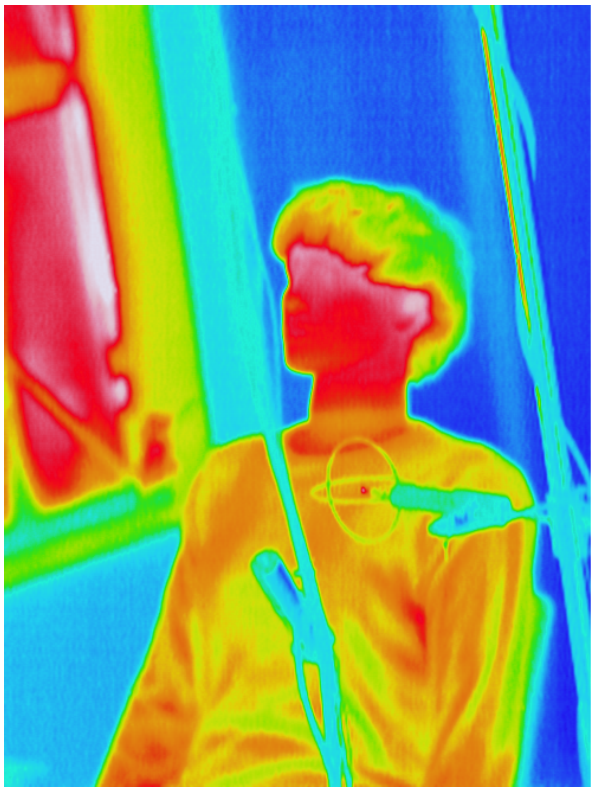

The evaluation of terminals cannot solely rely on numerical investigations, as several parameters are difficult to model accurately (e.g. interaction between ventilation and terminal, influence of the type of heat source, air temperature stratification). Therefore, full-scale experiments have been performed both under steady-state and dynamic conditions. The objective of these experiments is to perform a combined evaluation of the energy effectiveness and comfort obtained with different terminals using the same test facility. A detailed analysis of the air flow will be conducted to explain the differences between air-based and radiant terminals. Additionally, some local comfort parameters will be evaluated, using the classical methods and a thermal manikin.
This experimental investigation focuses on two high-temperature cooling systems: active chilled beam and radiant wall. The active chilled beam has been selected because the air handling process is limited to the minimum requirement, thus decreasing the fan usage and the first cost (cf. Introduction). The radiant wall has been chosen because the view factor between the occupant and the wall is relatively large for a regular office (Table 1) and also because few studies are available on such a terminal.

All accuracies specified in this part are given for a confidence interval of 95 % normally distributed. When no reference is indicated, the accuracy has been calculated by the author. The calculated uncertainties consider the calibration error (i.e. accuracy on the reference equipment, error on the type of calibration curve, etc.), the accuracy and logging frequency of the measuring device and other parameters specific to the type of measurement [102].

Figure 24: Southern facade of "The Cube".

1. Presentation of the test facility

The experiments have been performed from January to September 2013 in “The Cube” (Figure 24), which is an outdoor full-scale test facility located in Aalborg, Denmark (57.02°N, 10.0°E). In order to study the influence of solar radiation on the effectiveness of different terminals, an experimental room has been constructed inside the building with one wall connected to the outdoor environment (Figure 25). The experimental room consists of a wooden construction covered internally with 160 mm of expanded polystyrene (EPS). In order to increase the thermal mass of the room, 22 mm of plywood has been added to the floor, and plasterboards (13 mm) have been glued to the walls. The internal dimensions of the experimental room are 2.76 m × 3.60 m × 2.75 m (width × length × height) resulting in a floor area of around 10 m². The section of the test room is similar to the PASSYS test cell [93]. The south wall is equipped with a double layer glazing (2.76 m × 1.60 m), characterized by a U-value of 1.2 W/m².K and a g-value of 0.36. The thermal mass of the room is equal to 20 Wh/K.m², which corresponds to a light construction [103].

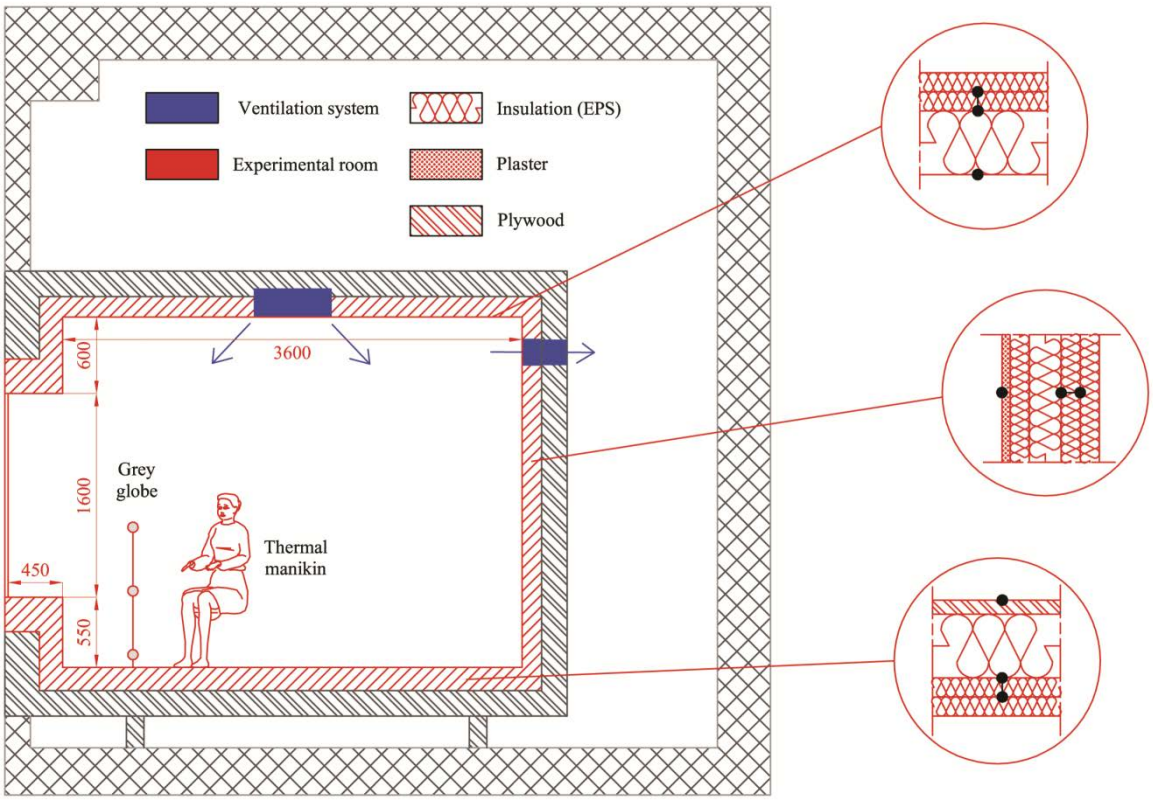

Figure 25: Vertical section of "The Cube" (dimensions in mm) with details on the construction elements (black dots indicate thermocouples).

Two terminals have been installed in the test room: a radiant wall and an active chilled beam (Figure 26). The west wall of the test room is equipped with 6 radiant panels, resulting in a total dimension of the activated surface equal to 3.6 m × 1.9 m (length × height). The radiant panels are composed of capillary pipes (3.35 mm diameter and 10 mm spacing) mounted at the back of a plasterboard. The water flow in each panel varies between 30 and 70 L/h and is laminar. The cooling capacity has been measured under experimental conditions and is equal to 21 W/m²$_{floor}$ (for $\Delta\theta_C = 8\,K$ [104]). Alternatively, maintaining comfort inside the test room can be achieved by the active chilled beam. The unit is located in the middle of the ceiling and has dimensions of 0.6 m × 0.6 m. The water flow in the cooling coil varies between 100 and 200 L/h, and the cooling capacity of the active chilled beam is equal to 25 W/m²$_{floor}$ (for $\Delta\theta_C = 8\,K$). The two terminals have similar time constants (around 3h10mn for the radiant wall and 3h45mn for the active chilled beam), but the initial response time of the active chilled beam is shorter.

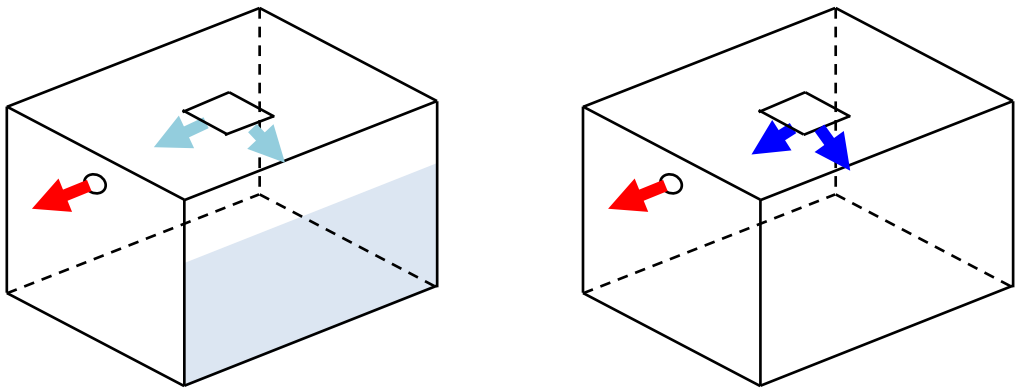

Figure 26: Cooling principles in the test room: radiant wall (on the left) or active chilled beam (on the right).

The control of the room temperature is performed through three grey globe temperature sensors of 40 mm diameter ($\alpha_{SW} = 0.62$), located 1 m far from the window and shielded from direct solar radiation (Figure 25). The three measurements of temperature at 0.1 m, 0.6 m and 1.1 m are then averaged to obtain the operative temperature for a person sitting [42].

In both cases, the fresh air is provided through the same unit as the active chilled beam. When the cooling is performed by the active chilled beam, the inlet consequently has two functions (cooling and ventilation inlet). The total air flow at the inlet is the sum of the air change rate and the recirculation rate induced by the active chilled beam. The air change rate can vary between 1 up to 4 ACH. The recirculation rate has been measured for different air change rates and is equal to around 1.5 times the air change rate. A circular outlet is located at the top of the north wall (diameter 125 mm, Figure 25). The extraction rate of the outlet is controlled so that there is no over- or under-pressure between the guarded zone and the experimental room. The infiltration between the guarded-zone and the test room is thus minimised. The air-tightness between the test room and outdoor has been tested by performing a blower door test, both in over- and under-pressure. The infiltration rate has been measured and is below 0.3 L/s.m$^2_{floor}$ at 50 Pa (i.e. 0.4 ACH at 50 Pa).

In order to simulate an office worker and assess the comfort level, a thermal manikin has been used (Comfortina [105], Figure 25 and Figure 27). The thermal manikin corresponds to a 1.7 meter tall woman, developed from a nearly anatomically-correct female manikin. The thermal manikin is sitting 1.2 m away from the south wall, on an open chair, which does not insulate or stop air movement. The clothing level of the whole thermal manikin ($I_{cl} = 0.83\ clo$) corresponds to a mid-season outfit [41], resulting in a thermal insulation from the body surface to the environment (I_T) equal to 1.47 clo. The manikin is made of a fibreglass shell covered with 0.3 mm diameter nickel wires, which are used sequentially to heat the manikin (accuracy on the heat flow ± 1 %) and to measure and control the skin temperature (accuracy ± 0.2 K). The manikin is divided into 17 parts, which can be controlled individually.
The thermal manikin is used for both simulating internal heat loads and evaluating local comfort in the experimental room. Local comfort evaluation can give additional information on the comfort level in a non-uniform environment [106, 107]. In fact, thermal comfort indices, such as the PPD, are based on the heat balance of the whole body, disregarding local effects. The analysis of local comfort will be performed using the heat flux from each body parts, from which can be calculated an equivalent temperature ($T_{skin} = 34$°C). The equivalent temperature is defined as the temperature of an imaginary space with uniform and still air condition, at which the body exchanges the same dry heat loss as in the actual environment [108].

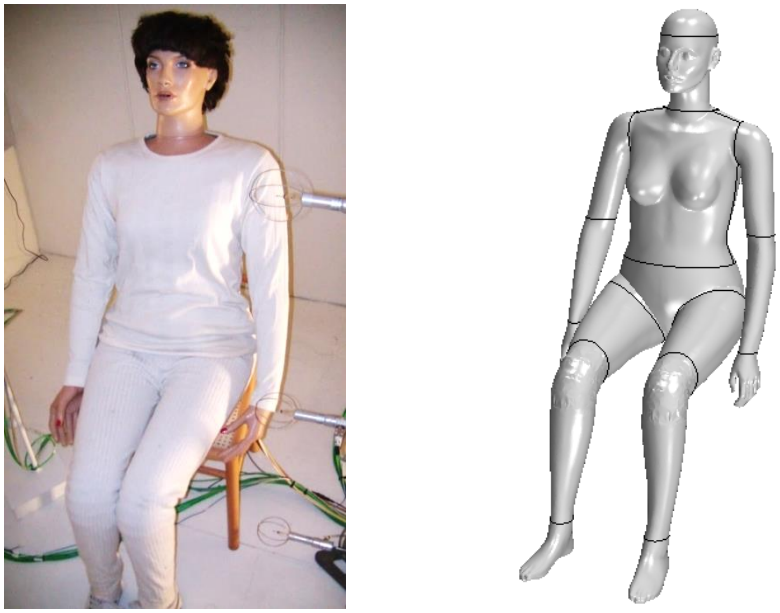

Figure 27: Thermal manikin used during the experiments (left) and the 17 individual parts (right).

2. Measurements and location of sensors

In order to evaluate with accuracy and precision the heat balance of the test room, a particular effort has been put in measuring the different parameters. More than 300 sensors have been placed in the experimental room, each of them calibrated individually. The logging frequency is varying between 0.1 Hz up to 5 Hz depending on the type of measurement.
The test room has been divided in 83 sub-surfaces to measure the heat flux going through the construction (Figure 28). The sub-surfaces have a smaller area where large temperature differences are expected (i.e. on the radiant panel, at the ceiling due to the inlet or at the floor because of solar radiation). For each of these sub-surfaces, thermopiles have been mounted inside the construction and thermocouples have been placed at the internal surface of the experimental room (accuracy ± 0.15 K [102]).

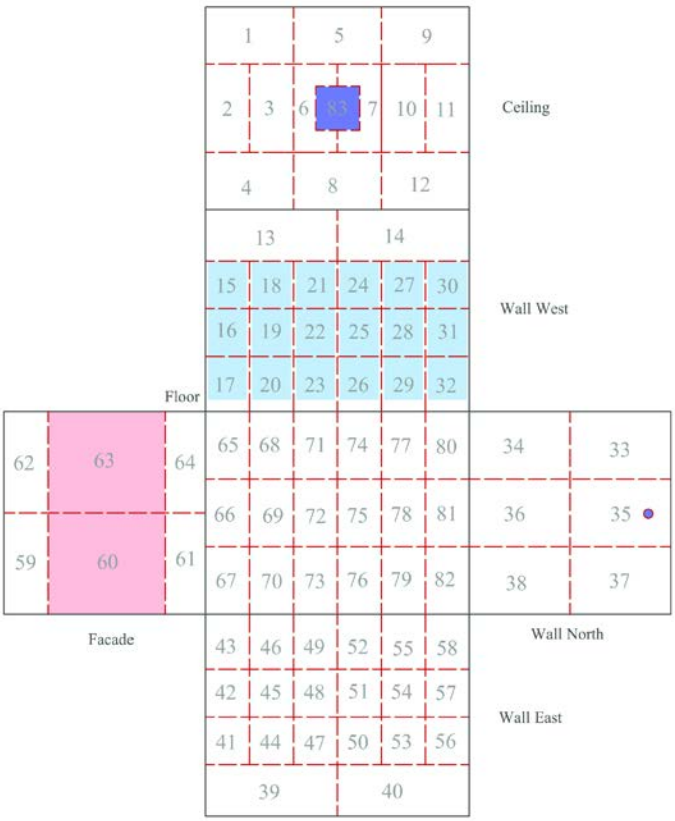

Figure 28: Subdivision of the test room into 83 sub-surfaces
(Light blue: radiant panel – Dark blue: ventilation inlet and outlet – Red: window).

To measure the air temperature distribution in the room, five columns of thermocouples have been installed in the test room: one in the middle and one in the centre of each wall (60 cm away from the south and north wall, and 25 cm away from the west and east wall). The thermocouples measure air temperature at 0.1, 0.6, 1.1, 1.7 and 2.65 m high. In order to decrease the influence of radiation on the measurement of air temperature, the thermocouples are silver-coated and protected by a mechanically ventilated silver shield (Figure 29).

Figure 29: Air temperature measurement.

Depending on the experiment, the active chilled beam or the radiant wall is used to cool down the test room. Seven energy meters have been mounted: one for the active chilled beam, and six for the radiant panels (one meter per panel). The accuracy of the measurement has been estimated to ± 0.9 L/h for the flow meters and ± 0.06 K for the Pt-500 sensors.

Irradiance is measured outside before the glazing using a CMP 21 pyranometer (accuracy ± 3 %). Another pyranometer has been placed on the roof of the experimental room and measures the global and diffuse solar radiation on a horizontal surface. A large carpet covers the ground in front of the south façade in order to control the ground reflectance ($\alpha_{SW} = 0.86$).

The measurement of the air flow through the ventilation system is performed using an orifice plate located before the inlet; the pressure difference is then converted into an air change rate (total accuracy: ± 7.5%). Twelve hot sphere anemometers have been placed in the test room for measuring air velocity. The sensors measure the turbulence intensity and the velocity at the ceiling, close to the thermal manikin (0.1, 0.6, 1.1 and 1.7 m high) and down the radiant wall (2 cm high and 30 cm far from the wall). The measurements are performed at a frequency of 10 Hz and integrated over 30 seconds.

3. Heat balance and uncertainty

The room heat balance has been performed for a time-step of 30 seconds and is expressed by Equation 8. The left part of the equation corresponds to the change of internal energy in the room, which includes both the capacitance of the air and of the equipment. The temperature swing of the equipment is assumed to follow the variation of the air temperature. The thermal mass of the equipment has been calibrated using the experimental results and is equal to 4.7 Wh/m$^2_{floor}$.K.

$$\left(V_{room}\,\rho_{air}\,C_{p\,air} + C_{m\,equipment}\right)\frac{\partial T_{air}}{\partial t} = \sum_i \left(Q_{cond\,i} + Q_{rad\,SW\,i}\right) + Q_{thermal\,manikin} + Q_{equipment} + Q_{ventilation} + Q_{chilled\,beam} \qquad (8)$$

The calculation of short-wave radiation ($Q_{rad\,SW\,i}$) includes both the angular-dependant properties of the glazing and the reflection of solar radiation in the room. First, the solar radiation measured at the façade level is decomposed into direct, diffuse and ground reflected solar radiation using the measured ratio of diffuse to global solar radiation and the ground reflectance. Then, the part of solar radiation transmitted through the glazing is calculated using the sun position and the angular-dependant properties of the glazing. Finally, the path of solar radiation inside the room is computed based on ray-tracing simulations (Figure 30). As the internal surfaces of the test room have a relatively high reflection coefficient ($\rho^*_{SW} = 0.73$), it is important to evaluate the portion of solar radiation, which is either absorbed by the glazing (after being reflected by the room surfaces) or redirected outside through the glazing. For diffuse radiation, the portion of solar radiation reflected by the room surfaces and then absorbed by the glazing is equal to 11 %, and the part of solar radiation redirected outside is equal to 7 % of the transmitted solar radiation.

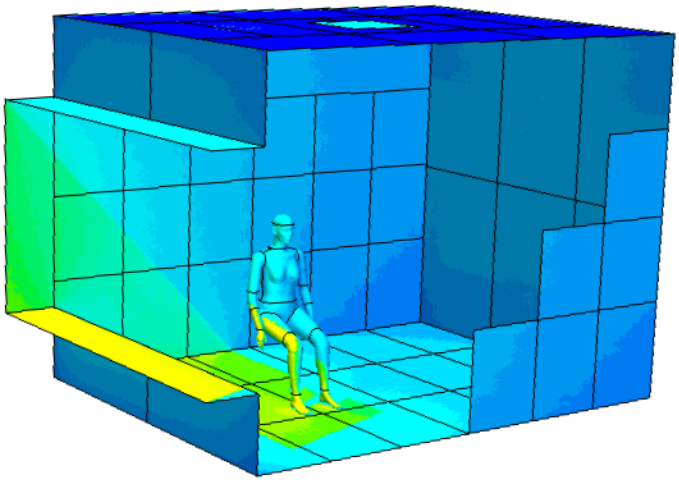

Figure 30: Example of ray-tracing calculation ($q_{SW\,direct}$ = 100 W/m² at an altitude of 45° - $q_{SW\,diffuse}$ = 100 W/m²).

A one-dimensional finite volume model with an explicit scheme [109] has been used to determine the conductive heat flux at the surface of each section ($Q_{cond\ i}$). The surface temperature and the temperature difference inside the construction over a 30 mm layer of EPS have been used as boundary conditions for the calculation (Figure 25). When the radiant wall is activated, an internal heat sink inside the construction layers is added to the numerical model. As the numerical model is one-dimensional, an equivalent layer has been defined to correctly model the two-dimensional heat flow at the pipes level.
Conductive heat transfer through the double-glazing unit has been calculated using the internal and external surface temperatures as boundary conditions, and taking into consideration the solar absorption of each pane. The thermal properties of the different layers have been estimated using EN 673 [110]: the thermal conductivity of the cavity is thus temperature-dependant.
Losses at the edges of the experimental room have been neglected due to the high level of thermal insulation (around 200 mm thick). But the thermal bridge of the window frame has been accounted because the temperature difference can be large and the window sealing does not ensure a full thermal insulation (Figure 31). Therefore, the software Therm [111], a two-dimensional finite element program, has been used to evaluate the heat transfer through the window frame ($\Psi_{frame} = 0.12\ W/m.K$).

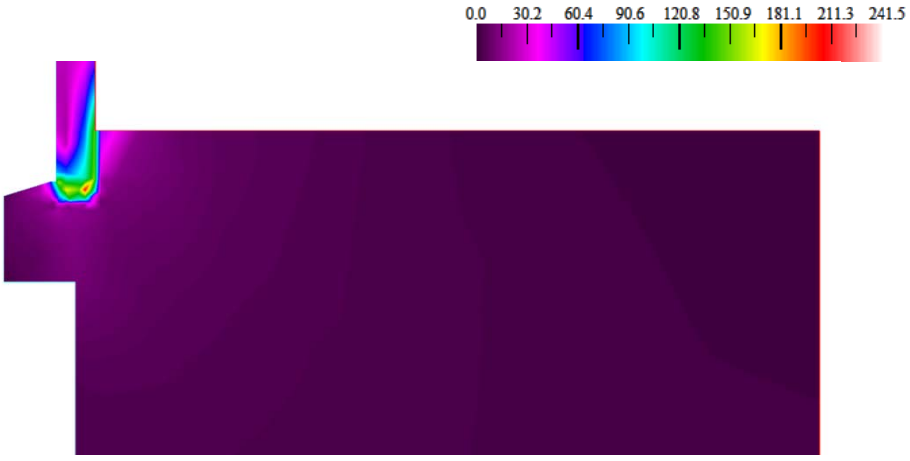

Figure 31: Cross section of the heat flux magnitude at the window frame (in W/m²).

An uncertainty analysis has been performed to assess the accuracy and the precision of the measurements [102]. This analysis is based on the heat balance experimentally derived (Equation 8). By comparing the difference between the gains and the losses, it is possible to estimate the error on the heat balance and, therefore, the uncertainty on the measurements.
The analysis has been performed for different intervals of calculation. The uncertainty on a single measurement point (i.e. representing 30 seconds of experiment) follows a normal distribution and is equal to ± 29 % (result based on ≈ 161 000 data points). This uncertainty did not show any correlation with the type of terminal or with the intensity of solar radiation. For hourly data, the accuracy is decreasing down to ± 17 % and down to ± 7 % for daily average.
A differential sensitivity analysis has also been performed to highlight the parameters having the largest influence on the accuracy of the heat balance. It has been observed that the optical properties of the glazing, the measurement of solar radiation, the measurement of the water flow and the evaluation of the ventilative flow influence the accuracy of the heat balance the most.

4. Comparison of the energy effectiveness

Two sets of experiments have been performed to analyse the performance of the radiant wall and the active chilled beam. First, steady-state experiments were conducted by placing a shading device on the external side of the window and 150 mm of EPS on the internal side. An electric carpet was mounted at the window level (Figure 32). In the second set of experiments, the window was cleared, so that the dynamic effects and the influence of solar radiation could be observed (Figure 33).

Figure 32: Panoramic view of the set-up with the electric carpet (steady-state).

Figure 33: Panoramic view of the set-up with the sun (dynamic).

4.1. Steady-state experiments

In a first set of experiments, an electric carpet has been mounted in front of the window, simulating the effect of internal solar shading (Figure 32). The power of the carpet and the air change rate have been set respectively to 36 W/m^2_{floor} and 2.2 ACH. The cooling power has been automatically adjusted to achieve an operative temperature of 26±0.2 °C. The cooling need of the two terminals has then been measured for different inlet temperatures, varying from 20°C up to 28°C (Figure 34). A linear relationship between the ratio cooling power/heat load and the temperature difference between the inlet and the operative temperature can be observed. The radiant wall is more energy-efficient than the active chilled beam. Under similar boundary conditions, the cooling power of the cooled wall is around 7–10 % lower. The linear cooling trend of the radiant wall and the active chilled beam was also observed in the numerical simulations (Figure 14, on the right) and shows the consistency and accuracy of the measurements. The higher the inlet air temperature, the larger the difference between the two terminals. Alternatively, one could say that the thermal sensation of a radiant wall is around 0.5–1 K lower than that of an active chilled beam for similar cooling power.

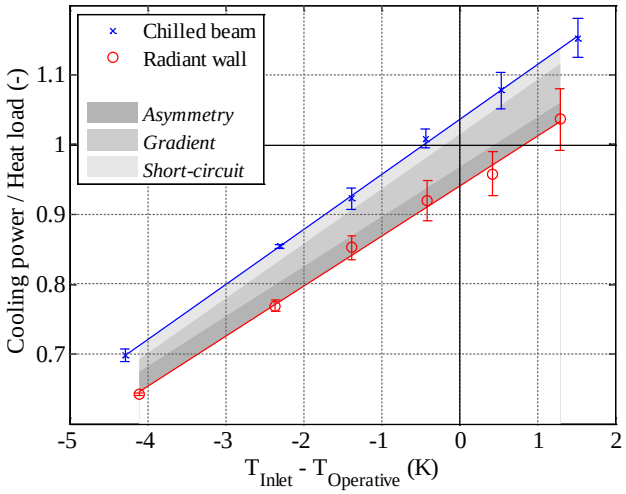

Figure 34: Cooling power/heat load ratio depending on the temperature difference between the inlet and operative temperature.

4.2. Dynamic experiments

The dynamic experiments have been performed during the months of July and August 2013, characterised by long days, relatively warm outdoor temperature at night (≈ 15–20°C) and solar radiation (up to 1000 W/m² on a horizontal surface). Contrary to the steady-state experiments, the inlet air temperature has been kept constant, equal to 25°C. During the day (7 am till 8 pm), the cooling set-point in the experimental room was set to 25°C. During the night, the test room was cooled down to 22°C. This night setback has a dual objective: obtain comparable results over the different days and simulate the lower outdoor temperature at night, which is providing a free cooling to buildings through the ventilation system.

When the heat load is lower than 400 Wh/m² per day (corresponding to an overcast day), the active chilled beam and the radiant wall achieved similar operative temperature. But when the heat load increases, the active chilled beam achieves a colder indoor environment than the radiant wall: the difference is up to 0.5 K for a clear day. This difference in the global comfort level is due to slightly different cooling capacities of the two terminals: the cooling capacity of the active chilled beam is 4 W/m^2_{floor} higher than the one of the radiant panel. This limited cooling capacity of the two terminals is also the explanation of the overheating period observed.

In order to compare the performance of the active chilled beam and the radiant panel, a similar analysis as for the steady-state case has been performed. The heat load and the cooling need have been calculated (Figure 35). In order to account for differences in the level of comfort, a correction on the cooling need of the radiant wall has been performed (cf. dashed line in Figure 35). Days with low heat load (below 400 Wh/m² per day), the cooling power is higher than the cooling need because the inlet air is warmer than the air inside the test room, thus generating additional heat gains. It can be observed that the radiant wall is slightly more efficient than the active chilled beam. When the heat load increases, the advantages of radiant terminals compared to convective terminals can be observed more clearly. Due to the higher air temperature, radiant terminals optimise the ventilation losses and save up to 15 % on the energy need for cooling.

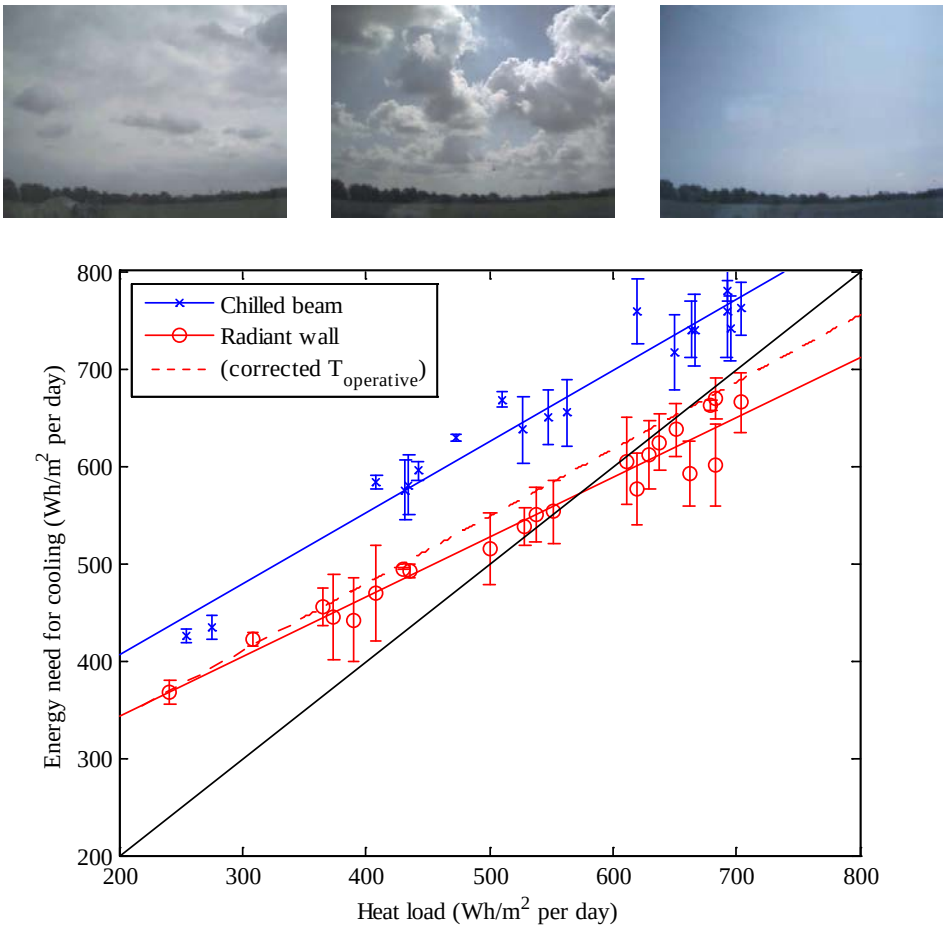

Figure 35: Cooling power as a function of the heat load (values calculated over 24h, starting from 1:30 am). The pictures of the sky shown above are on an indicative basis.

4.3. Discussion and comparison with simulations

From both the steady-state and the dynamic simulations, similar behaviour has been observed. The radiant wall has better energy effectiveness than the active chilled beam due to increased ventilation losses. The heat losses through ventilation are higher with the radiant wall than with the active chilled beam due to a higher outlet temperature, which can be caused by different factors: a temperature difference between the air and the surfaces ($\Delta T_{air\ occ.\ zone\ -\ radiant}$), an air temperature gradient ($\Delta T_{outlet\ level\ -\ air\ occ.\ zone}$) and/or a short-circuit between the inlet and the outlet ($\Delta T_{outlet\ -\ outlet\ level}$). By analysing these parameters, it is possible to prescribe correction factors on the ventilation heat balance depending on the type of terminal (Equation 9).

$$Q_{vent} = \dot{m} \cdot C_{p\,air} \cdot \left(T_{inlet} - T_{operative} - \frac{\Delta T_{air\ occ.\ zone\ -\ radiant}}{2} - \Delta T_{outlet\ level\ -\ air\ occ.\ zone} - \Delta T_{outlet\ -\ outlet\ level} \right) \quad (9)$$

In the experiments with the electric carpet simulating the solar load, the air temperature in the test room is around 0.5–1 K higher with the radiant wall than with the active chilled beam. This difference increases with the cooling power, which explains why the efficiency of radiant terminals increases with the heat load. Similar values of asymmetry between air and surfaces temperatures have been observed in the second set of experiments (Figure 36).

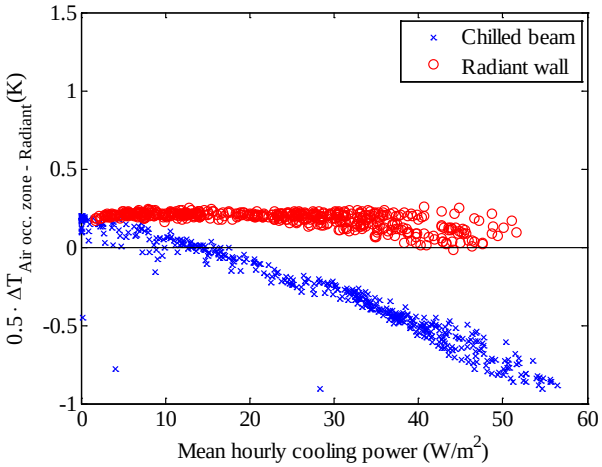

Figure 36: Difference between the air temperature in the occupied zone and the radiant temperature depending on the cooling power (hourly values, dynamic experiments only).

Additionally, a temperature gradient is achieved in the room when the radiant wall is activated (Figure 37). The temperature gradient increases the outlet temperature and thus the ventilation losses. The temperature gradient is highly dependent on the power and location of the heat load. For the steady-state experiments, the difference between the outlet and the mean air temperature in the occupied zone increases from 0.2 up to 1.3 K, when the cooling power rises from 25 W/m² up to 40 W/m². But when solar radiation is the main heat source, the temperature gradient with the radiant panel is not higher than 0.5 K. In fact, the direct solar radiation absorbed by the floor tends to homogenise the room air temperature, thereby decreasing the vertical temperature gradient.

It has also been observed that the difference between the outlet and the air temperature is negative for the active chilled beam. This is due to a short-circuit between part of the inlet air and the outlet.

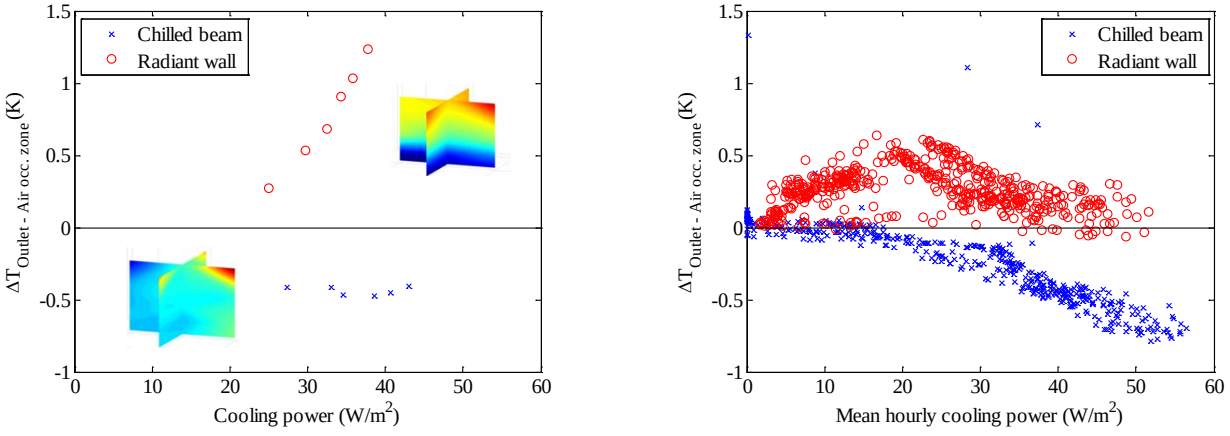

Figure 37: Difference between outlet temperature and the air temperature in the occupied zone depending on the cooling power for the steady-state experiments (on the left) and the dynamic (on the right).

By quantifying these different temperature differences ($\Delta T_{air\ occ.\ zone\ -\ radiant}$, $\Delta T_{outlet\ level\ -\ air\ occ.\ zone}$ and $\Delta T_{outlet\ -\ outlet\ level}$), it is possible to get a detailed explanation of the better energy effectiveness of the radiant wall compared to the active chilled beam (grey areas in Figure 34).

5. Comparison of the level of comfort

The comfort level achieved in the test room is evaluated by combining the results of both steady-state and dynamic experiments, as the results are similar. The analysis is performed on an hourly basis and during the working hours (i.e. from 8:30 am till 5:30 pm).
The radiant asymmetry and the vertical air temperature difference have been calculated for the different experiments, but no discomfort has been identified. Therefore, only the results about the draught rate and the local equivalent temperature will be presented.

The risk of draught has been evaluated in two critical locations: in the middle of the test room (down the inlet) and down the radiant panel (3 cm above the floor level).
Due to the higher air temperature, the risk of draught decreases when the cooling power increases. The risk of draught for the two terminals is below 20 %, which corresponds to the limit of category II (normal level of expectation). The risk of draught with the active chilled beam is higher due to the increased air velocity (around 0.12 m/s as compared to 0.07 m/s for the cooled wall). It has to be noted that the increased air velocity is too small to have a large impact on the global comfort [40].
The minimum surface temperature reached by the radiant panel is equal to 18°C, meaning higher than the due-point. This cold surface creates a down-draught, which can cause discomfort in the occupied zone. Therefore, the maximum velocity at the floor level close to the radiant panel has been measured in three different positions, and the PD (Percentage Dissatisfied) due to the down-draught has been calculated (Figure 38). The PD is below 14 % for all the experimental cases, even though the velocity down the panel rises up to 0.2 m/s. A similar relationship as Heiselberg [98] has been found between the air velocity and the temperature difference between the air and the surface.

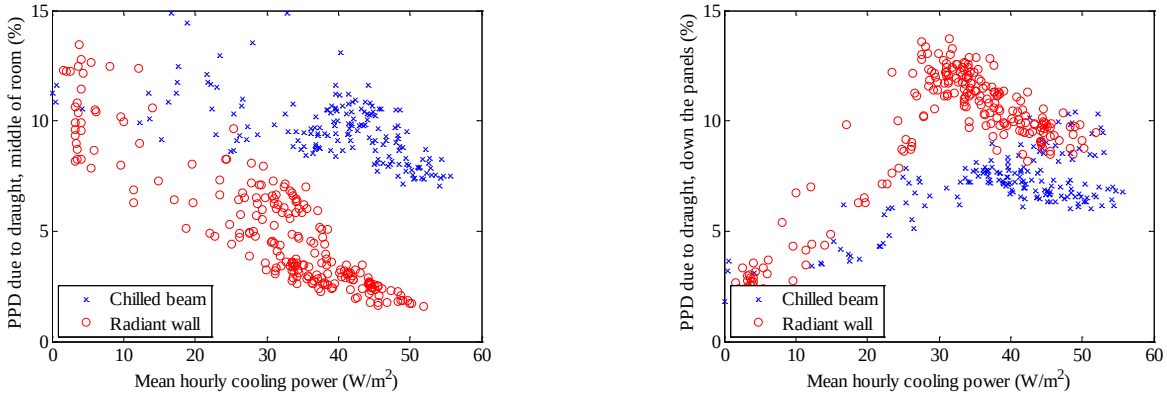

Figure 38: Risk of draught in the middle of the room (on the left) and down the radiant wall (on the right) as a function of the cooling power.

The local comfort has been evaluated using the thermal manikin, which was running at a constant skin temperature of 34°C. With the active chilled beam, the head, the chest, the left hand and forearm show a slightly lower equivalent temperature due to the cold air jet flowing close to these body segments. With the radiant wall activated, the top of the head and the back of the thermal manikin are slightly colder due to the radiation from the cold wall. But the decrease of equivalent temperature (lower than 2 K) is not significant enough to sense any local discomfort [112].

6. Conclusion

The two experimental set-ups are characterised by differences in the boundary conditions (steady-state vs. dynamic) and also in the level and type of heat load. The first set-up corresponds to the case of a building equipped with internal solar shadings, which stop most of the solar radiation, resulting in a heat load concentrated at the window level. The second set-up highlights the effect of direct solar radiation on the cooling performance as no shading device was placed at the window level.

Despite these differences, similar conclusions can be drawn out of these two sets of experiments. The radiant wall is more energy-efficient for cooling down a building than the active chilled beam. The energy savings can be estimated to around 10 % due to higher ventilation losses. A detailed analysis of the ventilation heat balance has been performed in order to isolate the effect of individual parameters, such as the asymmetry between air and radiant temperature, the air temperature gradient and the possible short-circuit between inlet and outlet. These three elements are the key parameters to characterise the effectiveness of emitters and can be used in standards and BES tools to differentiate the terminals (Equation 9).
In these experiments, the three parameters mentioned above play each an equally important role in decreasing the cooling need of the radiant wall compared to the active chilled beam. With the air-based terminals, it has been observed that the asymmetry between air and radiant temperature increases with the cooling power and leads to a lower air temperature than for the radiant panel. For a cooling power around 30 W/m², the air temperature with the radiant terminal is around 1 K higher than with the active chilled beam. Additionally, the cooled wall creates stratification in the test room, which increases the outlet temperature of around 0.5 K. This temperature gradient varies as a function of the intensity and type of heat load. In the case of a heat load concentrated at the window level, the increase of outlet temperature can even be up to 1.3 K. Finally, direct losses between the inlet and outlet have been observed. This short-circuit decreases by around 0.5 K the outlet temperature of the active chilled beam compared to the radiant wall.

Regarding comfort, both terminals met the general requirements except at high solar heat gains. Overheating was observed due to the absence of solar shading and the limited cooling capacity of the terminals. The local comfort conditions (radiant asymmetry, vertical air temperature gradient, risk of draught) were also evaluated and the measured parameters were within the comfort range. In addition to the traditional local comfort parameters, a thermal manikin was used to evaluate the discomfort in individual body parts. Even though a decrease of some segment temperatures was observed, this decrease was not large enough to create local discomfort.

For further information, the reader can refer to Paper 4:
“A full-scale experimental set-up for assessing the energy performance of radiant wall and active chilled beam for cooling buildings”

Part III

Characterisation of convective heat transfer at internal surfaces of buildings with different cooling terminals

As shown in Figure 16 (on the left), convective heat transfer plays an important role in the energy efficiency of air-based terminals. By increasing the convective heat transfer at specific surfaces, the interaction between the inlet air flow and the surfaces can be increased and thus modifying the asymmetry between surface and air temperature. Selecting the correct algorithm for modelling the convective heat transfer is, therefore, a key aspect to accurately evaluate the performance of different terminals.

On a global scale, convection has also been identified as one of the main sources of uncertainty in the simulation of building energy use. According to the ASHRAE Technical Committee 4.7, the modelling of internal surface convection in BES tools is ranked as one of the highest priority research topics [113]. Some sensitivity analyses have shown that the predicted heating/cooling need could vary in the order of 20 to 40 % depending on the model used for internal convection [34, 114]. Domínguez-Muñoz et al. [115] observed that the internal convective heat transfer coefficient (CHTC) was the second most influencing parameter on the peak cooling load. When modelling night-time ventilation, Goethals et al. [116] observed that the choice of the convection algorithm strongly affects the energy and thermal comfort predictions.
This uncertainty in the prediction is due to the complexity and diversity of flow that can be observed in buildings. The convective heat transfer can be either natural (driven by buoyancy forces), forced (caused by an external force) or mixed. As yearly simulations are required to analyse the building energy use, a detailed analysis of the flow around and in the building is not possible and the calculation of convective heat transfer has to be simplified by using correlations.

The objective of this part is specifically to study the influence of the air jet trajectory on CHTC. Even though this effect has not been studied as such, some evidences tend to prove that the air jet characteristics greatly influence the convective heat transfer. For example, the CHTC is 70 % larger with a radial ceiling diffuser [117] than with a side wall diffuser [118] at 5 ACH. Based on numerical simulations, Leenknegt et al. [119] also observed large differences in the resulting convective flow depending on the air jet trajectory. Alamdari and Hammond [120] and Jensen [121] have developed methodologies to calculate the convective heat transfer based on a detailed modelling of the flow close to the inlet. This thesis will propose alternative methods.
Another area of investigation is the interaction between the ventilation and the radiant terminals. The convective heat transfer coefficient at the surface of radiant terminals has been quite widely studied [35, 122, 123], but few experimental studies evaluate the effect of the air change rate on the heat release/absorption from the panel. Additionally, the convective heat transfer at non-activated surfaces will be studied to evaluate the accuracy of forced correlations when there is a small temperature difference between the inlet air and the surfaces.

1. Convection in buildings

Since the past 50 years, many researchers have studied experimentally CHTC in order to improve the accuracy of simulations [32, 38, 117, 118, 122, 124-126]. The first correlations were derived from flat plate experiments [127, 128]. Nevertheless, these correlations are not always applicable to buildings due to the scale effect and different flow characteristics. Awbi et. al. [122] showed that the CHTC for a heated wall tends to be higher than that of isolated plates with free edges. Therefore, full-scale measurements have been performed under different conditions [32, 38, 117, 118, 124-126]. Due to the diversity of indoor airflow patterns, a large scattering in the CHTC has been observed depending on the type of diffuser and its location. Studies under dynamic conditions have also been performed by some researchers to assess convective heat transfer over a wider range of situations [32, 126, 129]. The literature review from Peeters et al. [31] gives an overview of the current knowledge on the modelling of convective heat transfer.

The modelling of convection in Building Energy Simulation (BES) tools varies a lot with the software. Few BES tools use fixed coefficients; most of them use dynamic coefficients assuming natural convection (e.g. correlation from Alamdari & Hammond [127]). Lately, a couple of BES tools (EnergyPlus, ESP-r) have implemented the adaptive algorithm proposed by Beausoleil-Morrison [34], which consists in

coupling different correlations. This algorithm is the most advanced method available nowadays for modelling convection in buildings. One of the main advantages of this algorithm is that it can evolve over time by including more correlations and thus more types of flow.

Instead of using correlations, some BES tools (ESP-r, EnergyPlus) propose a coupling between energy simulation (BES) and computational fluid dynamic (CFD). This coupling improves the evaluation of the air flow and also the determination of the nature of convective flow (buoyant, forced or mixed) [34, 130-132]. Nevertheless, there is still a high uncertainty on the determination of CHTCs from CFD calculation because of the difficulty to model the heat exchange in the boundary layer close to the walls. Direct Numerical Simulation (DNS) or Large Eddy Simulation (LES) can be used to model turbulence, but these methods require a large computing power. Reynolds-Averaged Navier-Stockes equations (RANS) are thus used most of the time to model turbulence. If a standard wall function is chosen (log-law wall function), the boundary layer will be modelled assuming forced and fully turbulent convective flow. Alternatively, the Yuan wall function can be used for vertical surfaces with a buoyancy-driven flow. But besides these two cases, there is no clear agreement on which wall function best represents the convective flow. As an alternative to the standard wall function, a finer mesh can be used close to the wall to explicitly calculate the flow pattern in the boundary layer (low y^+). In this case, the turbulence model should be selected to match the flow properties (e.g. low turbulence models). Nevertheless none of these modelling techniques will accurately capture the convective flow and the computational time resulting from the coupling increases much. More experimental data is thus needed to validate the convective heat transfer calculated from CFD.

2. Deriving CHTCs from experiments

Two methodologies exist to derive convective heat transfer coefficients from experiments. The first method consists in obtaining specific surface temperatures using electric heaters or hydronic systems, and heat fluxes are measured at the different surfaces [117, 122, 124, 125, 133]. This method ensures a relatively uniform room temperature distribution, but it can result in a rather large conductive heat transfer. An alternative method consists in measuring the surface heat flux, without controlling its intensity. The conductive heat flow through the different surfaces can be measured/calculated in different ways. The air temperature gradient in the boundary layer can be measured by a Mayer ladder [126, 134], or heat flux sensors can be used [32, 35, 135], or thermocouples can be integrated to the construction to estimate the conductive flux knowing the thermal properties of materials [121, 123, 126, 129]. This technique results in a more realistic conductive flow at the surfaces, but the accuracy of the method is limited by the number of measuring points. In fact, the temperature distribution in the room can result in a highly inhomogeneous conductive heat flow, which is difficult to measure accurately.
In these experiments, the second technique has been used to establish the room heat balance. This technique has been chosen because it results in a more realistic surface temperature and heat flux inside the test room. The numerous sensors placed inside the test room ensure a correct tracking of the local changes in the heat flux.

The analysis of convection is divided in two parts. First, the total test room heat balance is established to ensure the accuracy of the overall results. This first step of the analysis is crucial to ensure the consistency of the results. Second, the convective heat flows at the surfaces are derived from the heat balance at the wall surfaces of the test chamber. By measuring/calculating the conductive and radiative heat flows together with air temperature measurements, the CHTCs can be obtained for each surface or sub-surface (Equation 10).
The CHTCs are calculated over a 30-minute period. This interval of time has been chosen because a similar period of analysis is usually selected in BES tools (between 15-minute and 1-hour time-step) and also because the uncertainty on the measured heat flow is smaller than for 30-second data.

$$h_{conv\ surface} = \frac{\sum_i (Q_{cond\ i} + Q_{rad\ SW\ i} - Q_{rad\ LW\ i})}{A_{surface} \cdot \Delta T_{surface-reference}} \qquad (10)$$

In order to study the convective heat transfer over a long period of time and for a wide range of conditions, experiments under dynamic boundary conditions have been performed in two different full-scale facilities. These facilities are presented below:

- **Indoor full-scale facility ("The little house in the prairie")**
  A test room located inside a laboratory at Aalborg University has been used in 2008 and 2009 by Artmann et al. [129] and Le Dréau et al. [26] to study different strategies for night-time ventilation (12 hours of discharge). The internal dimensions of the test room are 2.64 m × 3.17 m × 2.93 m (width × length × height) resulting in an internal volume of 24.5 m^3. The thermal mass of the room is concentrated at the ceiling, which is composed of 7 layers of 12.5 mm gypsum boards. The other walls are highly insulated by 230 mm of expanded polystyrene (EPS). The dynamic thermal mass of the room is equal to 26 $Wh/K.m^2_{floor}$, which corresponds to a light building [103].
  This test room is equipped with a slot side-wall diffuser (830 mm width × 80 mm height) and a displacement diffuser. A total of 34 experiments have been performed with different air change rates (2.3, 3.1, 6.7 and 13 ACH), different ventilation types (mixing and displacement), different types of floorings (normal and low emissivity) and different inlet temperatures (ΔT_0 varying between 2.9 up to 12.7 K, with ΔT_0 difference between the mean temperature at the ceiling before starting the experiment and the mean inlet temperature measured during the last 10 hours of the experiment).
  The heat balance of the test room has been established by evaluating the heat flow through the 37 sub-surfaces. The experimental uncertainty on the heat balance is equal to ± 18 % (hourly average).

- **Outdoor full-scale facility ("The Cube")**
  This test facility has already been presented in Part II (page 31). The test room has been placed inside a guarded zone with the exception of one wall, which is in direct contact with the outdoor environment (Figure 25). The internal dimensions of the test room are 2.76 m × 3.60 m × 2.75 m (width × length × height). The thermal mass of the room is equal to 20 $Wh/K.m^2$ [103].
  The test room is equipped with an active chilled beam (600 mm × 600 mm), which can be classified as a radial ceiling diffuser with induction effect. The purpose of these experiments is to analyse the convective flow with two types of cooling terminals (active chilled beam and radiant wall) and under realistic office conditions (thermal manikin, solar radiation). The effects of varying heat load, air change rate and inlet air temperature have been studied under both steady-state and dynamic conditions. More than 1400 hours of experiments have been used to analyse convective heat transfer in the test room.
  The test room has been subdivided in 83 sub-surfaces, and the experimental uncertainty on the heat balance has been estimated to ± 17 % (hourly average).

In a first part, the convective flow with air-based cooling systems will be studied. Two types of inlet will be considered (slot side-wall diffuser and active chilled beam). In a second part, the convective flow with radiant cooling system will be investigated.

3. Convective heat transfer with cooling from side-wall and radial diffusers

Pictures of the two diffusers are given in Figure 39. The slot side-wall diffuser is a class III diffuser, from which the jet is essentially two-dimensional. The active chilled beam is a Class II diffuser, from which the jet flows radially along the ceiling [136].
For both cooling systems, the local Richardson number calculated experimentally is below one, indicating that forced convection is dominating the convective heat transfer. It has also been observed that all surfaces have an influence on the total convective heat transfer and play an important role in the total convective heat flow removed from the test room. Therefore, all surfaces have to be included in the study in order to get accurate models for convection.

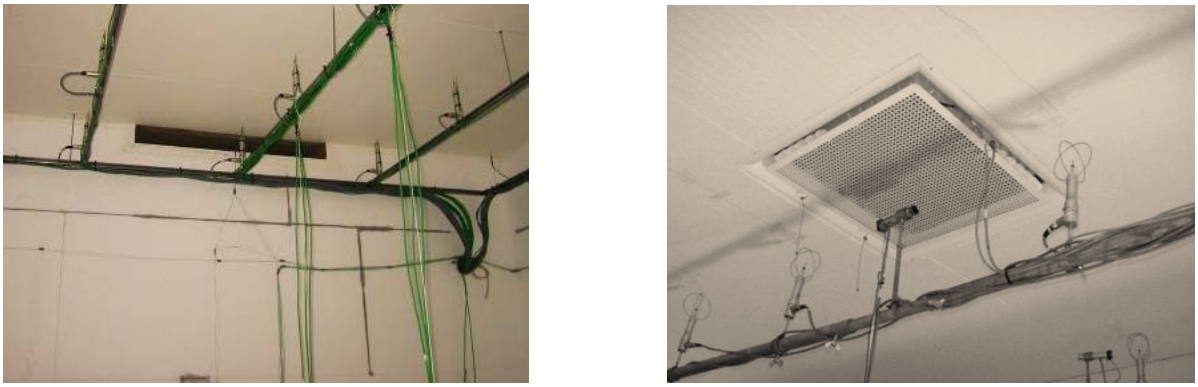

Figure 39: Pictures of the slot side-wall diffuser (on the left) and the active chilled beam (on the right).

3.1. Classic approach

As mentioned in the introduction, forced CHTCs are usually expressed as a function of the air change rate (ACR) and $q_{conv} = h_{forced} \cdot \Delta T_{Surface-Inlet}$, with $\Delta T_{Surface-Inlet}$ temperature difference between the surface and the inlet air. In the first part, the CHTCs of both experiments will be analysed using this classic approach and the limitations of this technique will be discussed.

In the indoor full-scale facility, the convective heat transfer with the slot side-wall diffuser has been investigated at the different surfaces (Figure 40). At the ceiling, measured CHTCs are lower than the one proposed by Fisher and Pedersen [117]. In fact, Fisher and Pedersen used a radial ceiling diffuser, which is more efficient than a side-wall diffuser because the air jet is covering a larger area. When comparing to the results of Fisher with the side-wall inlet [118], it can be observed that the measured CHTCs are lower or equal to the proposed correlation. The correlation matches the experimental results only for 13 ACH because the jet is flowing over the entire surface in both cases. When the air change rate is lower, the jet is not attached to the ceiling anymore, resulting in a lower CHTCs than the ones obtained by Fisher. At the floor, the correlations of Fisher and Pedersen estimates relatively well the convective heat transfer for the floor made of EPS, even though a slight underestimation can be observed at low air change rate (i.e. when the jet is dropping shortly after entering the room).
Similar results have been observed by other researchers studying forced convection with side-wall inlet. Goethals et al. [32] mentioned that the “correlations predict for all runs convective heat fluxes [at the ceiling], which are three to fourteen times as high as the measured ones”. Based on CFD simulations, Leenknegt et al. [119] concluded that “the CHTC resulting from Fisher and Pedersen correlations […] result in much higher values than were seen in the simulations”. In all cases, the discrepancy with the correlations of Fisher and Pedersen has been explained by the air jet dropping from the ceiling and therefore not exchanging as much heat as predicted by Fisher and Pedersen. Detachment of the jet from the ceiling was not observed by Fisher and Pedersen, even “for jet inlet temperature as low as 10°C and jet velocities as low as 1.3 m/s” [117].

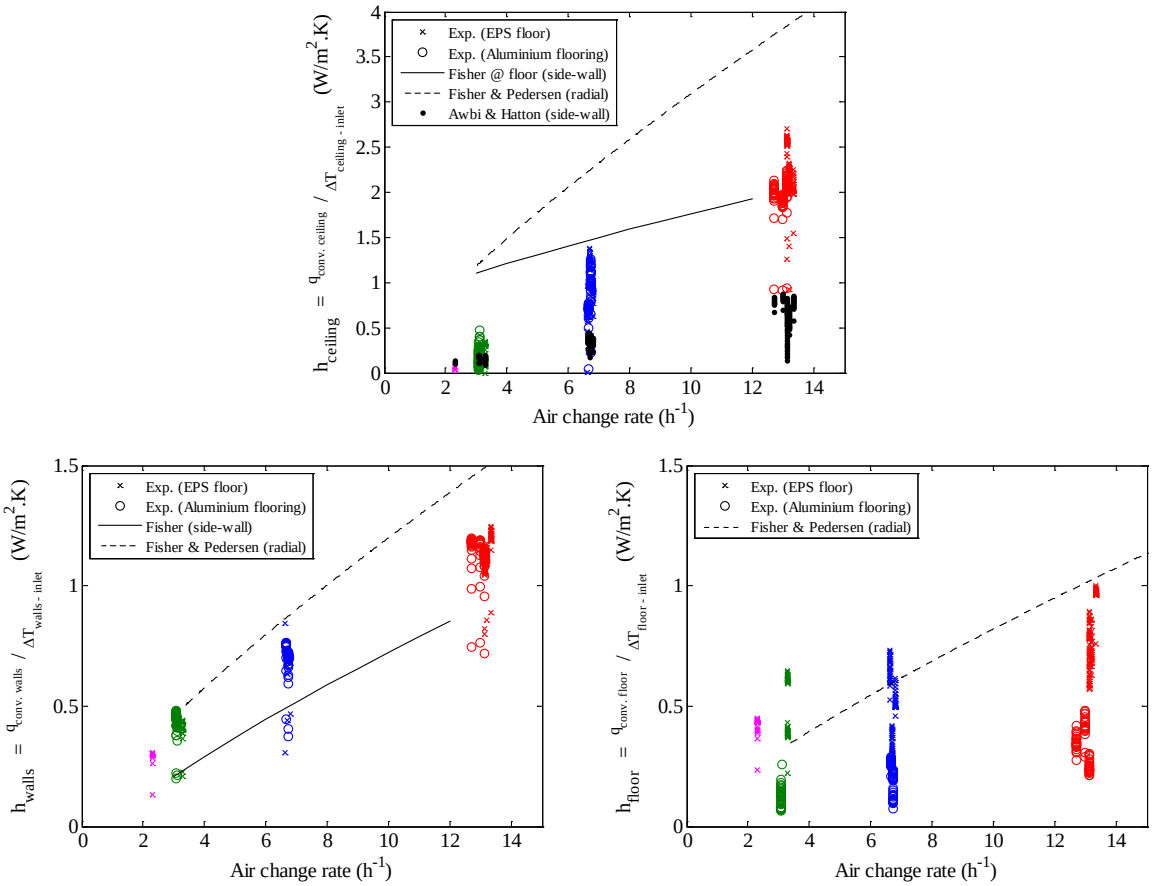

Figure 40: CHTCs at the surfaces of the test room depending on the air change rate (indoor full-scale facility with slot side-wall diffuser).

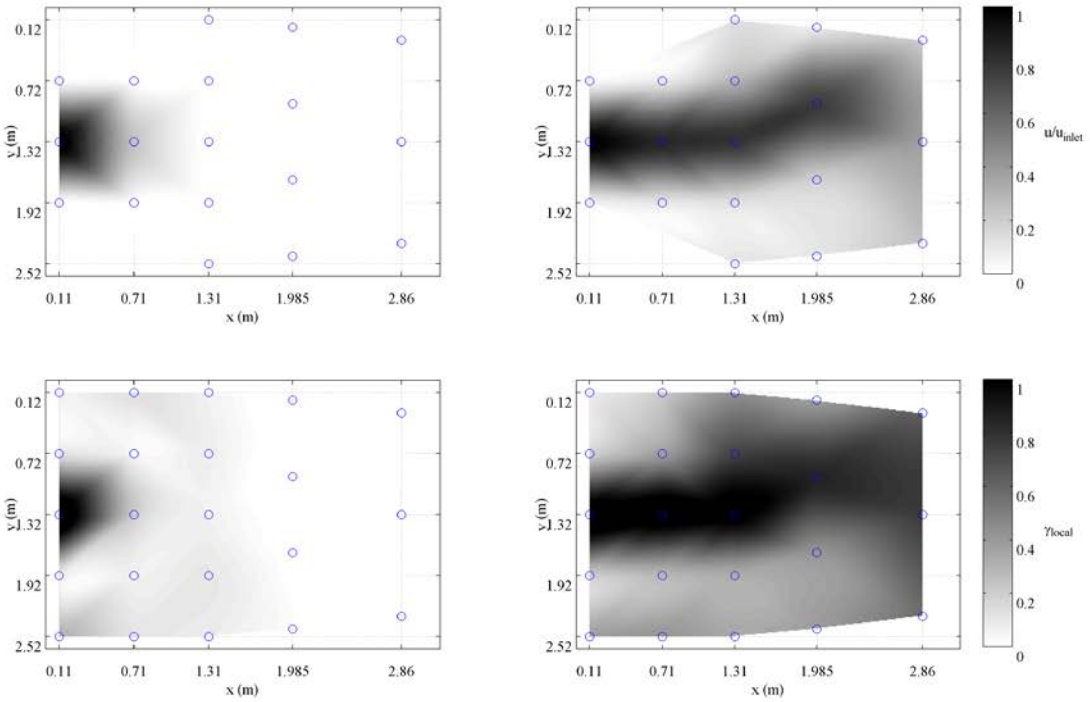

Figure 41: Comparison of the local dimensionless velocity (upper graphs) and the local convective ratio (lower graphs) at the ceiling for 3.3 ACH (on the left) and 13.2 ACH (on the right).

The differences in the air jet trajectory and the influence on the convective heat transfer are confirmed in Figure 41. The local dimensionless velocity at the ceiling (u/u_{inlet}) is compared to the local convective ratio (γ_{local}), with $\gamma_{local} = Q_{conv\,i} / Q_{cond\,i}$. At a low air change rate (3.2 ACH), the jet is falling down right after the inlet, resulting in a low convective ratio on the entire surface. The buoyant forces are dominating. Conversely, the jet covers a large part of the ceiling at high air change rate (13.2 ACH), resulting in a high convective ratio. The momentum forces are larger than the buoyancy forces. A strong relationship can be observed between the dimensionless velocity and the local convective ratio.

A similar analysis has been performed in the outdoor full-scale facility with the radial ceiling diffuser. In order to include a parameter describing the air jet trajectory, a modified Archimedes number ($Ar_{ratio} = (T_{outlet} - T_{inlet})/\dot{V}^2$) has been introduced. This number characterizes the ratio between thermal buoyancy and momentum forces and is often used when studying air distribution [137]. The colours of the experimental points are set as a function of this modified Archimedes number (Figure 42). The relationship between CHTC and air jet trajectory can be clearly observed. Its influence is of the same order as the type of inlet. The CHTC is decreasing at the ceiling, when the modified Archimedes number is increasing (i.e. when the jet is dropping). On the opposite, the CHTC at the walls and floor is increasing with increased Archimedes number due to the colder air reaching these surfaces.

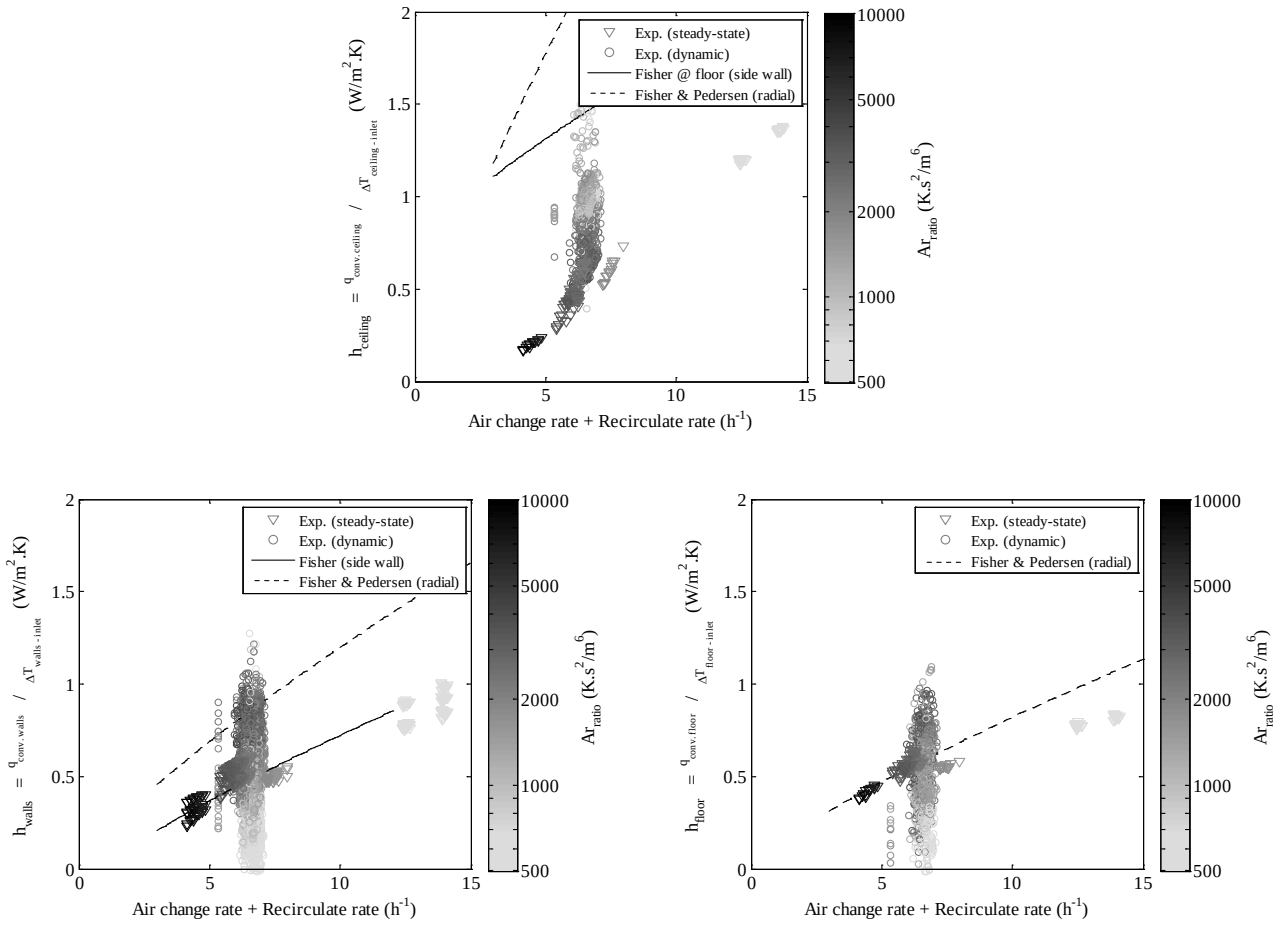

Figure 42: CHTCs at the surfaces of the test room depending on the air change rate and the recirculation rate (outdoor full-scale facility with active chilled beam).

These two analyses point out the specificity of existing correlations and the difficulty of extrapolating existing models to similar cases. Forced convective heat transfer is highly dependent on the inlet temperature and on the position, type and size of the inlet. Each configuration will lead to different correlations.
Despite these difficulties, CHTCs have to be defined accurately close to the inlet because a small error in the estimation of the CHTCs might result in a large error in the room heat balance due to the high temperature gradients involved. This thesis focuses on more precisely characterising the role of the air jet trajectory on the convective heat transfer. Two methods have been tested:

- In Method 1, the velocity profile at the ceiling has been used to derive the convective heat transfer. This method has been tested only on the results of the indoor full-scale experiments with the side-wall diffuser. It has to be noted that this technique has been investigated theoretically by Alamdari and Hammond [127] to model two- and three-dimensional turbulent wall jets.
- In Method 2, the Archimedes number has been used directly to derive new correlations. This method has been tested only on the results of the outdoor full-scale experiments with the radial diffuser.

3.2. Method 1: Local CHTC (side-wall diffuser)

In order to evaluate the accuracy of CHTC prediction using local velocity measurements, a mixed correlation has been developed based on these data (Equation 11). The mixed correlation is blending the natural convection term (correlation of Alamdari and Hammond for horizontal downward heat transfer [127]) and the forced convection term (correlation from ASHRAE for turbulent flow over a flat plate [128]), with a blending coefficient n equal to 6. The forced convective part is based on the measurements of local velocity u_i.

$$Q_{conv\ ceiling} = \sum_{i=1}^{22}\left[\left(\frac{6.02 \cdot u_i^{0.8}}{D_h^{0.2}}\right)^n\left(\frac{\Delta T_{Ceiling\ i\ -\ Inlet\ air}}{\Delta T_{Ceiling\ i\ -\ Room\ air}}\right)^n + \left(0.6 \cdot \left(\frac{\Delta T_{Ceiling\ i\ -\ Room\ air}}{D_h^2}\right)^{1/5}\right)^n\right]^{1/n} \cdot \Delta T_{Ceiling\ i\ -\ Room\ air} \cdot A_i \qquad (11)$$

An example of resulting convective heat transfer coefficients can be found in Figure 43. A 1:5 ratio can be observed between the lowest CHTC and the highest one, close to the inlet. Figure 44 compares the experimental data to the results obtained with the developed mixed correlation (side-wall diffuser). The predicted convective heat transfer lies within the uncertainty bands most of the time. The highest inaccuracy in the developed equation can be observed for low inlet temperature, when the ceiling is much warmer than the room air. This is due to the characteristics of the jet, which falls down after the inlet and creating large variations in the local air temperature, whereas the developed equation uses a constant air temperature. When comparing the calculated convective heat transfer with existing correlations (Table 10), it can be observed that the developed correlation gives better results than most of the correlations with an average error of ±17 % (excluding 3.3 ACH).

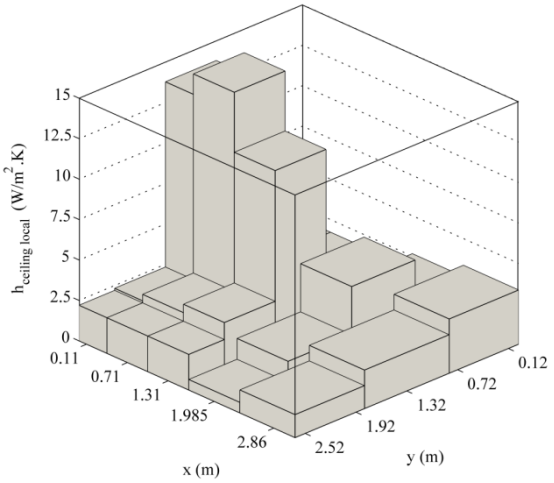

Figure 43: Calculated local convective heat transfer coefficient at the ceiling (slot side-wall diffuser at 6.6 ACH).

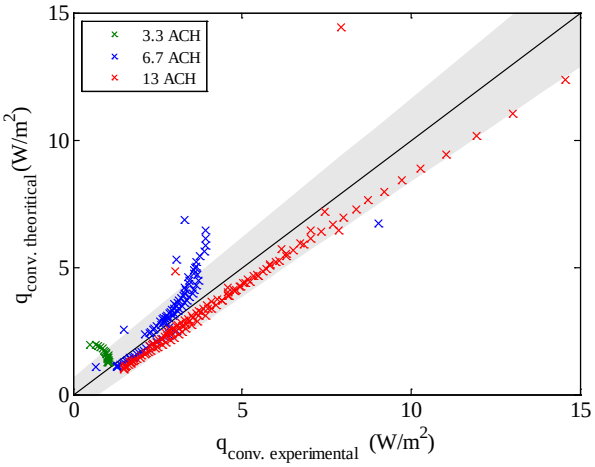

Figure 44: Comparison of the experimental and calculated convective heat flux at the ceiling (Equation 11).

Table 10: Comparison of the measured convective heat transfer with different CHTC correlations (12 hours data).

ACR (h^{-1})	3.3	6.7	6.8	6.6	13.1	13.2	13.1	13.3
ΔT_0 (K)	10.2	2.9	6.1	8.9	2.9	4.0	5.3	9.2
E_{exp} (Wh/m^2)	9.9	24.4	37.9	50.8	44.6	50.1	62.0	102.7
$\Delta E_{Fisher - Exp}$ (%)	900%	17%	74%	123%	-18%	-9%	0%	-1%
$\Delta E_{Fisher \& Pedersen - Exp}$ (%)	1017%	77%	167%	241%	55%	74%	90%	89%
$\Delta E_{Awbi \& Hatton - Exp}$ (%)	65%	-79%	-59%	-42%	-80%	-71%	-66%	-61%
$\Delta E_{Equation\ 11 - Exp}$ (%)	93%	-15%	21%	35%	-21%	-13%	-9%	-11%

3.3. Method 2: Archimedes number (radial diffuser)

The objective of this method is to make use of the Archimedes number to account for the air jet trajectory. This number characterizes the ratio between thermal buoyancy and momentum forces [137] and can be easily calculated by BES tools.

Based on the experimental results (radial diffuser), new correlations including the modified Archimedes number have been developed and validated. The new correlations keep the same structure as Fisher and Pedersen, but include a tuned coefficient, which is function of the modified Archimedes number (Equation 12). The exponent 0.8 associated with the air change rate is equal to the one used by Fisher, who studied convection over a large range of air change rate [118].

$$q_{conv} = \left(a \cdot \frac{T_{outlet} - T_{inlet}}{\dot{V}^2} + b\right) \cdot ACR^{0.8} \cdot \Delta T_{surface-inlet} \qquad (12)$$

The steady-state experiments (with varying air change rate) have been used to derive the coefficients a and b (Table 11 and Figure 45 on the left). It can be observed that the modified Archimedes number influences noticeably the CHTC only for values higher than 1000 K.s^2/m^6. The effect of the air jet trajectory has the opposite effect at the ceiling and at the floor. In fact, if the jet is dropping from the ceiling, the convective heat exchange is decreasing at the ceiling and increasing at the floor. Nevertheless, the coefficient a at the floor is lower than the absolute value at the ceiling due to the "mixing losses" between the top of the room and the floor. The walls did not show any strong dependency on the jet behaviour. It has to be noted that the negative coefficient a at the ceiling has a similar effect as the method of Jensen [121], which is adjusting the area affected by forced convection depending on the air jet trajectory.

Table 11: CHTC at the different surfaces with the active chilled beam (Equation 12).

Surface type	a	b	$a_{Fisher \& Pedersen}$ (for comparison)	$b_{Fisher \& Pedersen}$ (for comparison)
Ceiling	$-1.5 \cdot 10^{-5}$	0.19	0	0.49
Walls	0	0.15	0	0.19
Floor	$4.1 \cdot 10^{-6}$	0.14	0	0.13

The results of the dynamic experiments have then been used to validate the correlations developed (Figure 45 on the right). From the figure, it can be observed that the derived correlations improve the accuracy and the consistency of the calculation. The modified Archimedes number seems to be the right indicator of the jet behaviour, as the results from the steady-state experiments (varying $\dot{V}$) are in good agreement with the results from the dynamic experiments (varying $T_{outlet} - T_{inlet}$). The accuracy of the derived correlations has been estimated to ± 15 % with a minimum uncertainty on the derived convective heat flux equal to 1 W/m^2.

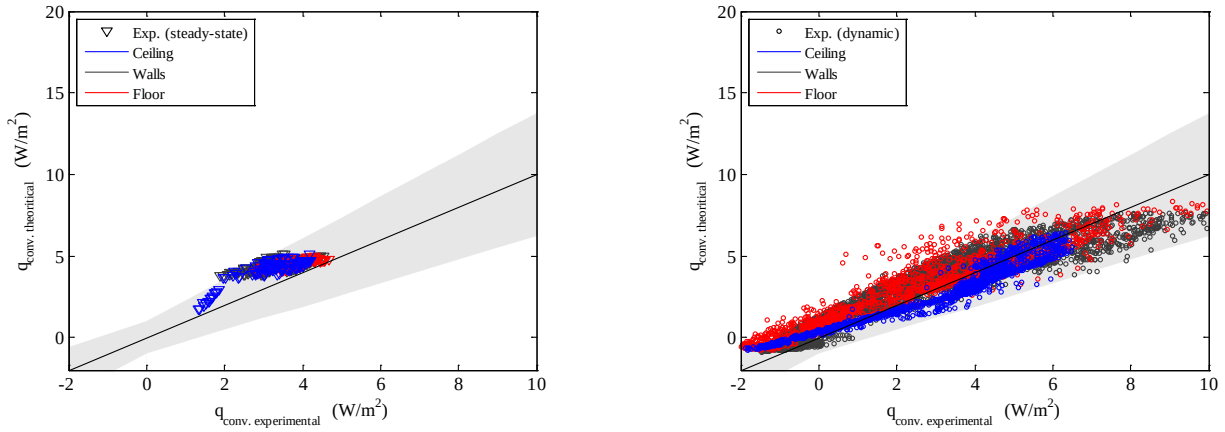

Figure 45: Comparison of the calculated (Equation 12) and measured convective heat flux at the different surfaces of the test room (steady-state experiments on the left / dynamic experiments on the right).

4. Convective heat transfer with cooling from radiant wall

In this part, the interaction between ventilation system and radiant wall and the accuracy of forced correlations when the inlet air temperature is close to the surface temperature will be evaluated. The experimental results from the outdoor full-scale facility will be used (radial diffuser).

The convective flow with the cooled wall is more complex than with air-based terminals as no main driving force exists. At the ceiling, the flow is dominated by the inlet momentum, but it can also be affected by the thermal plume from the window. The convective flow at the walls, except the activated wall, is also driven by the inlet momentum. The flow at the cooled wall is mainly driven by buoyancy forces, even though an influence of the inlet momentum has been observed (Figure 47). Finally, the convective heat transfer at the floor is probably the most complicated, as it is driven by the cold down-draught from the radiant wall, by the inlet momentum and also by the direct solar radiation.
Mixed convection correlations will thus be used to analyse the results. Instead of using mixed correlations, a selection of the convection algorithm based on the Richardson number has also been tested, but the discrepancy between experimental and theoretical results was larger.

The convective heat flux measured experimentally has been compared to the convective heat flux derived from mixed correlations (Figure 46). The mixed correlations have been calculated using the data from Alamdari and Hammond for natural convection [127] and Equation 12 with a blending coefficient $n = 6$. This coefficient will act as a selector between the two types of convective flow [31, 38]. Two special features have been used to improve the fitting between the experimental and theoretical data:

- The air temperature is modified to account for the air temperature gradient in the calculation of CHTCs. This temperature gradient is up to 1 K between the floor and the ceiling for a cooling power of 40 W/m^2 (Part II).
- Due to the presence of direct solar radiation on some surfaces, the convective flux has been calculated for each section instead of each surface. Local variations of surface temperatures are as such taken into consideration.

First of all, it can be observed that the uncertainty on the derived convective heat flux is much larger than for the active chilled beam (Figure 45). This is due to the lower temperature difference between the surfaces and the reference and also due to the large conductive heat flux at the cooled wall. A relatively large discrepancy can be observed at the floor due to the reference temperature used. In fact, the convective heat transfer is influenced by both the inlet air temperature and the cold air temperature flowing down the activated wall. At the ceiling, the convective heat transfer is overestimated, as it does not account for the locally warmer air close to the window. But it must be noted that the convective heat transfer at the cooled wall is relatively well modelled using the equation of Alamdari and Hammond [127]. As this surface has the largest share in the total convective flow from the room, it will result in a rather accurate estimation of convection despite the large scattering at other surfaces.

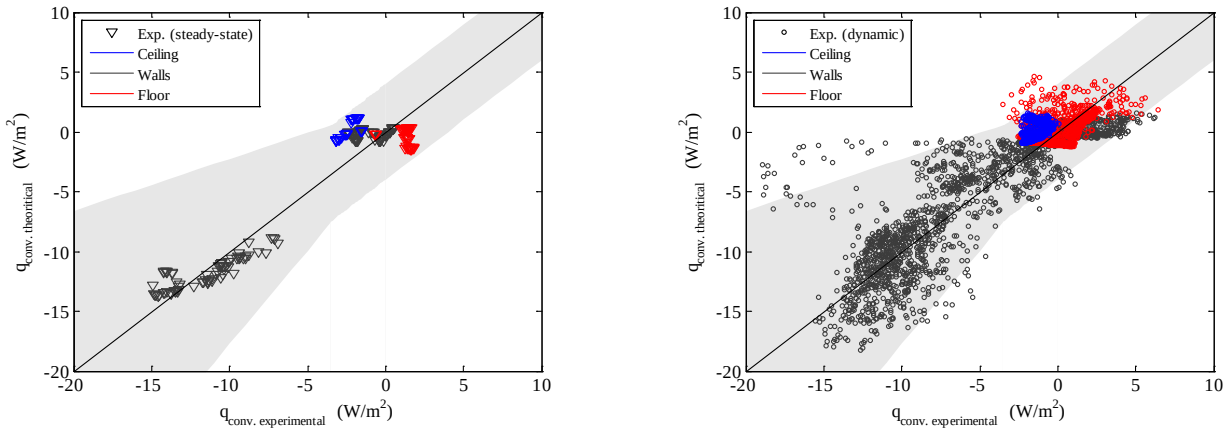

Figure 46: Comparison of the calculated (Alamdari & Hammond [127] blended with Equation 12) and measured convective heat flux at the different surfaces of the test room.

The CHTCs at the cooled wall have been expressed as a function of the temperature difference between the local air and the wall (Figure 47). As suggested by Figure 46, the convective heat transfer at the cooled wall is well modelled using the correlation of Alamdari and Hammond. Only when the temperature difference is lower than 3 K, the correlation does not fit because the convective heat transfer is driven by the inlet momentum (Richardson number lower than 4). On this figure, the effect of solar patches on the considered surface can also be observed. The convective heat transfer decreases due to the upward convective flow from the heated patches, which slows down and warms up the downward convective flow.
Finally, the effect of different air change rate has been tested. The points located inside the black circle correspond to the CHTCs obtained when increasing the air change rate from 2.2 ACH up to 3.6 ACH (Figure 47). The convective heat transfer is still dominated by natural convection and the correlations from Alamdari and Hammond model the convective heat transfer with a reasonable accuracy.

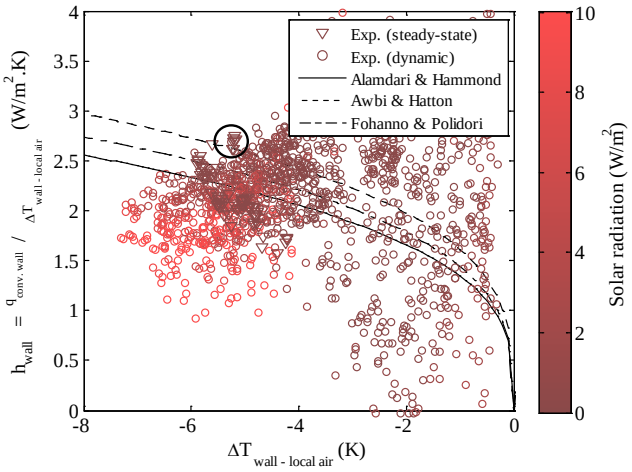

Figure 47: CHTCs at the radiant wall depending on the temperature difference between the surface and the local air.

5. Conclusion

Full-scale experiments in two test facilities have been performed to derive CHTCs for different types of diffusers and cooling terminals. The experimental set-ups proved to be accurate enough in both cases with an error on the heat balance of ± 17-18 % for hourly-averaged data. The experiments under both steady-state and dynamic conditions (with solar radiation entering the test room) have been used to derive CHTCs. So far, most of the research was focussed on steady-state analysis, disregarding the convective heat transfer at low heat load. This contribution analyses the convective flow over a longer period of time and, therefore, for a wide range of heat loads (intensity and repartition) and surface temperatures. Variations of the inlet air temperature and the air change rate have also been performed.

In a first part, the convective flow with air-based cooling systems has been investigated for two types of diffusers: slot side-wall diffuser and radial diffuser (active chilled beam). The convective flow with these cooling systems is dominated by forced convection and is relatively well-shared among the surfaces. The comparison with existing models pointed out the specificity of existing correlations and the limitation of their range of application. Because of differences in the air jet trajectory, existing correlations tend to overestimate the convective flow from the test room, especially at the ceiling (Figure 40 and Figure 42). Therefore, two approaches have been tested:

- One solution to overcome this problem could be to use local values of air velocity (Equation 11). This alternative way of deriving CHTCs has been investigated theoretically by Alamdari and Hammond [127]. Experimental results showed relatively accurate predictions (Figure 44). In practise, CHTC could be estimated for different types of inlet, providing local velocity data from the flow theory. This will require a better integration of the flow characteristics in the building simulation programs, but the complexity of this task would be limited as the surface of interest is only the one directly affected by the inlet air, avoiding the complexity of dealing with recirculation.
- Another solution tested is to include a modified Archimedes number in the correlations, in order to account for the jet behaviour (Equation 12 and Table 11). The convective heat flux calculated with the new correlations is in good agreement with experimental results (Figure 45) with an accuracy estimated to ± 15 % (and minimum uncertainty on the convective heat flux equal to 1 W/m^2). These correlations are valid under cooling conditions with the inlet located in the middle of the ceiling. Before implementing these correlations in BES tools, further validations are needed for other types and positions of inlet and other room geometries.

The convective flow with the radiant cooling system is more complex to study, due to the higher uncertainty on the derived CHTCs and also due to the complexity of the flow in the room. The cooled wall is dominated by natural convection, but the influence of forced convection has been observed when the temperature difference between the surface and the air is below 3 K, i.e. when the Richardson number is lower than 4 (Figure 47). The other surfaces are dominated by forced convection, but no accurate match between existing correlations and measured convective fluxes has been achieved. The largest scattering has been observed at the floor, where the convective flow is influenced by both the inlet and the down-draught from the cooled wall. The analysis also pointed out the importance of accounting for the air temperature gradient and the solar patches in the calculation of convection.

For further information, the reader can refer to Paper 5:
"Experimental investigation of convective heat transfer during night cooling with different ventilation systems and surface emissivities"

& Paper 6:
"Experimental investigation of the influence of the air jet trajectory on convective heat transfer with air-based and radiant cooling systems"

Conclusion of the thesis

This thesis presented various studies that aimed at characterising the comfort condition and energy need of radiant and air-based terminals. This work focussed on the energy performance in terms of delivered energy and not in terms of primary energy. The analysis was based on both numerical studies and full-scale experiments of office rooms. As the heating case has not been investigated in details, the conclusion will only address the cooling case. In addition to comparing the effectiveness of different terminals, the heat transfer in the space and the interaction between ventilation system and terminal have been investigated.

In the steady-state numerical analysis, the sensitivity of radiant and air-based terminals has been evaluated for different parameters. The difference between the two types of terminals is mainly due to changes in the ventilation losses (or gains). At low air-change rates (below 0.5 ACH), radiant and air-based terminals have similar energy needs. For higher air change rates, the energy need of radiant terminals is lower than that of air-based terminals (Figure 14). In fact, the ventilation losses are higher for radiant terminals due to the higher air temperature. For example, the cooling need of the radiant floor is 15 % lower than that of the active chilled beam at 2 ACH. Therefore, radiant cooling systems have a large potential of energy savings for buildings with high ventilation rates (e.g. shops, train station, industrial storage). From this study, it has also been observed that a vertical air temperature gradient greatly affects the cooling need (Figure 15). At 2 ACH, the cooling need of the terminal decreases by 15 % if a temperature gradient of 4 K is achieved between the floor and the ceiling. For the geometry considered, only small differences have been observed among radiant terminals when the occupants are standing. If the occupants are assumed to be sitting, the large view factor with floor can lead to a reduction of the energy need for floor cooling.
The performances of the active chilled beam and the radiant wall have then been tested in a full-scale test facility under different boundary conditions (steady-state and dynamic) and also different levels and types of heat loads. The experiments have confirmed the numerical analysis. The energy savings of a radiant wall compared to the active chilled beam can be estimated to around 10 % due to higher ventilation losses. The experimental results have also proved the importance of accounting for the air flow pattern in the calculation of the ventilation losses (or gains). The asymmetry between air and radiant temperature, the air temperature gradient and the possible short-circuit between inlet and outlet must be included in the heat balance in order to accurately model the different terminals. In these experiments, the three parameters played an equally important role in decreasing the cooling need of the radiant wall compared to the active chilled beam (Figure 34). The importance of accounting for air temperature stratification had already been pointed out in the work from the Annex 21, when comparing experimental and simulated heating need [138].
These conclusions on radiant and air-based terminals are valid for multi-storey or well-insulated buildings ($R > 5$ m^2.K/W). If a single storey-building with a low level of insulation is studied, the effectiveness of radiant terminal will decrease due to the larger back losses and an air-based terminal might become more energy-efficient than a radiant terminal in terms of delivered energy (Figure 23).

Regarding comfort, the radiant wall and the active chilled beam achieve similar global level of comfort in both numerical and experimental investigations. But due to the limited cooling capacity of the two systems, overheating has been observed with the two terminals during the dynamic experiments.
Variation of comfort in the space has been investigated numerically (Table 9). The active chilled beam theoretically achieves the most uniform comfort conditions (when disregarding the risk of draught), followed by the radiant ceiling. The least uniform conditions were obtained with the cooled floor, due to large differences between the sitting and standing positions. Local comfort conditions (radiant asymmetry, vertical air temperature gradient, risk of draught) have been evaluated both theoretically and numerically and no discomfort has been observed.

Figure 48 summarizes the advantages and drawbacks of terminals for cooling. Both energy and comfort parameters have been taken into account.

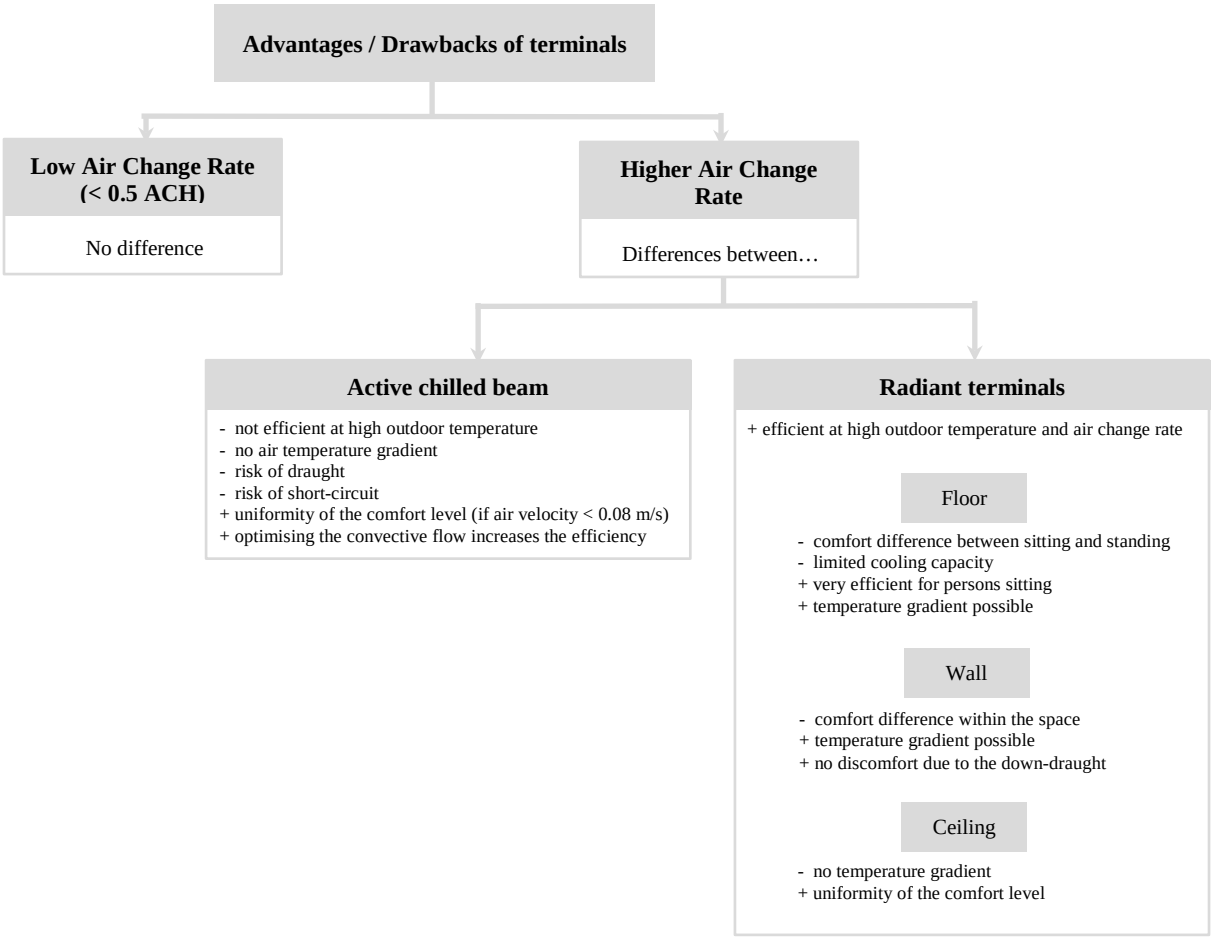

Figure 48: Advantages and drawbacks of terminals for cooling, + sign indicating advantages, - sign indicating drawbacks (valid for multi-storey or highly insulated buildings, R > 5 m^2.K/W)

The last part of the thesis focussed on characterising the convective heat transfer for different types of air flow and cooling systems. Convective heat transfer has a large influence on the asymmetry between surfaces and air temperature and thus on the terminal effectiveness (Figure 16). Additionally, convective heat transfer coefficients (CHTCs) have been identified as one of the main sources of uncertainty in BES tools. Based on two different experimental set-ups, the range of application of existing correlations has been tested. It has been observed that existing correlations for forced convection are specific to the case for which they have been developed and can lead to a relatively large error when the air flow pattern is different. The type of inlet, the inlet air temperature and the air change rate have a large influence on the convective heat transfer. Two approaches have been tested to better account for the air flow pattern in the definition of CHTC. In a first method, local values of air velocity are used to evaluate convection at the ceiling (Figure 44). This method results in a more accurate evaluation of convection with an average error of ± 17 %. The main drawback of this method is that the air flow pattern has to be evaluated using either flow element theory or CFD. An alternative approach consists in including a modified Archimedes number in the definition of CHTCs (Figure 45). Correlations have been developed for the radial inlet and a relatively good accuracy has been observed (± 15 % with a minimum uncertainty of 1 W/m^2).

When the space is cooled down with a radiant terminal, the accurate definition of CHTCs is more difficult due to the complexity of the flow pattern and the absence of a dominating effect (i.e. buoyancy or momentum). Forced correlations can be used at all surfaces except at the activated panels. For this surface, natural convection is dominating and the correlations from Alamdari and Hammond are suitable for modelling the convective heat transfer.

Finally, the study about CHTCs validates the base model (Alamdari and Hammond) used in the numerical comparison of radiant and air-based terminals (Part I). Using the forced convection correlations of Fisher and Pedersen would have led to an overestimation of the convective exchange at the surfaces for usual range of air change rates.

Future work

In order to better understand radiant terminals, further investigations are required. Similarly to the work of Fontana [139], a quantification of the effect of furniture on the effectiveness of radiant terminals is needed. In fact, obstruction between the activated surface and the occupant might lead to an increase of the cooling need of radiant terminals. This parameter has not been accounted for in this thesis.
In addition to steady-state analysis, a better characterisation of radiant systems under dynamic conditions is also required. This aspect is especially important when there is a strong thermal coupling between the radiant terminal and the structure of the building (e.g. for floor cooling systems).

Additional work is also required to improve the modelling of terminals, both in simplified and more advanced tools. A simplified calculation tool could be developed to assess the most efficient solution (radiant or air-based) depending on the geometry, the thermal insulation of the building and the characteristics of the ventilation system. This tool could be used for assessing different renovation strategies and also for countries, where the level of insulation is relatively low.
A more accurate modelling of the air temperature distribution in the space is also required for improving the accuracy of BES tools. It has been observed that the air temperature gradient and the shortcut between inlet and outlet play an important role in the space heat balance. Several studies have already been performed to characterise the vertical air temperature gradient with different ventilation and cooling/heating systems. The different correlations should be reviewed and tested with the objective of implementing them in design or BES tools.

Finally, more studies about convective heat transfer are needed. Forced convection and especially the influence of the air jet trajectory are still ill-defined. Gathering different experimental results would probably facilitate the comparison and the development of other algorithms. The integration of the jet theory in the calculation of CHTCs should also be tested against experimental data. More information on the airflow could be obtained by performing CFD simulations of the experimental cases.

References

[1] EC (European Commission), Communication from the Commission. Action Plan for Energy Efficiency, Realizing the Potential. (2006).

[2] V. Badescu, B. Sicre, Renewable energy for passive house heating: Part I. Building description, Energy Build. 35 (2003) 1077-1084.

[3] J. Babiak, B.W. Olesen, D. Petras, Low temperature heating and high temperature cooling, REHVA Guidebook Nbr. 7 (2007).

[4] B.W. Olesen, Radiant heating and cooling by embedded water-based systems, ASHRAE Trans. (2006).

[5] G. Hauser, C. Kempkes, B.W. Olesen, Computer simulation of the performance of a hydronic heating and cooling system with pipes embedded into the concrete slab between each floor, ASHRAE Trans. 106 (2000) 702-712.

[6] C. Roulet, J. Rossy, Y. Roulet, Using large radiant panels for indoor climate conditioning, Energy Build. 30 (1999) 121-126.

[7] R. Bean, B.W. Olesen, K.W. Kim, History of Radiant Heating & Cooling Systems: Part 1, ASHRAE J. 52 (2010) 40-41.

[8] R. Bean, B.W. Olesen, K.W. Kim, History of Radiant Heating & Cooling Systems: Part 2, ASHRAE J. 52 (2010) 50-55.

[9] M. De Carli, A. Zarrella, R. Zecchin, Comparison Between a Radiant Floor and Two Radiant Walls on Heating and Cooling Energy Demand, ASHRAE Trans. 115 (2009) 563.

[10] W. Kessling, S. Holst, M. Schuler, Innovative design concept for the new Bangkok international airport, NBIA (2004).

[11] J. Feng, S. Schiavon, F. Bauman, Cooling load differences between radiant and air systems, Energy Build. 65 (2013) 310-321.

[12] B. Lehmann, V. Dorer, M. Koschenz, Application range of thermally activated building systems tabs, Energy Build. 39 (2007) 593-598.

[13] K. Roth, J. Dieckmann, R. Zogg, J. Brodrick, Chilled beam cooling, ASHRAE J. 49 (2007) 84.

[14] B. Glück, Wärmeübertragung, Wärmeabgabe von Raumheizflächen und Rohren, VEB Verlag für Bauwesen. Berlin. (1989).

[15] M. Scarpa, K. Grau, B.W. Olesen, Development and validation of a versatile method for the calculation of heat transfer in water-based radiant systems, Eleventh International IBPSA Conference, Glasgow, Scotland (2009).

[16] EN 15377-1:2008 - Heating systems in buildings - Design of embedded water based surface heating and cooling systems - Part 1: Determination of the design heating and cooling capacity (2008).

[17] M. Koschenz, B. Lehmann, Thermoaktive Bauteilsysteme TABS, EMPA (2000).

[18] T. Weber, G. Jóhannesson, An optimized RC-network for thermally activated building components, Build. Environ. 40 (2005) 1-14.

[19] M.J. Ren, J.A. Wright, A ventilated slab thermal storage system model, Build. Environ. 33 (1998) 43-52.

[20] X. Xu, S. Wang, J. Wang, F. Xiao, Active pipe-embedded structures in buildings for utilizing low-grade energy sources: A review, Energy Build. 42 (2010) 1567-1581.

[21] R.K. Strand, C.O. Pedersen, Implementation of a radiant heating and cooling model into an integrated building energy analysis program, ASHRAE Trans. (1997).

[22] M. De Carli, M. Scarpa, R. Tomasi, A. Zarrella, DIGITHON: A numerical model for the thermal balance of rooms equipped with radiant systems, Build. Environ. 57 (2012) 126-144.

[23] EN 1264-2:2008, Water based surface embedded heating and cooling systems - Part 2: Floor heating: Prove methods for the determination of the thermal output using calculation and test methods (2008).

[24] A. Laouadi, Development of a radiant heating and cooling model for building energy simulation software, Build. Environ. 39 (2004) 421-431.

[25] P. Stefanizzi, A. Wilson, A. Pinney, Internal long-wave radiation exchange in buildings: Comparison of calculation methods: II Testing of algorithms, Building Services Engineering Research and Technology. 11 (1990) 87-96.

[26] J. Le Dréau, P. Heiselberg, R.L. Jensen, Experimental investigation of convective heat transfer during night cooling with different ventilation systems and surface emissivities, Energy Build. 61 (2013) 308-317.

[27] CIBSE Guide A, Environmental design, Chartered Institution of Building Services Engineers, London, UK (1999).

[28] J. Crabol, Transfert de Chaleur: Applications Industrielles, Tome 2, Masson, Paris (1990).

[29] J. Clarke, Energy Simulation in Building Design (second ed.), 7 – Energy-related subsystems, Butterworth-Heinemann, Oxford (2001) 202-280.

[30] A. Chapman, Fundamentals of Heat Transfer, 4th edition, New York, McMillan (1984).

[31] L. Peeters, I. Beausoleil-Morrison, A. Novoselac, Internal convective heat transfer modeling: Critical review and discussion of experimentally derived correlations, Energy Build. 43 (2011) 2227-2239.

[32] K. Goethals, M. Delghust, G. Flamant, M. De Paepe, A. Janssens, Experimental investigation of the impact of room/system design on mixed convection heat transfer, Energy Build. 49 (2012) 542-551.

[33] S.W. Churchill, R. Usagi, A general expression for the correlation of rates of transfer and other phenomena, American Institute of Chemical Engineers Journal. 18 (1972) 1121-1128.

[34] I. Beausoleil-Morrison, The adaptive coupling of heat and air flow modelling within dynamic whole-building simulation, PhD Thesis, University of Strathclyde Glasgow (2000).

[35] A. Novoselac, B.J. Burley, J. Srebric, New convection correlations for cooled ceiling panels in room with mixed and stratified airflow, HVAC&R Research. 12 (2006) 279-294.

[36] L. Neiswanger, G.A. Johnson, V.P. Carey, An Experimental Study of High Rayleigh Number Mixed Convection in a Rectangular Enclosure With Restricted Inlet and Outlet Openings, J. Heat Transfer. 109 (1987) 446-453.

[37] H.B. Awbi, A. Hatton, Mixed convection from heated room surfaces, Energy Build. 32 (2000) 153-166.

[38] A. Novoselac, B.J. Burley, J. Srebric, Development of new and validation of existing convection correlations for rooms with displacement ventilation systems, Energy Build. 38 (2006) 163-173.

[39] P.O. Fanger, Thermal comfort. Analysis and applications in environmental engineering, Danish Technical Press (1970).

[40] EN ISO 7730, Ergonomics of the Thermal Environment-Analytical Determination of Thermal Comfort by Using Calculations of the PMV and PPD Indices and Local Thermal Comfort Criteria (2005).

[41] EN 15251, Indoor environmental input parameters for design and assessment of energy performance of buildings addressing indoor air quality, thermal environment, lighting and acoustics (2007).

[42] EN ISO 7726, Ergonomics of the thermal environment-Instruments for measuring physical quantities (2001).

[43] Q. Chen, Comfort and energy consumption analysis in buildings with radiant panels, Energy Build. 14 (1990) 287-297.

[44] J.A. Myhren, S. Holmberg, Flow patterns and thermal comfort in a room with panel, floor and wall heating, Energy Build. 40 (2008) 524-536.

[45] R.D. Watson, K.S. Chapman, Radiant heating and cooling handbook, McGraw-Hill New York (2002).

[46] B.W. Olesen, Radiant floor heating in theory and practice, ASHRAE J. 44 (2002) 19-26.

[47] R. Zmeureanu, X. Yu Wu, Energy and exergy performance of residential heating systems with separate mechanical ventilation, Energy. 32 (2007) 187-195.

[48] F. Causone, F. Baldin, B.W. Olesen, S.P. Corgnati, Floor heating and cooling combined with displacement ventilation: Possibilities and limitations, Energy Build. 42 (2010) 2338-2352.

[49] B.W. Olesen, E. Mortensen, J. Thorshauge, Thermal comfort in a room heated by different methods, Technical Paper no. 2256, Los Angeles Meeting, ASHRAE Trans. 86 (1980).

[50] J. Hannay, L. Laret, J. Lebrun, D. Marret, P. Nusgens, Thermal comfort and energy consumption in winter conditions. A new experimental approach, ASHRAE Trans. 84 (1978).

[51] R. Howell, S. Suryanarayana, Sizing of radiant heating systems: Part I-Ceiling Panels, ASHRAE Trans. 96 (1990) 562-665.

[52] S. Suryanarayana, R. Howell, Sizing of radiant heating systems, Part II-Heated floors and infrared units, ASHRAE Trans. 96 (1990) 666-675.

[53] C. Inard, A. Meslem, P. Depecker, Energy consumption and thermal comfort in dwelling-cells: A zonal-model approach, Build. Environ. 33 (1998) 279-291.

[54] M. Tye-Gingras, L. Gosselin, Comfort and energy consumption of hydronic heating radiant ceilings and walls based on CFD analysis, Build. Environ. 54 (2012) 1-13.

[55] M. Krajčík, A. Simone, B.W. Olesen, Air distribution and ventilation effectiveness in an occupied room heated by warm air, Energy Build. 55 (2012) 94-101.

[56] R. Tomasi, M. Krajčík, A. Simone, B. Olesen, Experimental evaluation of air distribution in mechanically ventilated residential rooms: Thermal comfort and ventilation effectiveness, Energy Build. 60 (2013) 28-37.

[57] EN 15316-2-1, Heating systems in buildings - Method for calculation of system energy requirements and system efficiencies - Part 2-1: Space heating emission systems (2007).

[58] J. Niu, J.v.d. Kooi, H.v.d. Rhee, Energy saving possibilities with cooled-ceiling systems, Energy Build. 23 (1995) 147-158.

[59] Y. Yao, Z. Lian, W. Liu, Z. Hou, M. Wu, Evaluation program for the energy-saving of variable-air-volume systems, Energy Build. 39 (2007) 558-568.

[60] E. Fabrizio, S.P. Corgnati, F. Causone, M. Filippi, Numerical comparison between energy and comfort performances of radiant heating and cooling systems versus air systems, HVAC&R Research. 18 (2012) 692-708.

[61] G. Salvalai, J. Pfafferott, M.M. Sesana, Assessing energy and thermal comfort of different low-energy cooling concepts for non-residential buildings, Energy Conversion and Management. 76 (2013) 332-341.

[62] T. Imanari, T. Omori, K. Bogaki, Thermal comfort and energy consumption of the radiant ceiling panel system.: Comparison with the conventional all-air system, Energy Build. 30 (1999) 167-175.

[63] M. Brunk, Cooling ceilings-an opportunity to reduce energy costs by way of radiant cooling, ASHRAE Trans. 99 (1993) 479-479.

[64] J.L. Niu, L.Z. Zhang, H.G. Zuo, Energy savings potential of chilled-ceiling combined with desiccant cooling in hot and humid climates, Energy Build. 34 (2002) 487-495.

[65] J. Jeong, S.A. Mumma, W.P. Bahnfleth, Energy conservation benefits of a dedicated outdoor air system with parallel sensible cooling by ceiling radiant panels, ASHRAE Trans. 109 (2003) 627-636.

[66] Z. Tian, J.A. Love, Application of radiant cooling in different climates: assessment of office buildings through simulation, Eleventh International IBPSA Conference, Glasgow, Scotland (2009).

[67] C. Stetiu, Energy and peak power savings potential of radiant cooling systems in US commercial buildings, Energy Build. 30 (1999) 127-138.

[68] B. Olesen, Radiant floor cooling systems, ASHRAE J. 50 (2008) 16-22.

[69] I. Knight, G. Dunn, Measured energy consumption and carbon emissions of air-conditioning in UK office buildings, Building Services Engineering Research and Technology. 26 (2005) 89-98.

[70] D. Alexander, M. O'Rourke, Design considerations for active chilled beams, ASHRAE J. 50 (2008) 50-58.

[71] K. Loudermilk, Designing chilled beams for thermal comfort, ASHRAE J. 51 (2009) 58.

[72] J. Stein, VAV Reheat vs. Active Chilled Beams & DOAS Response, ASHRAE J. 55 (2013) 13-13.

[73] A. Livchak, C. Lowell, Don't turn active beams into expensive diffusers, ASHRAE J. (2012) 52-60.

[74] T. Kim, S. Kato, S. Murakami, J. Rho, Study on indoor thermal environment of office space controlled by cooling panel system using field measurement and the numerical simulation, Build. Environ. 40 (2005) 301-310.

[75] F. Causone, S.P. Corgnati, M. Filippi, B.W. Olesen, Solar radiation and cooling load calculation for radiant systems: Definition and evaluation of the Direct Solar Load, Energy Build. 42 (2010) 305-314.

[76] M. Behne, Indoor air quality in rooms with cooled ceilings.: Mixing ventilation or rather displacement ventilation?, Energy Build. 30 (1999) 155-166.

[77] A. Novoselac, J. Srebric, A critical review on the performance and design of combined cooled ceiling and displacement ventilation systems, Energy Build. 34 (2002) 497-509.

[78] S. Schiavon, F. Bauman, B. Tully, J. Rimmer, Temperature stratification and air change effectiveness in a high cooling load office with two heat source heights in a combined chilled ceiling and displacement ventilation system, UC Berkeley: Center for the Built Environment (2012).

[79] A. Keblawi, N. Ghaddar, K. Ghali, L. Jensen, Chilled ceiling displacement ventilation design charts correlations to employ in optimized system operation for feasible load ranges, Energy Build. 41 (2009) 1155-1164.

[80] S. Schiavon, F. Bauman, B. Tully, J. Rimmer, Room air stratification in combined chilled ceiling and displacement ventilation systems, HVAC&R Research. 18 (2012) 147-159.

[81] S.A. Mumma, B.W. Lee, Extension of the multiple spaces concept of ASHRAE Standard 62 to include infiltration, exhaust/exfiltration, interzonal transfer, and additional short-circuit paths, ASHRAE Trans. 104 (1998) 1232-1244.

[82] J. Jeong, S.A. Mumma, Impact of mixed convection on ceiling radiant cooling panel capacity, HVAC&R Research. 9 (2003) 251-257.

[83] S. Venko, D. Vidal de Ventós, C. Arkar, S. Medved, An experimental study of natural and mixed convection over cooled vertical room wall, Energy Build. 68, Part A (2014) 387-395.

[84] L. Fang, G. Clausen, P.O. Fanger, Impact of Temperature and Humidity on Perception of Indoor Air Quality During Immediate and Longer Whole-Body Exposures, Indoor Air. 8 (1998) 276-284.

[85] D. Kalz, J. Pfafferott, Impact of Cooling on Energy Use, in: , Springer International Publishing, 2014, pp. 1-14.

[86] W. Hoenmann, F. Nuessle, Kuehldecken verbessern Raumklima, Kuehldecke an Raumlueftung, Fachinstitut Gebaeude-Klima eV, Bietigheim-Bissingen, Germany (1991).

[87] F. Sodec, Economic viability of cooling ceiling systems, Energy Build. 30 (1999) 195-201.

[88] J. Adnot, P. Riviere, D. Marchio, S. Becirspahic, C. Lopes, I. Blanco, L. Perez-Lombard, J. Ortiz, N. Papakonstantinou, P. Doukas, Energy efficiency and certification of central air conditioners (EECCAC), Final report. 1 (2003).

[89] L. Pérez-Lombard, J. Ortiz, C. Pout, A review on buildings energy consumption information, Energy Build. 40 (2008) 394-398.

[90] E. Djunaedy, J. Hensen, Q. Chen, M. Loomans, Simulating radiative cooling/heating using BES-CFD coupled simulation, Proceedings Indoor Air (2005).

[91] Danish Building Regulations 01.01.2013 (Bygningsreglementet, in Danish), http://bygningsreglementet.dk/ (2013).

[92] EN 1264-4:2009, Water based surface embedded heating and cooling systems - Part 4: Installation. (2009).

[93] L. Vandaele, P. Wouters, The PASSYS services: Summary report, Belgian Building Research Institute for the European Commission (1994).

[94] EN ISO 13790:2008, Energy performance of buildings - Calculation of energy use for space heating and cooling (2008).

[95] R. Judkoff, J. Neymark, Building energy simulation test (BESTEST) and diagnostic method., International Energy Agency (1995).

[96] T. Blomberg, Heat conduction in two and three dimensions: Computer Modelling of Building Physics Applications, Rapport TVBH. 1008 (1996).

[97] N. Giglioli, A. Saltelli, SimLab 1.1, Software for Sensitivity and Uncertainty Analysis, tool for sound modelling (2000).

[98] P. Heiselberg, Draught risk from cold vertical surfaces, Build. Environ. 29 (1994) 297-301.

[99] H. Karlsson, An innovative floor heating application-transfer of excess heat between two building zones, Proceedings of the 10th International Building Performance Simulation Association Conference and Exhibition (2007).

[100] D. Müller, T. Haase, A. Hoh, T. Tschirner, Absclussbericht – Niedriexergiesysteme für di Heiz- und Raumlufttechnik: Systemuntersuchung. (2008).

[101] SBi, BSim, version 6.11.1.14 (2011).

[102] J. Le Dréau, P. Heiselberg, R.L. Jensen, Experimental data from a full-scale facility investigating radiant and convective terminals : Uncertainty and sensitivity analysis, Description of the experimental data, Aalborg University, DCE Technical Reports No. 168. http://vbn.aau.dk/files/197208203/Experimental_data_from_a_full_scale_facility_investigating_radiant_and_convective_terminals.pdf (2014).

[103] EN ISO 13786, Thermal performance of building components–Dynamic thermal characteristics–Calculation methods (2007).

[104] EN 1264-3, Water based surface embedded heating and cooling systems - Part 3: Dimensioning (2009).

[105] PT Teknik, Comfortina, http://pt-teknik.dk/ (1999).

[106] S. Tanabe, E.A. Arens, F. Bauman, H. Zhang, T. Madsen, Evaluating thermal environments by using a thermal manikin with controlled skin surface temperature, ASHRAE Trans. 100, Part 1 (1994).

[107] L. Schellen, M.G.L.C. Loomans, B.R.M. Kingma, M.H. de Wit, A.J.H. Frijns, W.D. van Marken Lichtenbelt, The use of a thermophysiological model in the built environment to predict thermal sensation: Coupling with the indoor environment and thermal sensation, Build. Environ. 59 (2013) 10-22.

[108] H.O. Nilsson, I. Holmér, Comfort climate evaluation with thermal manikin methods and computer simulation models, Indoor Air. 13 (2003) 28-37.

[109] S.V. Patankar, Numerical heat transfer and fluid flow, Taylor & Francis (1980).

[110] EN 673, Glass in building - Determination of thermal transmittance (U value) - Calculation method (2011).

[111] Lawrence Berkeley Laboratory (LBL), Berkeley, USA, THERM 6.3 - A PC program for analyzing the two-dimensional heat transfer through building products (2012).

[112] H.O. Nilsson, Thermal comfort evaluation with virtual manikin methods, Build. Environ. 42 (2007) 4000-4005.

[113] ASHRAE, ASHRAE Technical Committee 4.7: Energy Calculations, Technical Report June (2004).

[114] P.A. Strachan, G. Kokogiannakis, I.A. Macdonald, History and development of validation with the ESP-r simulation program, Build. Environ. 43 (2008) 601-609.

[115] F. Domínguez-Muñoz, J.M. Cejudo-López, A. Carrillo-Andrés, Uncertainty in peak cooling load calculations, Energy Build. 42 (2010) 1010-1018.

[116] K. Goethals, H. Breesch, A. Janssens, Sensitivity analysis of predicted night cooling performance to internal convective heat transfer modelling, Energy Build. 43 (2011) 2429-2441.

[117] D.E. Fisher, C.O. Pedersen, Convective heat transfer in building energy and thermal load calculations, ASHRAE Trans. 103 (1997) 137-148.

[118] D.E. Fisher, An experimental investigation of mixed convection heat transfer in a rectangular enclosure, PhD Thesis, University of Illinois at Urbana-Champaign (1995).

[119] S. Leenknegt, R. Wagemakers, W. Bosschaerts, D. Saelens, Numerical study of convection during night cooling and the implications for convection modeling in Building Energy Simulation models, Energy Build. 64 (2013) 41-52.

[120] F. Alamdari, G. Hammond, Time-dependent convective heat transfer in warm-air heated rooms, Proc. 3rd Int. Symp. Energy Conservation in the Built Environment, Dublin. 4 (1982) 209-220.

[121] R.L. Jensen, Modellering af naturlig ventilation og natkøling - ved hjælp af ringmetoden (in Danish), PhD Thesis, Center for Hybrid Ventilation, Aalborg University (2005).

[122] H.B. Awbi, A. Hatton, Natural convection from heated room surfaces, Energy Build. 30 (1999) 233-244.

[123] A.J.N. Khalifa, R.H. Marshall, Validation of heat transfer coefficients on interior building surfaces using a real-sized indoor test cell, Int. J. Heat Mass Transfer. 33 (1990) 2219-2236.

[124] J. Spitler, C. Pedersen, D. Fisher, Interior convective heat transfer in buildings with large ventilative flow rates, ASHRAE Trans. 97 (1991) 505-515.

[125] K. Goldstein, A. Novoselac, Convective Heat Transfer in Rooms with Ceiling Slot Diffusers (RP-1416), HVAC&R Research. 16 (2010) 629-655.

[126] P. Wallentén, Convective heat transfer coefficients in a full-scale room with and without furniture, Build. Environ. 36 (2001) 743-751.

[127] F. Alamdari, G.P. Hammond, Improved data correlations for buoyancy-driven convection in rooms, Building Services Engineering Research and Technology. 4 (1983) 106-112.

[128] ASHRAE, ASHRAE – Handbook Fundamentals – Chapter 4: Heat Transfer, American Society of Heating, Refrigeration and Air-Conditioning Engineers Inc., Atlanta, GA. (2009).

[129] N. Artmann, R.L. Jensen, H. Manz, P. Heiselberg, Experimental investigation of heat transfer during night-time ventilation, Energy Build. 42 (2010) 366-374.

[130] E. Djunaedy, J. Hensen, M. Loomans, External coupling between CFD and energy simulation: implementation and validation, ASHRAE Trans. 111 (2005) 612-624.

[131] Z.J. Zhai, Q.Y. Chen, Performance of coupled building energy and CFD simulations, Energy Build. 37 (2005) 333-344.

[132] M. Mirsadeghi, B. Blocken, J. Hensen, Validation of external BES-CFD coupling by inter-model comparison, 29th AIVC Conference (2008) 14-16.

[133] T. Min, L. Schutrum, G. Parmelee, J. Vouris, Natural convection and radiation in a panel heated room, ASHRAE Trans. 62 (1956) 337-358.

[134] S.R. Delaforce, E.R. Hitchin, D.M.T. Watson, Convective heat transfer at internal surfaces, Build. Environ. 28 (1993) 211-220.

[135] C. Qingyan, C.A. Meyers, J. van der Kooi, Convective heat transfer in rooms with mixed convection, International Seminar on Air Flow Patterns in Ventilated Spaces, Liège, Belgium (1989) 69.

[136] EN 12238:2001 , Ventilation for buildings - Air terminal devices - Aerodynamic testing and rating for mixed flow application (2001).

[137] D. Müller, R. Kosonen, C. Kandzia, A.K. Melikov, P.V. Nielsen, Mixing Ventilation - Guidebook on mixing air distribution design, REHVA Guidebook Nbr. 19, REHVA (2013).

[138] K.J. Lomas, H. Eppel, C. Martin, D. Bloomfield, Empirical validation of thermal building simulation programs using test room data, vols. 1-2: Final Report, Annex 21 and IEA Solar Heating and Cooling Programme Task 12 (1994).

[139] L. Fontana, Thermal performance of radiant heating floors in furnished enclosed spaces, Appl. Therm. Eng. 31 (2011) 1547-1555.

Publications for the thesis

- Paper 1: Le Dréau J., Heiselberg P. “Potential use of radiant walls to transfer energy between two building zones”. Proceedings of ISHVAC. Vol. 1 Tsinghua University Press, 2011. p. 120-126.

- Paper 2: Le Dréau J., Heiselberg P. “Comparison of the thermal performances of radiative and convective terminals: A conceptual approach”. PLEA 2012 Lima Peru - Opportunities, Limits & Needs: Towards an environmentally responsible architecture. 2012.

- Paper 3: Le Dréau J., Heiselberg P. “Sensitivity analysis of the thermal performance of radiative and convective terminals”. Energy and Buildings 82, 2014. p. 482-491.

- Paper 4: Le Dréau J., Heiselberg P., Jensen R.L. “A full-scale experimental set-up for assessing the energy performance of radiant wall and active chilled beam for cooling buildings”. Building Simulation: An International Journal, 2014.

- Paper 5: Le Dréau J., Heiselberg P., Jensen R.L. "Experimental investigation of convective heat transfer during night cooling with different ventilation systems and surface emissivities”. Energy and Buildings 61, 2013. p. 308-317.

- Paper 6: Le Dréau J., Heiselberg P., Jensen R.L. “Experimental investigation of the influence of the air jet trajectory on convective heat transfer with air-based and radiant cooling systems”. Journal of Building Performance Simulation, 2014.

Other publications

(Available online on http://vbn.aau.dk)

- Paper: Le Dréau J., Karlsen L.R., Litewnicki M., Michaelsen L., Møllerskov A., Ødegaard H., Svendsen L., Jensen R.L., Marszal A.J. “Experimental Investigation of the Influence of Different Flooring Emissivity on Night-Time Cooling using Displacement Ventilation”. Proceedings of the 9th Nordic Symposium on Building Physics: NSB 2011. ed. / J. Vinha; J. Piironen; K. Salminen. Vol. Volume 1 Tampere, Finland : Tampere University Press, 2011. p. 491-498.

- Paper: Le Dréau J., Heiselberg P., Jensen R.L., Selman A.D. “Modelling The Energy Performance Of Night-Time Ventilation Using The Quasi-Steady State Calculation Method”. Building Simulation 2013: BS2013. 2013. p. 3307-3313.

- Report: Le Dréau J., Heiselberg P., Jensen R.L., Selman A.D. “Thermal Mass & Dynamic Effects Danish Building Regulation”. Aalborg University. Department of Civil Engineering, 2013. 93 p. (DCE Technical Reports; No. 152).

- Report: Le Dréau J., Heiselberg P., Jensen R.L., “Experimental data from a full-scale facility investigating radiant and convective terminals : Uncertainty and sensitivity analysis, Description of the experimental data”. Aalborg University. Department of Civil Engineering, 2014. 32 p. (DCE Technical Reports; No. 168).

Paper 1

Potential use of radiant walls to transfer energy between two building zones

ISHVAC 2011 - 7th International Symposium on Heating, Ventilation and Air Conditioning – Shanghai, China 6-9 November 2011

POTENTIAL USE OF RADIANT WALLS TO TRANSFER ENERGY BETWEEN TWO BUILDING ZONES

J. Le Dréau[1,*], P. Heiselberg[1]

[1] Department of Civil Engineering, Aalborg University
9000 Aalborg, Denmark

ABSTRACT
Due to a reduced energy demand in low energy buildings, low temperature heating and high temperature cooling can be used to control thermal comfort. Nevertheless, highly varying heat loads due to solar radiation can create sometimes an imbalanced energy demand inside the building. Instead of being considered as a disturbance, this asymmetry can be used as a heat source for another zone of the building. By means of computer simulations, the possibility of shifting the energy demand between two office rooms with different thermal loads has been studied. Due to the small temperature difference between the two zones, capillary tubes embedded in the surface of walls are used to exchange heat from a south-facing room to a north-facing room. In addition to having a better indoor climate, the total heating and cooling consumption decreases when running the system. A comparison has also been performed with a system exchanging room air directly.

KEYWORDS
Capillary pipes, Interzonal heat transfer, Radiant cooling, Solar radiation, Air exchange

ISBN: 978-962-85138-0-2

POTENTIAL USE OF RADIANT WALLS TO TRANSFER ENERGY BETWEEN TWO BUILDING ZONES

J. Le Dréau[1,*], P. Heiselberg[1]

[1] Department of Civil Engineering, Aalborg University
9000 Aalborg, Denmark

ABSTRACT
Due to a reduced energy demand in low energy buildings, low temperature heating and high temperature cooling can be used to control thermal comfort. Nevertheless, highly varying heat loads due to solar radiation can create sometimes an imbalanced energy demand inside the building. Instead of being considered as a disturbance, this asymmetry can be used as a heat source for another zone of the building. By means of computer simulations, the possibility of shifting the energy demand between two office rooms with different thermal loads has been studied. Due to the small temperature difference between the two zones, capillary tubes embedded in the surface of walls are used to exchange heat from a south-facing room to a north-facing room. In addition to having a better indoor climate, the total heating and cooling consumption decreases when running the system. A comparison has also been performed with a system exchanging room air directly.

KEYWORDS
Capillary pipes, Interzonal heat transfer, Radiant cooling, Solar radiation, Air exchange

INTRODUCTION
In order to fulfil the EU objectives regarding climate changes and energy efficiency, Denmark has planned to reduce the energy demand of new buildings by 2020 by 66% compared to the present energy regulation (71 kWh/m^2 per year) (EBST 2009). Better insulated walls and intelligent glazed façades will be required to decrease heat losses. Moreover the performance of the heating and cooling systems can be improved through the application of low temperature heating and high temperature cooling.
The focus of this paper will be on developing a new heating and cooling system, capable as well of transferring energy inside the building thanks to a smart hydraulic layout. The south-facing rooms of office buildings are frequently overheated during daytime because of high solar heat gains. In low energy buildings, this load can be used as a heat source for the north-facing room, which is usually colder because it is unaffected by the direct solar radiation. This kind of system is therefore taking advantage of the asymmetry of the building loads, instead of considering it as a disturbance. During the winter season, the transfer of energy aims at heating the north-facing room, whereas this energy shifting will have the purpose of cooling the south-facing room during the summer season.
Karlsson (2007) has studied the possibility of transferring excess heat between two rooms via a floor heating system. The building located in Sweden had a highly glazed facade (56%) but no shading was applied. When running the system, the heating consumption decreased of 2.8% during the months of March and April. Another way of transferring energy between rooms with different heat loads is to use a surface system composed of capillary tubes, embedded at the inner surface of walls. The studies on this new technology are relatively recent: Glück (2003) has investigated the thermal and energetic properties of such a system, and Müller et al. (2008) has studied experimentally different configurations of capillary mats

* Corresponding e-mail: *jld@civil.aau.dk*

(floor, walls, ceiling) to transfer energy between two rooms. The experiments showed that up to 70% of the load difference (34 W/m^2) can be compensated thanks to the energy shifting.

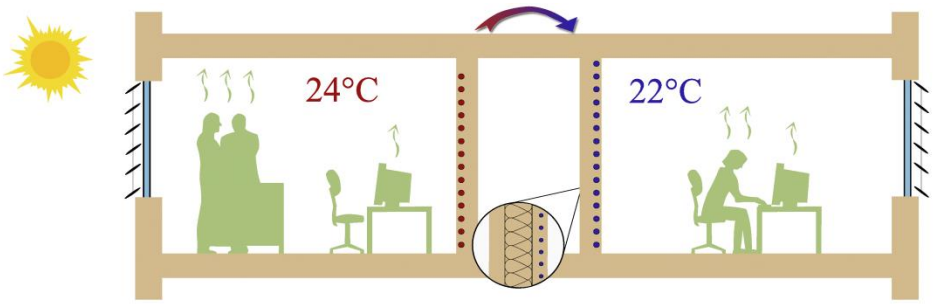

***Figure 1**. The concept of interzonal heat transfer applied to an office building.*

In the study case, a system which can harness low temperature difference is needed. Therefore this paper will be focused on the potential of using a surface system embedded in walls (cf. figure 1). In the first part, the building studied will be presented, especially its thermal characteristics; the model used and its assumptions will be detailed. Then the potential of this system will be investigated. Finally the potential of shifting energy in another type of building will be analysed, and a comparison with a direct air exchange will be performed.

METHOD

Presentation of the study case

In order to assess the potential of interzonal heat transfer, an office building has been considered. The characteristics of the building have been chosen similar to the one studied by Winther et al. (2010) in his report about intelligent glazed facades. The office is located in Denmark and the meteorological ambient boundary conditions correspond to the weather conditions in Copenhagen for the Design Reference Year. The time of occupancy of the building is Monday to Friday, from 8am to 5pm; holidays are not considered

Two office rooms, one facing the south and another one facing the north, represent the energy consumption of the whole building. The floor area of each office is equal to 26 m² and 77% of the façade is glazed. The surrounding offices are assumed to be at the same temperature, so that there is no heat loss through the internal walls and floors. The building components are characteristic of a low energy building, respecting the Danish Building Regulation 2020 (i.e. consuming less than 25 kWh/m² per year for heating, cooling, ventilation, lighting and domestic hot water). The external walls are insulated with 20 cm of glass wool, and the overall U-value of the window is equal to 0.7 W/m².K. The building thermal mass is equal to 80 Wh/K.m², which corresponds to a medium light construction; the construction with the highest thermal mass is the ceiling, with 10 cm of exposed concrete.

Moreover a dynamic control of the windows has been set up, so that heat losses and heat gains are optimised. The shadings can be activated during the day if the operative temperature is getting close to the upper bound of the comfort range; nevertheless they are never fully closed, so that the daylight level should be sufficient enough to work without artificial lighting. The shutters (R = 5 K.m²/W) are activated outside the period of occupancy, when the outside temperature is below 20°C. Thanks to this intelligent control of windows, a dynamic average U-value of the external envelope (wall & window) is achieved, which can increase from 0.20 to 0.59 W/m².K depending on the meteorological conditions.

Table 1 describes the main parameters used to define the building and the different systems regulating the indoor climate. The internal heat loads are equal to 20 W/m², lighting not included. The values used in the simulations correspond to standard values for a low energy building.

***Table 1**. Main parameters of the building*

GENERAL INFORMATION	Location	Denmark
	Aspect	South-North
	Internal dimension of a single room L·W·H	7.54m x 3.5m x 3.2m
	Floor area	26.4 m²
VENTILATION	Decentralized ventilation combined with natural ventilation	
	Specific Fan Power factor	0.4 kJ/m³
	Air change rate per office	200 m³/h = 2.4 h⁻¹
	Heat recovery efficiency	85%
INFILTRATION	Air change rate	12.7 m³/h = 0.15 h⁻¹
PEOPLE	Number of persons per office	2 persons, light work
	Heat load per office (dry heat)	200 W
EQUIPMENT	Heat load per office	300 W
LIGHTING	Type	Continuous daylight control
	Luminance on a horizontal work surface	200 lux

System transferring energy inside the building

In order to assess the potential of transferring energy, a third function has been added to the heating and cooling system: transferring energy thanks to a smart hydraulic layout. Capillary tubes embedded at the surface of walls have been chosen for these applications. The tubes, usually made of polypropylene, have an outer diameter of around 5 mm and are embedded in 10 mm of plaster. This system is characterized by the large area of heat exchange, so that low temperature differences can be used for heating and cooling of the building.

The building and the system used to transfer energy in space have been simulated using the software BSim, which has been developed by the Danish Building Research Institute (SBi). In order to model the heat exchange, thermal zones integrated inside the wall structure have been created. These zones of 1 mm thickness are located at the same position as the capillary tube mats. These mats are represented by a fully convective surface, with a heat transfer coefficient on the water side equal to 1000 W/m².K, which corresponds to the value used by Glück in his report about the performance of capillary tubes (2003). These thermal zones are exchanging heat with the thermal zones of the opposite room, so that a thermal homogenisation between the two cavities occurs over the time. In order to assess the potential of the system, the three walls are activated and the system is running as soon as a temperature difference exists.

Thermal comfort

Based on the operative temperature obtained from the simulation, the thermal comfort has been assessed during working hours using the international standard EN 1525. In this standard, the thermal environment is divided in four different categories (I, II, III and IV), category I corresponding to a high level of expectation. For all the simulations performed in this paper, the indoor environment has been evaluated in both rooms, with and without activating the heat exchange and corresponds at least to category II (normal level of expectation). During the winter season (from November to April in this case), the temperature has to be kept within the range of 20 to 24°C to achieve category II. A deviation outside the comfort range up to 5% of the working hours is allowed. Figure 2 represents the thermal comfort in the south-facing room when transferring energy for the optimised solution (case 3 of figure 3). It can be seen that the temperature is slightly warmer than what could be expected during winter: this is due to the low heat losses of the building studied.

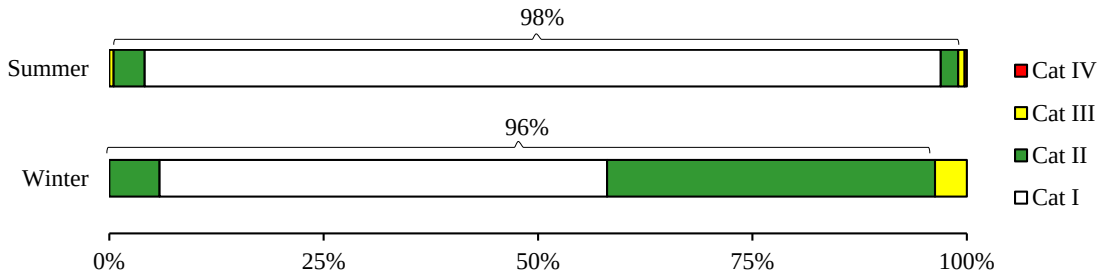

***Figure 2**. Indoor thermal quality expressed in percentage of time in 4 categories (met=1.2 – clo=1 during winter, 0.5 during summer)*

RESULTS

Overall energy consumption

The potential of this system has been evaluated by performing several simulations on the low energy office building described before. Different parameters, such as the shading control, the lighting control, or the thermal mass, have been tested in order to optimise the efficiency of the system. The heating and cooling consumptions of three different combinations are represented in figure 3. The left columns represent the energy consumption without transferring energy between the south-facing room and the north-facing room. The decrease in the heating and cooling consumption defines the efficiency of the system; this efficiency is given as a percentage at the top of the right columns. The energy for running pumps has not been taken into consideration in this paper.

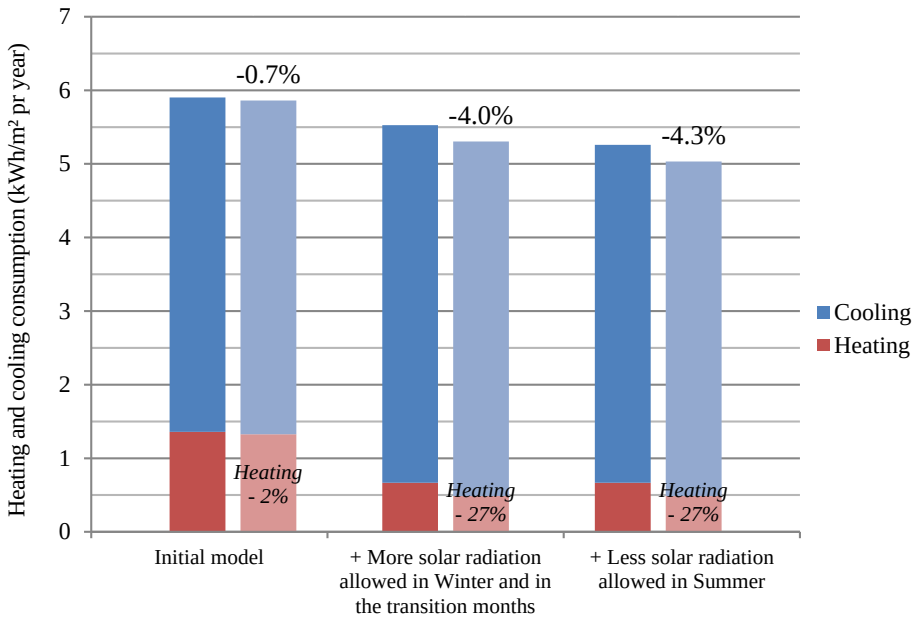

***Figure 3**. Influence of different control strategies on the heating and cooling consumption and on the energy shifting.*

It can be seen that the heating and cooling consumption can be decreased by activating the heat exchange. For this building, the system can reach 4.3% efficiency, which represents a diminution in the heating and cooling consumption of 0.23 kWh/m² per year. An appropriate control of the sun radiation increases this diminution in the heating and cooling consumption. It has to be noted that the heating demand is decreasing much when activating the system: 27% of the heating consumption can be saved. Moreover the efficiency is only slightly influenced by the number of walls activated: when activating only one wall (instead of 3) for exchanging energy, the total efficiency decreases from 4.3% to 3.7%.

Changes in the heat transfer over the year

Figure 4 describes the variation in the heat exchange over a year. It can be seen that the highest amount of energy is exchanged during the winter months, when the asymmetry is high and both room are not overheated. During warmer months, the heat exchange can occur from the north-facing room to the south-facing room because the high direct solar radiation on the south-facing window necessitates the shading being closed.

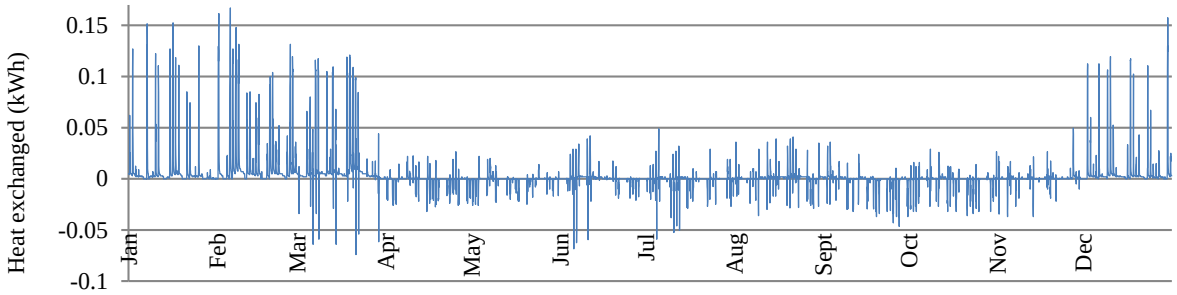

***Figure 4**. Fluctuation over the year in the heat exchanged between the 2 rooms; the value is positive if the heat is exchanged from the south to the north. Case 3 (cf. figure 3).*

Effect on the indoor climate

Figure 5 shows the operative temperature variation during 3 days of the heating season. As it can be seen on the left figure, the operative temperature in the south-facing room is decreasing when activating the heat exchange. Conversely the operative temperature is increasing in the north-facing room (cf. right figure). By activating the heat transfer within the building, the number of degree-hours is decreasing by 694 Kh per year in the south-facing room.

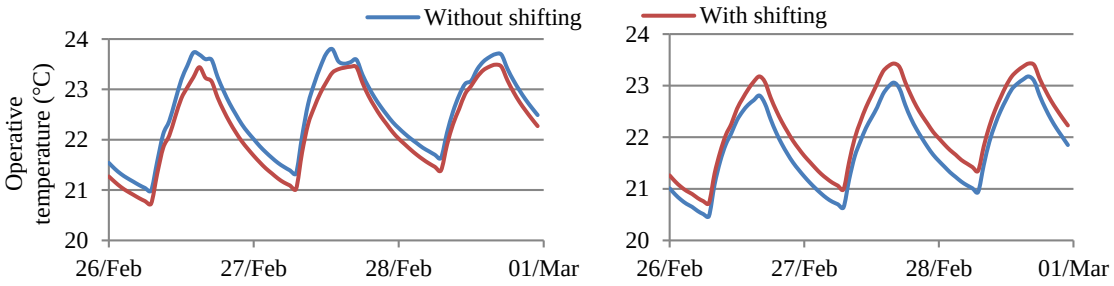

***Figure 5**. Operative temperature in the south-facing room (left plot) and north-facing room (right plot) during 3 working days in February. Case 3 (cf. figure 3).*

ANALYSIS OF THE POTENTIAL IN OTHER CASES

The building studied in the previous part corresponded to a very low energy building, which respects the Building Regulation 2020 (BR 20). A comparison has been performed with a building built according to the Building Regulation 2015 (BR 15), in order to evaluate the influence on the potential of shifting. Figure 6 presents a comparison between these two types of buildings. The efficiency of the system is slightly higher in the case of a building respecting BR 15 (4.5% instead of 4.3%). This can be explained by the higher heating demand of this building, compared to the building built according to BR 20.

In the same figure, it can be seen the influence of the type of heat exchange: water-based (3-walls exch.) or air-based system (direct air exch.). In the case of a direct air exchange (10 ACH), the efficiency is lower than with a wall exchange in both cases. When having a closer look to the results, it can be seen that mainly the heating consumption decreases in the case of a wall exchange, whereas both cooling and the heating consumption decreases in the case of a direct air exchange. This can be explained by the fact that the surface temperature is higher

than the air temperature for a low energy building. Therefore, if a wall exchange occurs, relatively high temperature is transferred, which leads to a high efficiency for heating.

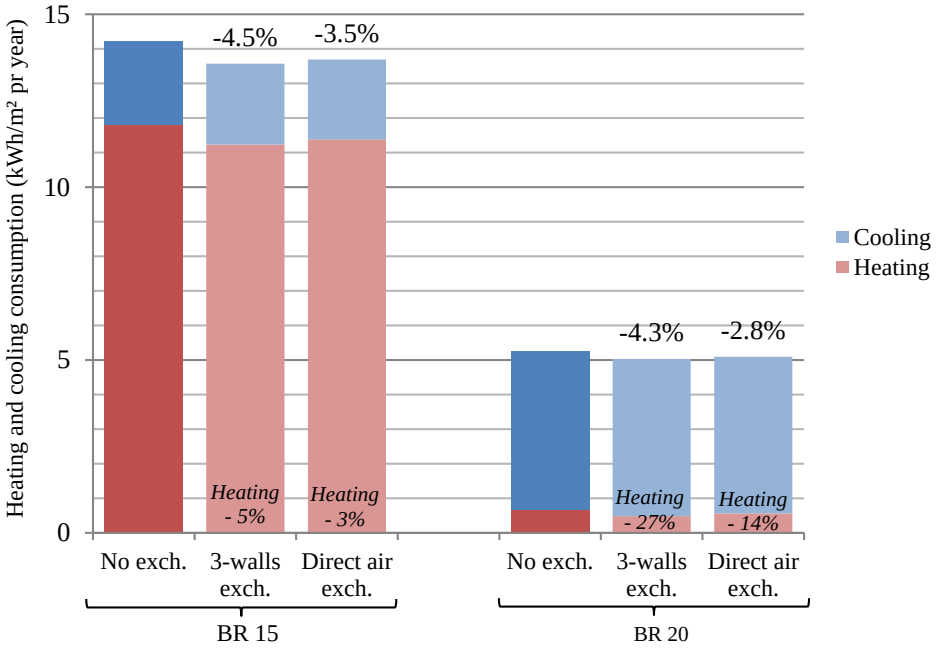

***Figure 6**. Comparison of different buildings and techniques to exchange heat.*

CONCLUSION

The potential of transferring energy between two building zones thanks to a surface system has been studied by means of computer simulations. Two different kinds of office building located in Denmark have been simulated, one with a predominant cooling demand and the other one with a predominant heating demand. The efficiency of the system is mainly influenced by the solar shadings, which have to be set carefully in order to optimize both the energy consumption and the interzonal heat transfer. Thanks to this transfer, the total energy consumption of the building is decreasing and an improvement in the indoor climate can be observed, due to the thermal homogenisation of the building. Nevertheless the energy savings reached with this system are not sufficient enough for the two types of buildings studied: the decrease in the heating and cooling consumption was always lower than 5%. A comparison with a direct air exchange has also been performed, but it didn't show better results.

REFERENCES

CEN. 2007. Standard ISO EN 15251. Indoor environmental input parameters for design and assessment of energy performance of buildings. Brussels.

EBST. http://www.ebst.dk/, Tight energy requirements for new buildings (Stramme energikrav til nye bygninger), last accessed on 24 May 2010.

Glück B. 2003. Entwicklung von Produkten mit Kunststoff-Kapillarrohrmatten zur umweltschonenden Raumheizung und –kühlung.

Karlsson, H. 2007. An Innovative Floor Heating Application – Transfer of Excess Heat Between Two Building Zones, *In: Proceedings of the 10th International Building Performance Simulation (IBPSA) Conference*, pp. 148–155, Beijing, China.

Müller D., Haase T., Hoh A. and Tschirner T. 2008. Absclussbericht – Niedriexergiesysteme für di Heiz- und Raumlufttechnik: Systemuntersuchung.

SBi-BSim, version 6,11,1,14. 2011.

Winther F., Heiselberg P. and Jensen R. 2010. Intelligent glazed facades for fulfilment of future energy regulations, *In: 3rd Nordic Passive House Conference*, Aalborg, Denmark.

Paper 2

Comparison of the thermal performance of radiative and convective terminals: A conceptual approach

Comparison of the thermal performance of radiative and convective terminals: A conceptual approach

J. LE DRÉAU[1], P. HEISELBERG[1]

[1]Department of Civil Engineering, Aalborg University, Aalborg, Denmark

ABSTRACT: During the last decades, the use of radiant terminals for heating or cooling buildings has rapidly increased and the activation of different construction elements has been tested: floor, ceiling or walls. Radiant systems are usually used instead of air conditioning systems: it is therefore of interest to compare the energy efficiency of the two types of terminals for heating and cooling buildings. Convective terminals (i.e. air conditioning systems) have been widely used in buildings, but the level of comfort is not always acceptable due to high air velocity. On the other hand radiant terminals can provide a better indoor climate, and be more energy efficient because they can make use of low-grade sources. The output of this conceptual approach is a better understanding of the advantages and drawbacks of the two technologies under different conditions. The analysis has been performed by simulating the energy consumption of an office room, located in Denmark. Different outdoor conditions have been tested, in order to compare their performance during the winter season and the summer season. Different types of activated surface have also been simulated. The results of this analysis show that the efficiency of convective terminals is highly dependent on the ventilation losses of the building. Radiant terminals are less sensitive to this parameter.
Keywords: Radiant terminal, Air conditioning, Energy efficiency, Heating, Cooling, Steady state, Solar Absorption

ISBN: 978-612-4057-89-2

Comparison of the thermal performance of radiative and convective terminals: A conceptual approach

J. LE DRÉAU[1], P. HEISELBERG[1]

[1]Department of Civil Engineering, Aalborg University, Aalborg, Denmark

ABSTRACT: During the last decades, the use of radiant terminals for heating or cooling buildings has rapidly increased and the activation of different construction elements has been tested: floor, ceiling or walls. Radiant systems are usually used instead of air conditioning systems: it is therefore of interest to compare the energy efficiency of the two types of terminals for heating and cooling buildings. Convective terminals (i.e. air conditioning systems) have been widely used in buildings, but the level of comfort is not always acceptable due to high air velocity. On the other hand radiant terminals can provide a better indoor climate, and be more energy efficient because they can make use of low-grade sources. The output of this conceptual approach is a better understanding of the advantages and drawbacks of the two technologies under different conditions. The analysis has been performed by simulating the energy consumption of an office room, located in Denmark. Different outdoor conditions have been tested, in order to compare their performance during the winter season and the summer season. Different types of activated surface have also been simulated. The results of this analysis show that the efficiency of convective terminals is highly dependent on the ventilation losses of the building. Radiant terminals are less sensitive to this parameter.
Keywords: Radiant terminal, Air conditioning, Energy efficiency, Heating, Cooling, Steady state, Solar Absorption

INTRODUCTION

Conventional forced-air systems have been widely used to control indoor climate, but the use of radiant systems has rapidly increased during the last decades [1]. During the 70's, the use of floor heating systems became very popular, especially in the residential sector. In the 90's, cooled radiant ceilings have been increasingly installed in European offices because of longer overheated periods during summer time. More recently radiant walls have been introduced on the market, principally for cooling. Radiant systems are an efficient way of transporting energy [2], mainly due to the higher heat capacity of water. Moreover the large surface of exchange of radiant systems allows the use of source temperature closer to the room temperature, especially in low energy buildings.

Differences between radiant and forced-air systems can also be observed in the way of emitting energy. In fact, instead of transferring heat only by convection, this occurs partly by radiation to (or from) the neighbouring surfaces, and partly by convection to (or from) the indoor air with a radiant system [3]. The influence of the terminal type will be the focus of this paper. Therefore four different terminals are selected (air conditioning, radiant floor, radiant wall and radiant ceiling) and their thermal performance will be compared for an office room located in Denmark. The heating and cooling seasons will be studied through numerical simulations under steady state conditions. The output of this study will be a better understanding of the parameters influencing their performance and also the advantages and drawbacks of the different solutions.

CASE STUDY

In order to study the influence of the terminal type on the energy efficiency, an office room located in Denmark has been considered. The internal dimensions of the room have been chosen similar to the PASSYS test cell: 5×2.76×2.75 m (length × width × height), resulting in a floor area of 13.8 m² [4]. 25% of the south facing wall is glazed: the window is double glazed with a g-value of 0.6. The construction elements are selected in accordance to the Danish Building Regulation 2010, meaning that the building energy need is lower than 71 kWh/m² per year for heating, cooling, ventilation, lighting and domestic hot water. The thermal characteristics of the building components are given in Table 1: ε corresponds to the surface emissivity (considering long-wave radiation) and α to the surface absorptivity (considering short-wave radiation). It has to be noticed that the window has a low-emissivity coating (low-e).

Four different terminals for cooling have been tested: radiant walls, radiant floor, radiant ceiling and air conditioning. The three radiant systems can be compared at the same level, as the activated areas are similar. Radiant terminals are embedded close to the surface, so that their radiant effect applies directly on the internal

constructions. The cooling or heating power of these terminals is assumed to be constant over the entire surface, therefore not taking into account the inhomogeneity due to the pipes layout.
Two different ventilation strategies have been tested: fully mixed or with a temperature gradient. The system is not equipped with heat recovery.

Table 1: Thermal properties of the construction elements (U-value given without including surface heat transfer coefficient).

	U' (W/m².K)	$\varepsilon_{long\text{-}wave}$ (-)	$\alpha_{short\text{-}wave}$ (-)
Wall	0.15	0.8	0.6
Window	1.40	0.2	0.14
Floor	0.10	0.8	0.6
Roof	0.10	0.8	0.6

The outdoor conditions have been selected from the weather data of the Design Reference Year (DRY) in Copenhagen. Using these boundary conditions, dynamic simulations of an office room facing south have been performed using the software BSim [5] and two cases have been selected: one representing the winter season, and another one the summer season. The studied cases have been chosen so that, 95% of the time, the climate is less severe and leads to a lower energy consumption. Therefore it makes possible to compare the capacity of different terminals to provide an acceptable indoor climate over the year with a tolerance of 5%; this value has been chosen according to [6] and can be interpreted as a design parameter. The selected cases are summarised in Table 2.

Table 2: Definition of the winter conditions (26th of December, 12 o'clock) and summer conditions (13th of July, 15pm).

	WINTER	SUMMER
T_{ext} (°C)	0.0	23.0
$Q_{solar\ normal}$ (W/m²)	11	296
$Q_{solar\ diffuse}$ (W/m²)	33	389
Solar azimuth (°)	174	234
Solar height angle (°)	11	47

PHYSIC OF THE ROOM

Modelling accurately the heat transfer in the room is essential when studying the influence of the terminal type. In fact, the only difference between radiant terminals and air conditioning is the nature of the heat or cold provided to the room, i.e. either convective or radiative. But this parameter will highly influence the indoor climate.

In order to establish the room heat balance, the surfaces are discretized in a total of 61 sub-surfaces, and the room air is assumed to be fully mixed (single zone model). A nodal scheme is then used to solve the heat transfer between the different elements. The conduction (Q_{cond}) through walls is calculated using the U-values (Table 1). The heat transfer is assumed to be one-dimensional, and thermal bridges are not considered. The effect of thermal mass does not need to be treated as only steady state conditions are studied in this paper. The different models used for convection, long-wave radiation and short-wave radiation are explained in the following paragraphs.

On the external side of the walls, a combined heat transfer coefficient is used to model the convective and radiative exchange with the ambient environment. This coefficient has been chosen equal to 29.3 W/m².K, which corresponds to the value for brick or rough plaster [7].

On internal surfaces, the convective heat transfer (Q_{conv}) is assumed to be natural and is modelled by a constant coefficient selected according to the surface slope and the type of convective flow observed. For a horizontal surface, the flow can either be facing upward or downward, depending on the temperature difference between the air and the surface considered. For example, in the case of a heated floor, the relatively hot, lighter fluid has a tendency to be convected upward in the form of plumes, being replaced by colder, denser fluid from above. This configuration is gravitationally unstable and the buoyancy forces will drive the convective motion. The associated convective heat transfer coefficient will be rather high. On the other hand, in the case of a cooled floor, the fluid is gravitationally stable and it leads to the formation of a stable layer. The downward flow will result in a low convective heat transfer coefficient [8].

Table 3: Definition of the convective heat transfer coefficients at the internal surfaces of the room [9, 10].

	h_{conv} (W/m².K)
Vertical surface	2.5
Horizontal upward	4.0
Horizontal downward	0.7

The radiative exchange can be split in two categories: (1) Short-wave radiation, also called solar radiation, is coming from a body heated at 5800 K. 75% of the flux is therefore emitted at a wavelength lower than 1 µm. (2) Long-wave radiation is emitted by objects at ambient temperature, around 300 K, and is concentrated in the infra-red region (wavelength around a few micrometres). For example a black body heated at 300 K has a peak emission at 10 µm.

The material properties are changing with the type of radiation considered, i.e. the type of spectrum (Table 1).

Long-wave radiative heat transfer between surfaces ($Q_{rad\ j\to i}$) has to be modelled accurately when establishing the room heat balance. Diffuse grey surfaces are assumed, and the window is taken to be opaque to long-wave radiation. The difficulty comes from the non-linearity of radiative exchange, which implies the use of either simplified linear models or iteration techniques. The algorithm chosen in this study is the one developed by Clarke [11]: it is a non-linear model, including direct reflection between two surfaces, but also indirect reflections on a third surface. The use of this model implies several iterations before convergence is reached (assessed by a change in the surface temperature smaller than 10^{-7} %). This method has been compared to the exact method, the radiosity method, and the obtained radiative heat fluxes do not differ by more than 3% for the considered cases.

One of the main issues, when calculating the cooling load in a building, is the computation of the incoming solar radiation (Q_{solar}). There are three main steps in the calculation of the solar load: (1) determination of the irradiation on the south façade, (2) separation of solar radiation absorbed and reflected by the glazing, and transmitted to the room, (3) calculation of the solar repartition in the room. Once the solar radiation is distributed on the different internal surfaces, radiation is treated as long-wave radiation.
(1) The irradiation on a vertical surface is calculated according to [12]. It takes into consideration direct, diffuse and reflected solar radiation.
(2) The part of solar radiation absorbed by the glazing and transmitted to the room is calculated using the software Window 6 [13]. In this program, the detailed calculation of reflection between the panes and the absorption and transmission of each pane is performed hemispherically for diffuse radiation and in steps of 10° incidence angle for direct solar radiation. Thanks to this program, it is possible to define the part of solar radiation directly transmitted (T_{sol}) and the part absorbed and then reemitted ($SHGC - T_{sol}$), with $SHGC$ Solar Heat Gain Coefficient. In the studied case, around 5 % of the solar radiation is absorbed and 50-55 % is transmitted to the room (these values vary with the solar angle).
(3) Finally the part of transmitted solar radiation has to be distributed on the room surfaces. In BESTEST [7], a method is proposed to calculate the interior solar distribution of short-wave radiation depending on the solar absorptivity of surfaces. This technique assumes that no solar radiation is directly absorbed by the zone air; all incident solar radiation initially hits the floor and is then reflected over the other surfaces according to their view factors. The remaining amount of original solar radiation is then assumed to be absorbed by all surfaces in proportion to their area-absorptance products. For the considered case, the distribution is: 63 % at the floor, 10 % at the ceiling, between 4 and 9 % at each wall, and 1 % lost through the window. This type of distribution is proper to cases with low diffuse radiation.

The internal heat gains from equipment, lights and people are modelled as sensible heat load (no latent heat load), assuming that 40% of this heat load is convective ($Q_{conv\ int}$), and 60% is radiative ($Q_{rad\ int}$) [7]. The radiative heat loads are distributed on the different surfaces according to their relative area; no radiative internal heat load is applied to the window (low-e).

Finally the temperatures at the different nodes are determined by solving the room heat balance composed of 62 equations:

$$\begin{cases} Q_{ventilation} = \sum_i Q_{conv\ \{i\}} + Q_{conv\ int} + Q_{conv\ terminal} \\ Q_{cond\ \{i\}} = Q_{conv\ \{i\}} + \sum_j Q_{rad\ j\to i} + Q_{solar\ \{i\}} + Q_{rad\ int\ \{i\}} + Q_{rad\ terminal\ \{i\}} \end{cases}$$

$Q_{conv\ terminal}$ and $Q_{rad\ terminal}$ represent the heating (if positive) or cooling (if negative) power of the terminal. The validity of the code has been checked by comparing the obtained results with the software BSim [5]. A good agreement has been observed despite differences in the model used for representing the room physics.

EVALUATION OF COMFORT

The thermal comfort has been evaluated at a global scale using the operative temperature, but local thermal comfort parameters have also been assessed.

The operative temperature is defined as the mean value of the radiant temperature and air temperature; this evaluation of the operative temperature is valid for relative air velocity below 0.2 m/s [14].
As we consider the case of an office building, the air temperature is calculated at a height of 0.6 m, which corresponds to the height of a seated person.
The mean radiant temperature ($\boldsymbol{T_{rad}}$) is also evaluated for a seated person (orientation not fixed). It can be expressed by the following equation [14]:

$$T_{rad} = 0.13\left(T_{pr\,[up]} + T_{pr\,[down]}\right) + 0.185\left(T_{pr\,[right]} + T_{pr\,[left]} + T_{pr\,[front]} + T_{pr\,[back]}\right)$$

with T_{pr} plane radiant temperature
$T_{pr}{}^4 = \sum_i T_i{}^4 F_{p-i}$ (for high emissivity)
F_{p-i} view factors between the plane and the surface i (calculated according to [14])

The factors used in the calculation of the radiant temperature correspond to the projected area factor of a seated person in the 6 directions. This calculation method has been preferred to the area-weighted method because it leads to more accurate results. Otherwise the radiant

temperature would have been underestimated in case of cooled floor and overestimated in case of cooled ceiling (with an error up to 2 K).

As the focus of this project is on radiant solutions, two local comfort parameters have been evaluated: the radiant temperature asymmetry, which corresponds to the difference between the plane radiant temperatures on two opposite sides of a small plane element, and the surface temperatures. In all the simulations performed, it has been verified that the local discomfort parameters are within the range of category II, corresponding to a normal level of expectation: the limit values can be found in [15].

RESULTS FOR HEATING

In order to study the influence of the terminal type on the heating consumption of buildings, several simulations have been performed under typical winter conditions (Table 2). Several parameters can influence the energy efficiency of terminals: outdoor temperature, air change rate, temperature gradient… Therefore a sensitivity analysis has been conducted by setting the operative temperature equal to 21°C for all cases, and observing the influence of the different parameters on the energy performance and local comfort. Internal heat loads are not considered in the winter case.

Figure 1 presents the influence of the air change rate on the energy efficiency of convective and radiative terminals. It can be observed that, at low air change rate, the differences between the four terminals are rather small; the convective terminal is slightly more energy efficient at low air change rate. Nevertheless, when increasing the air change rate, radiant terminals show significant advantages. They are taking advantage of the high portion of radiative exchange, which is therefore not greatly influenced by the air temperature and the air change rate. No significant differences can be observed between the three radiant terminals. At 3 ACH, the energy need for a radiant system is around 10% lower than for a convective system.

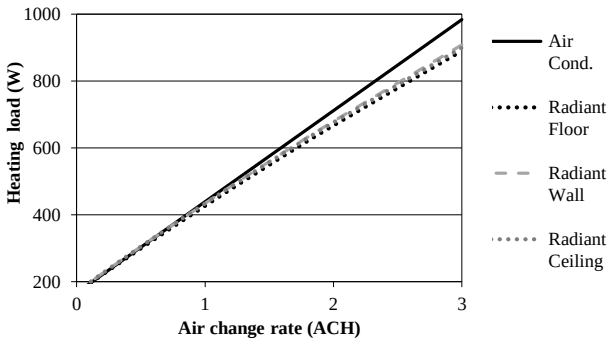

Figure 1: Heating consumption of the terminal depending on the air change rate and terminal type.

Even though all systems achieve the same level of global comfort, the local comfort conditions are not identical. Local parameters are changing only in the case of radiant terminal. When increasing the air change rate, a higher asymmetry between the air and the surface temperature can be observed. The air temperature is decreasing whereas the radiant temperature is increasing: at 3 ACH, this asymmetry can be up to 5 K. The maximum surface temperature is therefore increasing, as it can be seen in Figure 2. The radiant floor has the lowest surface temperature due to its high convective heat transfer (Table 3), whereas the ceiling has the highest one. The local comfort criteria are respected in all cases, except for the radiant ceiling: at air change rate higher than 2.5 ACH, the vertical radiant asymmetry is larger than 5 K.

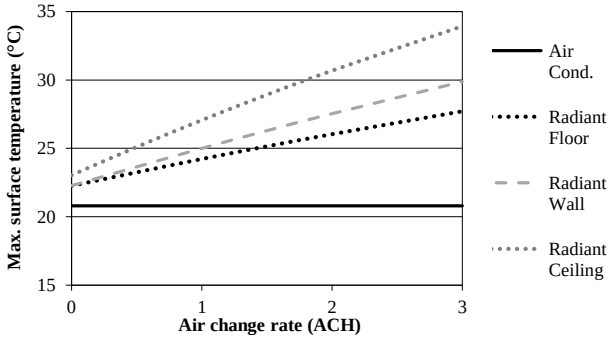

Figure 2: Maximum surface temperature depending on the air change rate and terminal type.

In order to study the influence of the type of ventilation system, a temperature gradient of 4 K between the floor and the ceiling has been imposed to the room air. Thanks to this model, it is possible to simulate the effect of displacement ventilation. The temperature gradient chosen ensures that the local thermal comfort is achieved, i.e. that the vertical air temperature between 1.1 m and 0.1 m is lower than 3 K [15]. The temperature gradient leads to an increase of the heating consumption (Figure 3) because of warmer outlet air. At 3 ACH, the increase is of the order of 10 % for the heated wall; similar results are obtained with other types of terminal.

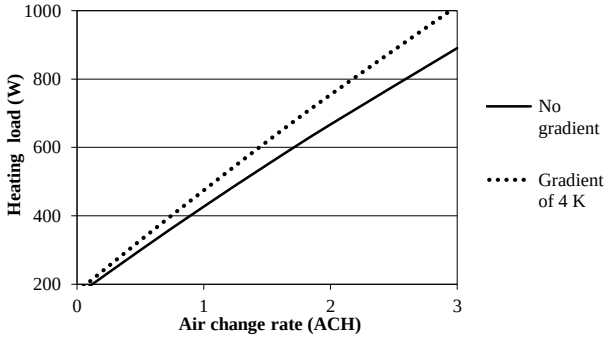

Figure 3: Influence of a temperature gradient on the heating consumption of a radiant wall.

RESULTS FOR COOLING

The influence of the terminal type on the cooling consumption has also been investigated under typical summer conditions (Table 2). Obviously the amount of solar radiation and the internal heat loads are important factors for determining the cooling consumption. But these parameters are (almost) independent of the architectural choices; therefore their influence will not be presented in this paper. The focus will be on the influence of design parameters, such as the ventilation rate, the surface properties and the type of ventilation. For all the simulations, the operative temperature has been set to 26°C and the energy efficiency has been compared. Internal heat loads are equal to 20 W/m^2 (value close to the solar heat load) and the shading due to the opening width is taken into consideration.

The influence of the air change rate has been investigated (Figure 4), and comments similar to the heating case can be made: at low air change rate, air conditioning can be more efficient, but radiant terminals require less power when the air change rate is increasing. It can also be observed that, under these conditions, the ventilation is assisting the cooling process.

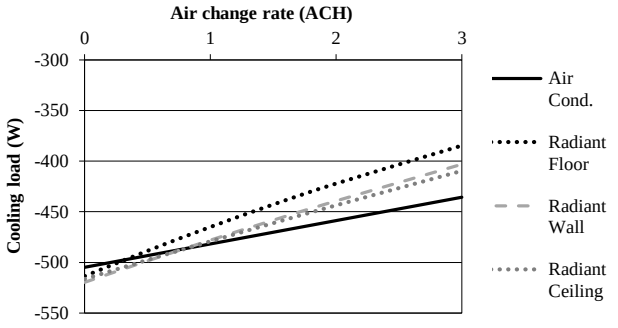

Figure 4: Cooling consumption of the terminal depending on the air change rate and terminal type.

In the summer case, more differences appear between the different radiant terminals. Radiant floor is the most efficient system despite the low convective heat transfer coefficient: this is due to the direct solar absorption (Figure 5). Radiant ceiling is the less efficient radiant terminal despite the high convective heat transfer coefficient: it can be explained by the low amount of solar radiation reflected to this surface and by the location of the operative temperature sensor. Moreover it can be observed that the portion of radiation in the terminal heat balance is almost constant, around 50%. Only the convective part varies greatly according to the type of terminal: for floor cooling, it represents only 7% of the heat exchange, whereas it represents around 30-40% for the other radiant terminals. Similar results have been obtained experimentally by Novoselac et al. [16] in their study about cooled ceiling.

When having a closer look to local comfort, it can be observed that all the solutions achieved an acceptable indoor climate. The minimum surface temperature is always above 21°C, and the temperature asymmetry is within the recommended range. But radiant terminals, and especially the cooled ceiling and the cooled wall, create a more uniform environment, i.e. with a lower temperature difference between air and surfaces.

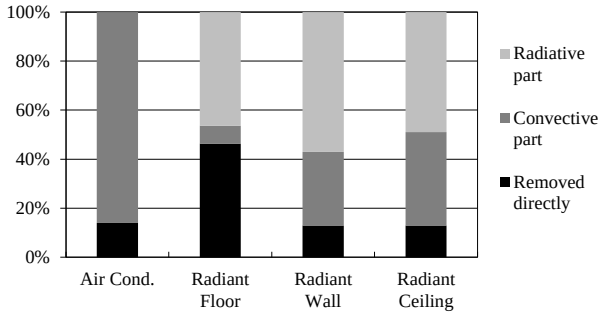

Figure 5: Heat balance of the different terminals (ventilation set to 2 ACH).

Simulations with different outdoor temperatures have also been performed (Figure 6) and they showed that the energy efficiency of air conditioning is highly dependent on the ambient conditions. In fact, as air conditioning terminals are cooling down the air, more energy will be needed if warmer air penetrates the building. Radiant systems are less sensitive to the inlet air temperature because these systems are principally cooling down the surfaces and can achieve the same level of comfort than air conditioning with warmer air.

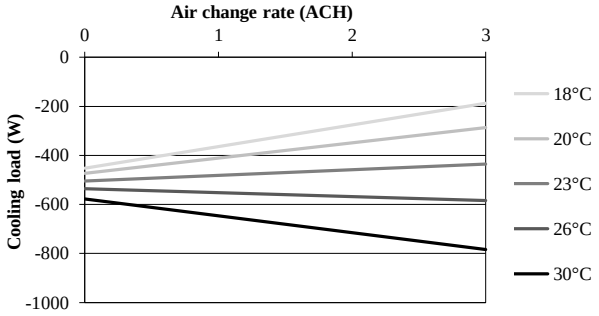

Figure 6: Influence of the outdoor temperature on the cooling consumption of air conditioning.

The influence of the type of ventilation has been studied (Figure 7). Contrary to the heating case, the cooling power needed to achieve thermal comfort is reduced with a temperature gradient in the room. At 3 ACH, the required power is decreasing by 30%.

Figure 8 presents the cooling consumption depending on the floor absorptivity with an air change rate set to 2 ACH. When the floor absorptivity is decreasing, the cooling consumption is decreasing. This is due to the part

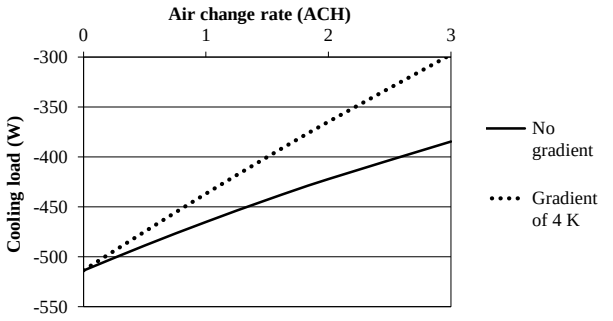

Figure 7: Influence of a temperature gradient on the cooling consumption of a radiant wall.

of solar radiation redirected outside the building, which is changing: for a floor absorptivity of 0.8, this part is only 0.7%, whereas it increases up to 2.9% for an absorptivity of 0.2. Because of the small window area and the shape of the room, the influence on the cooling consumption is not so important, but it can become rather high for highly glazed surfaces like atria [17].

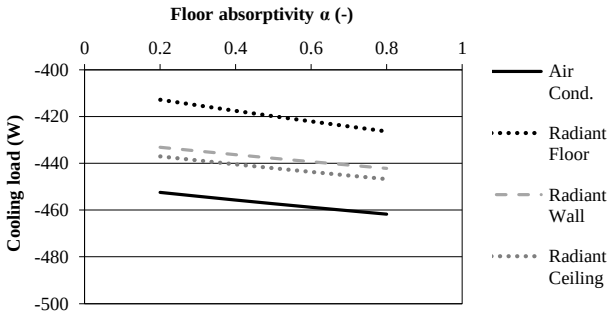

Figure 8: Cooling consumption of the terminal depending on the floor absorptivity and terminal type (ventilation set to 2 ACH).

CONCLUSION

The thermal performance of four types of terminal (air conditioning, radiant floor, radiant wall and radiant ceiling) has been investigated numerically. The case of an office room located in Denmark has been simulated under winter and summer conditions. Not only has the energy efficiency been analysed, but also the local thermal comfort.

The parameter, which is influencing the most the thermal performance of terminals, is the air change rate.

During winter, the ventilation rate should be minimised in order to decrease heat losses; in that case the four types of terminal have similar efficiency. Only at high air change rate radiant terminals show better performance. It has to be noticed that the heated ceiling has limited capacity due to the constraint on radiant asymmetry.

During summer, radiant panels show significant advantages compared to air conditioning. In fact outdoor air is often a few degrees above or below the cooling set-point. For air conditioning, this characteristic is a drawback because the cooling consumption will be highly dependent on the outdoor temperature. On the contrary, radiant terminals are much less sensitive because they are operating at higher air temperature: the ventilation system is therefore often assisting the cooling process. Moreover radiant systems create a more uniform indoor environment. Significant differences between radiant terminals can only be observed in the summer case due to high solar radiation. Floor cooling is the most efficient solution thanks to the direct solar absorption, but the repartition of solar radiation plays an important role in this efficiency. The results and conclusions made in this paper might differ with other assumptions.

Finally the effect of displacement ventilation has been simulated. The temperature gradient created leads to an increase of the heating consumption, whereas the cooling consumption is reduced.

REFERENCES

1. De Carli, M. (2009). Comparison Between a Radiant Floor and Two Radiant Walls on Heating and Cooling Energy Demand. *ASHRAE Transactions*, 115 (2).

2. Olesen, B.W. (2000). Hydronic radiant heating and cooling of buildings using pipes embedded in the building structure. *41st AICARR Conference*, Milano, Italy.

3. Roulet, C., J. Rossy, Y. Roulet (1999). Using large radiant panels for indoor climate conditioning. *Energy and Buildings*, vol. 30, no. 2, pp. 121-126.

4. Vandaele, L., P. Wouters (1994). The PASSYS summary report, *European Commission Publication*, EUR 15113 EN.

5. Danish Building Research Institute (2012). SBi-BSim, Version 6,11,1,14.

6. EN 15251 (2007). Indoor environmental input parameters for design and assessment of energy performance of buildings.

7. Judkof R., Neymark J. (1995) International Energy Agency Building Energy Simulation Test (BESTEST) and Diagnostic Method, *National Renewable Energy Laboratory (NREL)*.

8. Alamdari, F., Hammond, G.P. (1983). Improved data correlations for buoyancy-driven convection in rooms, *Building Services Eng. Research and Tech.*, vol. 4, no. 3, pp. 106-112.

9. EN 15265 (2007). Energy performance of buildings - Calculation of energy needs for space heating and cooling.

10. Causone, F., Corgnati, S.P., Filippi, M., Olesen, B.W. (2009). Experimental evaluation of heat transfer coefficients between radiant ceiling and room, *Energy and Buildings*, vol. 41, no. 6, pp. 622-628.

11. Clarke, J. (2001). *Energy Simulation in Building Design (2nd Edition)*. Butterworth-Heinemann, Oxford, pp. 202-280.

12. ASHRAE (2009). Handbook of Fundamentals, Chapter 14 - Climatic Design Information, Atlanta GA.

13. University of California. (2012) Window 6.3.

14. EN 7726 (2001). Ergonomics of the thermal environment - Instruments for measuring physical quantities.

15. EN 7730 (2005). Ergonomics of the thermal environment - PMV and PPD.

16. Novoselac, A., B.J. Burley (2006). New Convection Correlations for Cooled Ceiling Panels in Room with Mixed and Stratified Airflow, *HVAC&R Research 12*, pp. 279-294.

17. Wall M. (1995). A design tool for glazed spaces. Part I: description. *ASHRAE Trans.*, 101, 1261.

Paper 3

Sensitivity analysis of the thermal performance of radiative and convective terminals

Energy and Buildings 82 (2014) 482–491

Contents lists available at ScienceDirect

Energy and Buildings

journal homepage: www.elsevier.com/locate/enbuild

Sensitivity analysis of the thermal performance of radiant and convective terminals for cooling buildings

J. Le Dréau, P. Heiselberg

Department of Civil Engineering, Aalborg University, Sohngaardsholmsvej 57, DK-9000 Aalborg, Denmark

ARTICLE INFO

Article history:
Received 22 September 2013
Received in revised form 27 April 2014
Accepted 1 July 2014
Available online 9 July 2014

Keywords:
Floor cooling
Cooled wall
Cooled ceiling
Active chilled beam
Emitters
Sensitivity analysis
Cooling need
Convective heat transfer coefficient
Air temperature stratification
Comfort

ABSTRACT

Heating and cooling terminals can be classified in two main categories: convective terminals (e.g. active chilled beam, air conditioning) and radiant terminals. The mode of heat transfer of the two emitters is different: the first one is mainly based on convection, whereas the second one is based on both radiation and convection. In order to characterise the advantages and drawbacks of the different terminals, steady-state simulations of a typical office room have been performed using four types of terminals (active chilled beam, radiant floor, wall and ceiling). A sensitivity analysis has been conducted to determine the parameters influencing their thermal performance the most. The air change rate, the outdoor temperature and the air temperature stratification have the largest effect on the cooling need (maintaining a constant operative temperature). For air change rates higher than 0.5 ACH, differences between terminals can be observed. Due to their higher dependency on the air change rate and outdoor temperature, convective terminals are generally less energy effective than radiant terminals. The global comfort level achieved by the different systems is always within the recommended range, but differences have been observed in the uniformity of comfort.

DOI: http://doi.org/10.1016/j.enbuild.2014.07.002

Paper 4

A full-scale experimental set-up for assessing the energy performance of radiant wall and active chilled beam for cooling buildings

A full-scale experimental set-up for assessing the energy performance of radiant wall and active chilled beam for cooling buildings

Jérôme Le Dréau (✉), Per Heiselberg, Rasmus Lund Jensen

Department of Civil Engineering, Aalborg University, Sohngaardsholmsvej 57, DK-9000 Aalborg, Denmark

Abstract

Full-scale experiments under both steady-state and dynamic conditions have been performed to compare the energy performance of a radiant wall and an active chilled beam. From these experiments, it has been observed that the radiant wall is a more secure and efficient way of removing heat from the test room than the active chilled beam. The energy saving, which can be estimated to around 10%, is due to increased ventilation losses. The asymmetry between air and radiant temperature, the air temperature gradient and the possible short-circuit between inlet and outlet play an equally important role in decreasing the cooling need of the radiant wall compared to the active chilled beam. It has also been observed that the type and repartition of heat load have an influence on the cooling demand. Regarding the comfort level, both terminals met the general requirements, except at high solar heat gains: overheating has been observed due to the absence of solar shading and the limited cooling capacity of the terminals. No local discomfort has been observed although some segments of the thermal manikin were slightly colder.

Keywords

full-scale experiments,
cooling need,
terminal,
emitter,
radiant wall,
active chilled beam,
energy effectiveness,
air temperature stratification,
local comfort

Article History

Received: 9 January 2014
Revised: 20 May 2014
Accepted: 17 June 2014

DOI: http://doi.org/10.1007/s12273-014-0190-7

BUILD SIMUL
DOI 10.1007/s12273-014-0190-7

A full-scale experimental set-up for assessing the energy performance of radiant wall and active chilled beam for cooling buildings

Jérôme Le Dréau (✉), Per Heiselberg, Rasmus Lund Jensen

Department of Civil Engineering, Aalborg University, Sohngaardsholmsvej 57, DK-9000 Aalborg, Denmark

Abstract

Full-scale experiments under both steady-state and dynamic conditions have been performed to compare the energy performance of a radiant wall and an active chilled beam. From these experiments, it has been observed that the radiant wall is a more secure and efficient way of removing heat from the test room than the active chilled beam. The energy saving, which can be estimated to around 10%, is due to increased ventilation losses. The asymmetry between air and radiant temperature, the air temperature gradient and the possible short-circuit between inlet and outlet play an equally important role in decreasing the cooling need of the radiant wall compared to the active chilled beam. It has also been observed that the type and repartition of heat load have an influence on the cooling demand. Regarding the comfort level, both terminals met the general requirements, except at high solar heat gains: overheating has been observed due to the absence of solar shading and the limited cooling capacity of the terminals. No local discomfort has been observed although some segments of the thermal manikin were slightly colder.

Keywords

full-scale experiments,
cooling need,
terminal,
emitter,
radiant wall,
active chilled beam,
energy effectiveness,
air temperature stratification,
local comfort

Article History

Received: 9 January 2014
Revised: 20 May 2014
Accepted: 17 June 2014

1 Introduction

In low energy buildings, the cooling and heating need is greatly reduced and allows the use of renewable sources (e.g. ground water, ambient air). New types of terminals, such as thermo-active building systems (Lehmann et al. 2007) or active chilled beams (Roth et al. 2007), have been developed to promote the use of low temperature heating (25–40℃) and high temperature cooling systems (13–20℃) (Babiak et al. 2007). Terminals (or emitters) can be classified in two main categories: air-based and radiant terminals. With air-based terminals, the indoor temperature is maintained within a certain range by controlling the air temperature, whereas radiant terminals control the surface(s) temperature through a water-based system. These two terminals emit or absorb heat in different ways and will lead to different levels of comfort and energy performance.

Different numerical and experimental studies have been performed to compare the energy effectiveness of terminals. In the 1980s, most of the research focussed on the heating case. The thermal comfort in a room heated by different emitters (radiator, convector, heated floor, etc.) has been studied experimentally by Hannay et al. (1978) and Olesen et al. (1980). The thermal comfort conditions achieved with different terminals were similar, but differences of temperature gradient in the space have been observed. The flow pattern in a room heated with panel, floor and wall heating has been investigated numerically by Myhren and Holmberg (2008): they calculated that the annual energy savings with a radiant heating terminal could be around 7% due to the lower air temperature. In addition to terminals for heating, cooling systems have raised interest in the past ten years due to the increased level of insulation and air-tightness of buildings. Fabrizio et al. (2012) have compared numerically the performance of radiant heating and cooling systems versus all-air and fan coil systems for

E-mail: jld@civil.aau.dk

List of symbols

C_p	heat capacity (J/(kg·K))
C_m	effective heat capacity (J/K)
I_{cl}	thermal insulation from the skin surface to the outer clothing surface (clo)
I_T	thermal insulation from the body surface to the environment, including all clothing, enclosed air layers and boundary air layer (clo)
$\dot{m}$	mass flow (kg/s)
PPD	predicted percentage dissatisfied (%)
PD	percentage dissatisfied (%)
Q	heat flow (W)
t	time (s)
T	temperature (℃)
ΔT_{i-j}	temperature difference, T_i–T_j (K)
α	solar absorptance
ε	emissivity
λ	thermal conductivity (W/(m·K))
ρ	density (kg/m³)
Ψ	linear thermal transmittance (W/(m·K))
ρ^*	solar reflectivity
τ	solar transmittance

Subscripts

1	outermost surface
2	innermost surface
eq	equivalent
LW	long-wave radiation
SW	short-wave radiation
vent	ventilation

different European countries: the use of radiant technologies showed a good potential for warm climates (e.g. 10%–15% primary energy savings in Rome). Most of the research focused on the primary energy use, but some studies also compared the energy delivered to the space and differences in the heat balance were noted in several publications. The variations of the air temperature and of the conductive flux through the outer walls were pointed out by Imanari et al. (1999) and Feng et al. (2013). Le Dréau and Heiselberg (2014) have identified the parameters influencing the effectiveness of terminals through a sensitivity analysis and showed that the radiant terminals are more efficient than air-based terminals when the air change rate is higher than 0.5 ACH.

The interaction between the ventilation system and the terminals has usually been investigated experimentally. Causone et al. (2010) studied the interaction between a radiant floor and the ventilation system: large vertical air temperature difference between head and ankles has been observed when the cooled floor was combined with displacement ventilation. Tomasi et al. (2013) made similar observations in their study of air distribution with different mixing ventilation design. Additionally, a short-circuit has been noticed when both supply and extract air terminals were located at high level.

The evaluation of terminals cannot solely rely on numerical investigations as several parameters are difficult to model accurately (e.g. interaction between ventilation and terminals, effect of the type of heat source, air temperature stratification). Therefore, full-scale experiments have been performed under both steady-state and dynamic conditions. This paper focuses on two high-temperature cooling systems: active chilled beam and radiant wall. The objective of these experiments is to perform a combined evaluation of the energy effectiveness and comfort obtained with the two terminals using the same test facility. A detailed analysis of the airflow will be conducted to explain the differences between air-based and radiant terminals. Additionally, some local comfort parameters will be evaluated, using the parameters from EN ISO 7730 (2005) and a thermal manikin.

2 Presentation of the test facility

The experiments have been performed from January to September 2013 in "The Cube", which is an outdoor full-scale test facility located in Aalborg, Denmark (57.02°N, 10.0°E). This facility has been used by Kalyanova to investigate double-skin facades (Kalyanova 2008), by Winther to characterise intelligent glazed facades (Winther 2013) and by Le Dréau et al. to study convective heat transfer (Le Dréau et al. 2014b). In order to observe the influence of solar radiation on the effectiveness of different cooling terminals, an experimental room has been constructed inside the building with one wall connected to the outdoor environment (Fig. 1). The experimental room consists of a wooden construction covered internally with 160 mm of expanded polystyrene (EPS). In order to increase the thermal mass of the room, 22 mm of plywood has been added to the floor and plasterboards (13 mm) have been glued to the walls. The internal dimensions of the experimental room are 2.76 m × 3.60 m × 2.75 m (width × length × height) resulting in a floor area of around 10 m². The section of the test room is

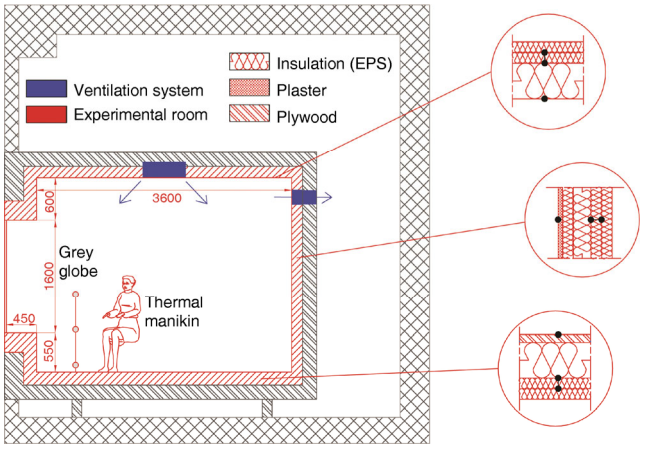

Fig. 1 Vertical section of "The Cube" (dimensions in mm) with details on the construction elements (black dots indicate thermocouples)

similar to the PASSYS test cell (Vandaele and Wouters 1994). The south wall is equipped with a double-layer glazing (2.76 m × 1.60 m) characterized by a *U*-value of 1.2 W/(m²·K) and a *g*-value of 0.36. The thermal mass of the room is equal to 20 Wh/(m²·K), which corresponds to a light construction (EN ISO 13786 2007).

All uncertainties specified in this paper are given for a confidence interval of 95%, normally distributed. The uncertainty analysis and the experimental data are described in detail in a technical report (Le Dréau et al. 2014a).

2.1 Construction elements

The thermal and optical properties of the materials used in the experimental room are given in Table 1. With the exception of the specific heat capacity, all parameters and associated uncertainties have been derived from measurements (i.e. hot plate apparatus, infrared camera or spectrometer). The specific heat capacity C_p of materials has been estimated using the European standard (EN 12524 2000).

The double-layer glazing used in the test room is composed of a 6 mm glass with low-e coating (Pilkington Suncool 66/33), a 15 mm cavity filled with Argon and a 6 mm clear glass (Pilkington Optifloat Clear). The thermal and optical properties of the double-glazing unit are given in Table 2. The optical properties have been evaluated using Window (Lawrence Berkeley Laboratory (LBL) 2012a): the calculation of the normal-incidence properties is based on the standard EN ISO 15099 (2003) and the angular-dependant properties are determined from a fourth order polynomial regression, whose coefficients change depending on the coating. The window frame is made of wood and sealed with silicone.

2.2 Cooling principles

Two terminals have been installed in the test room: a radiant wall and an active chilled beam (Fig. 2). The west wall of the test room is equipped with six radiant panels, resulting in a total dimension of the activated surface equal to 3.6 m × 1.9 m (length × height). The radiant panels are composed of capillary pipes (3.35 mm diameter and 10 mm spacing) mounted at the back of a plasterboard. The water flow in each panel varies between 30 and 70 L/h and is laminar. The cooling capacity has been measured under experimental conditions and is equal to 21 W/m²$_{floor}$ (for $\Delta\theta_C$ = 8 K (EN 1264-3 2009)). Alternatively, maintaining

Table 1 Thermal and optical properties of the materials used in the experimental room

Material		λ (W/(m·K))	ρ (kg/m³)	C_p (J/(kg·K))	ε_{LW}	$\rho^*_{SW\ hemis}$
Expanded polystyrene		0.041 ± 0.002	20.0 ± 0.2	1450 ± 100	0.73 ± 0.05	0.94 ± 0.01
Plywood (white finish)		0.13 ± 0.01	532 ± 10	1600 ± 100	0.95 ± 0.05	0.73 ± 0.01
Gypsum (white finish)		0.21 ± 0.01	680 ± 10	1000 ± 100	0.95 ± 0.05	0.73 ± 0.01
Extruded polystyrene		0.035 ± 0.004	40.0 ± 0.4	1450 ± 100	—	—
Thermal manikin	Skin	—	—	—	0.95 ± 0.05	0.70 ± 0.01
	Clothes	—	—	—	0.77 ± 0.05	0.70 ± 0.01
Electric carpet		—	—	—	0.74 ± 0.05	—
Ground carpet		—	—	—	—	0.14 ± 0.01

Table 2 Thermal and optical properties of the window

Element	Thickness (mm)	λ (W/(m·K))	ρ (kg/m³)	C_p (J/(kg·K))	$\varepsilon_{1\ LW}$	$\varepsilon_{2\ LW}$	$\tau_{SW}(0°)$	$\alpha_{SW}(0°)$
Outer pane	5.9 ± 0.1	1.0 ± 0.1	2300 ± 10	840 ± 50	0.84 ± 0.05	0.03 ± 0.01		0.32 ± 0.02
Cavity	12.0 ± 1.0	0.017 ± 0.005	1.64 ± 0.10	522 ± 30	—	—	0.30 ± 0.03	—
Inner pane	5.9 ± 0.1	1.0 ± 0.1	2300 ± 10	840 ± 50	0.84 ± 0.05	0.84 ± 0.05		0.027 ± 0.020

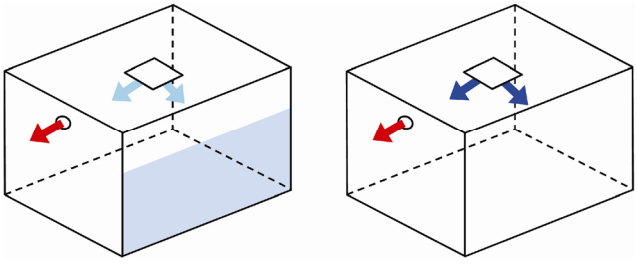

Fig. 2 Cooling principles in the test room: radiant wall (on the left) or active chilled beam (on the right)

comfort inside the test room can be achieved by the active chilled beam. The unit is located in the middle of the ceiling and has the dimensions of 0.6 m × 0.6 m. The water flow in the cooling coil varies between 100 and 200 L/h, and the cooling capacity of the active chilled beam is equal to 25 W/m$^2_{floor}$ (for $\Delta\theta_C$ = 8 K).

The cooling systems are connected to a chiller, which provides cold water at a constant temperature of around 12℃. The control of the room temperature is performed through three grey globe temperature sensors of 40 mm diameter ($\rho^*_{SW\ hemis}$ = 0.38), located 1 m away from the window and shielded from direct solar radiation (Fig. 1). The three measurements of temperature at 0.1 m, 0.6 m and 1.1 m are then averaged to obtain the operative temperature for a person sitting (EN ISO 7726 2001). This measured temperature is used as input for the PI controller, which is controlling the inlet water temperature of the activated element (3-way valve). The two systems have similar time constants (around 3h10min for the radiant wall, against 3h45min for the active chilled beam), but the initial response time of the active chilled beam is smaller. These time constants have been determined experimentally, by applying a step change to the inlet water temperature.

2.3 Ventilation and air-tightness

Providing fresh air to the test room is performed using the same unit as the active chilled beam. Therefore, the inlet has two functions (cooling and ventilation inlet) when the test room is cooled down by the active chilled beam. The fresh air is supplied at a constant air change rate (around 2.3 ACH), which corresponds to the basic requirement in the case of one occupant sitting in a low-polluting office (EN 15251 2007). The inlet air temperature is kept constant (varying between 20℃ up to 28℃ depending on the experiments). In order to ensure a stable temperature, the inlet air is taken from the guarded zone, which is temperature-controlled.

A circular outlet is located at the top of the north wall (diameter 125 mm, Fig. 1). The extraction rate of the outlet is controlled so that there is no over- or under-pressure between the guarded zone and the experimental room. The infiltration between the guarded zone and the test room is thus minimised. The air-tightness between the test room and outdoor has been tested by performing a blower door test both in over- and under-pressure. The infiltration rate is below 0.3 L/(s·m$^2_{floor}$) at 50 Pa.

2.4 Thermal manikin

In order to simulate an office worker and assess the comfort level, a thermal manikin has been used (Comfortina (PT Teknik 1999), Fig. 1). The thermal manikin corresponds to a 1.7 m tall woman, developed from a nearly anatomically-correct female manikin (DuBois area equal to 1.5 m^2). The manikin is made of a fibreglass shell covered by 0.3 mm diameter nickel wires, which are sequentially used to heat the manikin (uncertainty on the heat flow: ± 1%) and to measure and control the skin temperature (uncertainty: ± 0.2 K). The 17 parts of the manikin can be individually controlled.

The thermal manikin is sitting 1.2 m away from the south wall, on an open chair, which does not insulate or stop air movement. The clothing ensemble consists of cotton stockings, tennis shoes, cotton panties, cotton vest, two pairs of cotton tights and two tight-fitting and high-necked cotton blouses with long sleeves. The clothing level of the whole thermal manikin (I_{cl} = 0.83 clo) corresponds to a mid-season outfit EN 15251 (2007), resulting in a thermal insulation from the body surface to the environment (I_T) equal to 1.47 clo.

The thermal manikin is used for both simulating internal heat loads and evaluating local comfort in the experimental room. Local comfort evaluation can give additional information on the comfort level in a non-uniform environment (Schellen et al. 2013; Tanabe et al. 1994). In fact, thermal comfort indices, such as the PMV, are based on the heat balance of the whole body, disregarding local effects. The analysis of local comfort will be performed using both the parameters defined in EN ISO 7730 (2005) and the equivalent temperature derived from the thermal manikin. The equivalent temperature is defined as the temperature of an imaginary space with uniform and still air condition, at which the body exchanges the same dry heat loss as in the actual environment (Nilsson and Holmér 2003). The heat flux from each body parts is used to calculate the equivalent temperature, using Eq. (1) (T_{skin} = 34℃):

$$T_{eq\,i} = T_{skin} - Q_i \cdot I_{T\,i} \cdot 0.155 \quad (1)$$

2.5 Sensors

In order to evaluate with precision the heat balance of the

test room, a particular effort has been put in measuring accurately the different parameters. More than 300 sensors have been placed in the experimental room, each of them calibrated individually. The logging frequency is varying between 0.1 Hz up to 5 Hz depending on the type of measurement.

In order to measure the heat flux going through the construction, the test room has been divided in 83 sub-surfaces (Fig. 3). The sub-surfaces have a smaller area where large temperature differences are expected (i.e. at the radiant wall, at the ceiling due to the inlet or at the floor because of solar radiation). For each of these sub-surfaces, thermopiles have been mounted inside the construction and thermocouples have been placed at the internal surface of the experimental room (type K thermocouples, with an uncertainty of ± 0.15 K (Le Dréau et al. 2014a)). To measure the air temperature distribution in the room, five columns of thermocouples have been installed in the test room: one in the middle and one in the centre of each wall (60 cm away from the south and north wall, and 25 cm away from the west and east wall). The thermocouples measure the air temperature at 0.1, 0.6, 1.1, 1.7 and 2.65 m high. In order to decrease the influence of radiation on the measurement of air temperature, the thermocouples are silver-coated and protected by a mechanically ventilated silver shield.

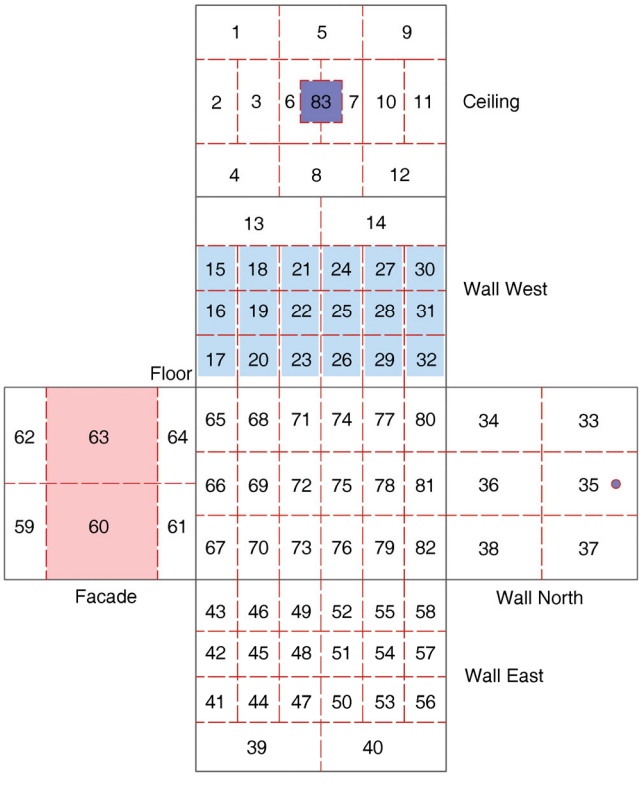

Fig. 3 Subdivision of the test room into 83 sub-surfaces (light blue: radiant wall; dark blue: ventilation inlet and outlet; red: window)

Depending on the experiment, the active chilled beam or the radiant wall is used to cool down the test room. Seven energy meters have been mounted: one for the active chilled beam and six for the radiant panels (one meter per panel). Each meter has been calibrated individually, and the uncertainty of the measurement has been estimated to ± 0.9 L/h for the flow meters and ± 0.06 K for the Pt-500 sensors.

Irradiance is measured outside before the glazing using a CMP 21 pyranometer (uncertainty: ± 3%). Another pyranometer has been placed on the roof of the experimental room to measure the global and diffuse solar radiation on a horizontal surface. A large carpet covers the ground in front of the south facade in order to control the ground reflectance ($\rho^{*}_{\text{SW carpet}} = 0.14$).

The measurement of the airflow through the ventilation system is performed using an orifice plate located before the inlet; the pressure difference is then converted into an air change rate (total uncertainty: ± 7.5%). Twelve hot sphere anemometers have been placed in the test room for measuring air velocity. The measurements are performed at a frequency of 10 Hz and integrated over 30 seconds. The sensors measure the turbulence intensity and the velocity at the ceiling, close to the thermal manikin (0.1, 0.6, 1.1 and 1.7 m high) and down the radiant wall (2 cm high and 30 cm away from the wall).

3 Analysis of the data

3.1 Heat balance of the test room

The room heat balance has been performed for a time-step of 30 seconds and is expressed by Eq. (2). The left part of the equation corresponds to the change of internal energy in the room, which includes both the capacitance of the air and of the equipment. The temperature swing of the equipment is assumed to follow the variation of the air temperature. The thermal mass of the equipment has been calibrated using the experimental results and is equal to 4.7 Wh/(m^2_{floor}·K).

$$\begin{aligned}\left(V_{\text{room}}\rho_{\text{air}}C_{\text{p air}} + C_{\text{m equipment}}\right)\frac{\partial T_{\text{air}}}{\partial t} \\ = \sum_i \left(Q_{\text{cond}\,i} + Q_{\text{rad SW}\,i}\right) + Q_{\text{thermal manikin}} \\ + Q_{\text{equipment}} + Q_{\text{ventilation}} + Q_{\text{chilled beam}}\end{aligned} \quad (2)$$

The calculation of short-wave radiation ($Q_{\text{rad SW}\,i}$) includes both the angular-dependant properties of the glazing and the reflection of solar radiation in the room. First, the solar radiation measured at the facade level is decomposed into direct, diffuse and ground reflected solar radiation using

the measured ratio of diffuse to global solar radiation and the ground reflectance. Then, the part of solar radiation transmitted through the glazing is calculated using the sun position and the angular-dependant properties of the glazing. Finally, the path of solar radiation inside the room is computed based on ray-tracing simulations. As the internal surfaces of the test room have a relatively high reflection coefficient (Table 1), it is important to evaluate the portion of solar radiation, which is either absorbed by the glazing (after being reflected by the room surfaces) or redirected outside through the glazing. For diffuse radiation, the portion of solar radiation reflected by the room surfaces and then absorbed by the glazing is equal to 11% and the part of solar radiation redirected outside is equal to 7% of the transmitted solar radiation.

A one-dimensional finite volume model with an explicit scheme (Patankar 1980) has been used to determine the conductive heat flux at the surface of each section ($Q_{cond\,i}$) (Fig. 3). The surface temperature and the temperature difference inside the construction over a 30 mm layer of EPS have been used as boundary conditions for the calculation (Fig. 1). When the radiant wall is activated, an internal heat sink inside the construction layers is added to the numerical model. As the numerical model is one-dimensional, an equivalent-layer has been defined to correctly model the two-dimensional heat flow at the pipes level.

Conductive heat transfer through the double-glazing unit has been calculated using the internal and external surface temperatures as boundary conditions, and taking into consideration the solar absorption of each pane. The thermal properties of the different layers have been estimated using EN 673 (2011): the thermal conductivity of the cavity is thus temperature-dependant.

Losses at the edges of the experimental room are neglected due to the high level of thermal insulation (around 200 mm thick). But the thermal bridge of the window frame has been accounted because the temperature difference can be large and the window sealing does not ensure a full thermal insulation. Therefore, the software Therm (Lawrence Berkeley Laboratory (LBL) 2012b), a two-dimensional finite element program, has been used to evaluate the heat transfer through the window frame (Ψ_{frame} = 0.12 W/(m·K)).

3.2 Uncertainty of measurements

An uncertainty analysis has been performed to assess the accuracy and the precision of the measurements. This analysis is based on the heat balance experimentally derived (Eq. (2)). By comparing the difference between the gains and the losses, it is possible to estimate the error on the heat balance and therefore the uncertainty on the measurements.

The analysis has been performed for different intervals of calculation (Le Dréau et al. 2014a). The uncertainty on a single measurement point (i.e. representing 30 seconds of experiment) follows a normal distribution and is equal to ± 29% (result based on around 161 000 data points). This uncertainty did not show any correlation with the type of terminal or with the intensity of solar radiation. For hourly data, the uncertainty is decreasing down to ± 17% and down to ± 7% for daily average.

A differential sensitivity analysis has also been performed to highlight the parameters having the largest influence on the accuracy of the heat balance. It has been observed that the optical properties of the glazing, the measurement of solar radiation, the measurement of the water flow and the evaluation of the ventilative flow influence the uncertainty of the heat balance the most.

4 Comparison of the energy effectiveness

Two sets of experiments have been performed to analyse the performance of the radiant wall and the active chilled beam. First, steady-state experiments were conducted by placing a shading device on the external side of the window and 150 mm of EPS on the internal side. An electric carpet was mounted at the window level (Fig. 4). In the second set of experiments, the window was cleared, so that the dynamic effects and the influence of solar radiation could be observed (Fig. 5).

4.1 Steady-state experiments

In a first set of experiments, an electric carpet has been mounted in front of the window, simulating the effect of internal solar shading (Fig. 4). The power of the carpet and the air change rate have been set to a constant value of 36 W/m^2_{floor} and 2.2 ACH respectively. The cooling effect

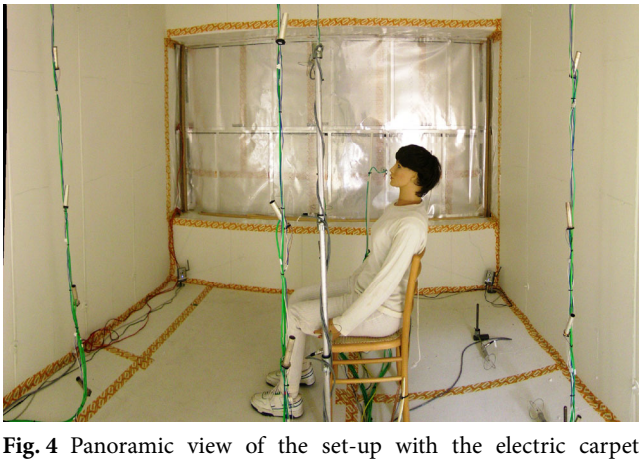

Fig. 4 Panoramic view of the set-up with the electric carpet (steady-state)

Fig. 5 Panoramic view of the set-up with the sun (dynamic)

has been automatically adjusted to achieve an operative temperature of (26 ± 0.2)℃. The cooling need of the two terminals has then been measured for different inlet temperatures, varying from 20℃ up to 28℃ (Fig. 6). It has to be noted that the inlet temperature corresponds to the temperature before the cooling coil of the active chilled beam. In order to account for changing outdoor conditions, the cooling need to maintain a constant operative temperature is not given as an absolute value, but as a ratio cooling need/heat load. The heat load has been calculated using Eq. (3). It takes into account the regular heat loads (from the sun, the thermal manikin and the equipment), to which are subtracted the conduction losses through the facade.

$$Q_{\text{heat load}} = Q_{\text{rad SW}} + Q_{\text{thermal manikin}} + Q_{\text{equipment}} + Q_{\text{cond\{facade\}}} \quad (3)$$

A linear relationship between the ratio cooling need/heat load and the temperature difference between the inlet and the operative temperature can be observed. The radiant wall is more energy effective than the active chilled beam. Under similar boundary conditions, the cooling need of the cooled wall is around 7%–10% lower. The higher the inlet air temperature, the larger the difference between the two terminals. Alternatively, one could say that the thermal sensation of a radiant wall is around 0.5–1 K lower than the one of an active chilled beam for similar cooling power.

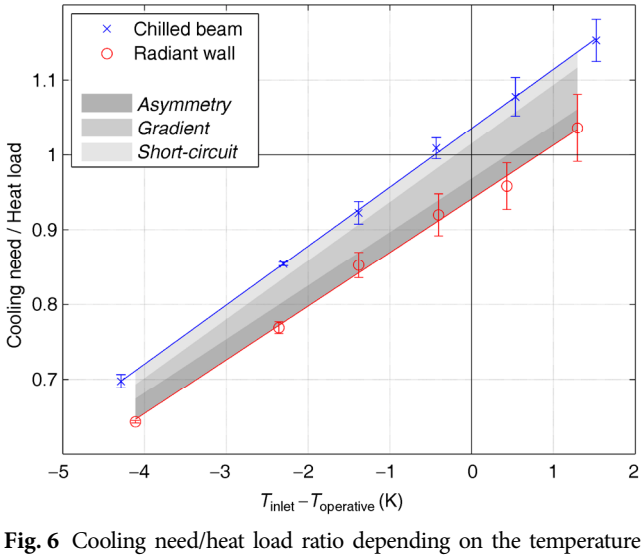

Fig. 6 Cooling need/heat load ratio depending on the temperature difference between the inlet and operative temperature (6-hour average)

4.2 Dynamic experiments

The influence of solar radiation has been studied by removing the insulation placed in front of the window. The experiments have been performed during the months of July and August of 2013, characterised by long days, relatively warm outdoor temperature at night (≈ 15–20℃) and high level of solar radiation (up to 1000 W/m² on a horizontal surface). Contrary to the steady-state experiments, the inlet air temperature has been kept constant, equal to 25℃. The air change rate has been set to 2.4 ACH. During the day (7 a.m. till 8 p.m.), the cooling set-point in the experimental room was set to 25℃. During the night, the test room was cooled down to 22℃. This night setback has a dual objective: obtain comparable results over the different days and simulate the lower outdoor temperature at night, which is providing a free cooling to buildings through the ventilation system.

Before comparing the energy need of the two terminals, the global comfort level achieved with the two emitters should be verified. Even though the operative temperature achieved at 1:30 a.m. is always equal to 22℃, the temperature profile during the day can be different. Therefore, the heat load has been calculated over a 24-hour period (Eq. (3)) and the mean operative temperature in the test room has been compared for the two terminals (Fig. 7). When the heat load is lower than 400 Wh/m² per day (corresponding to

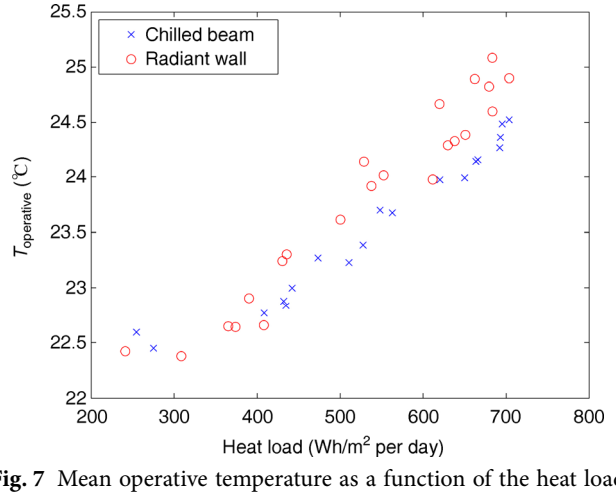

Fig. 7 Mean operative temperature as a function of the heat load (values calculated over 24 hours, starting from 1:30 a.m.)

an overcast day), the active chilled beam and the radiant wall achieved a similar operative temperature. But when the heat load increases, the active chilled beam achieves a colder indoor environment than the radiant wall: the difference is up to 0.5 K for a clear day. This difference in the global comfort level is due to slightly different cooling capacities of the two terminals: the cooling capacity of the active chilled beam is 4 W/m^2_{floor} higher than the one of the radiant wall. The limited cooling capacity of the two terminals is also the explanation of the overheating period observed for both terminals.

Similarly to the steady-state case, the performances of the active chilled beam and the radiant wall have been compared. The heat load and the cooling need have been measured and the results are shown in Fig. 8. In order to account for differences in the level of comfort, a correction on the cooling need of the radiant wall has been performed based on Eq. (2) (cf. dashed line in Fig. 8). Days with low heat load (below 400 Wh/m^2 per day) are characterised by intermittent solar radiation and therefore intermittent cooling demand in the test room. The cooling system does not need to be active all the time and on/off periods can be observed. Under these conditions, the cooling need is higher than the heat load because the inlet air is warmer than the air inside the test room, thus generating additional heat gains. It can be observed that the radiant wall is slightly more efficient than the active chilled beam. When the heat load increases, the advantages of radiant terminals compared to convective terminals can be observed more clearly. Due to the higher air temperature, radiant terminals can optimise the ventilation losses and save around 10%–15% on the cooling need.

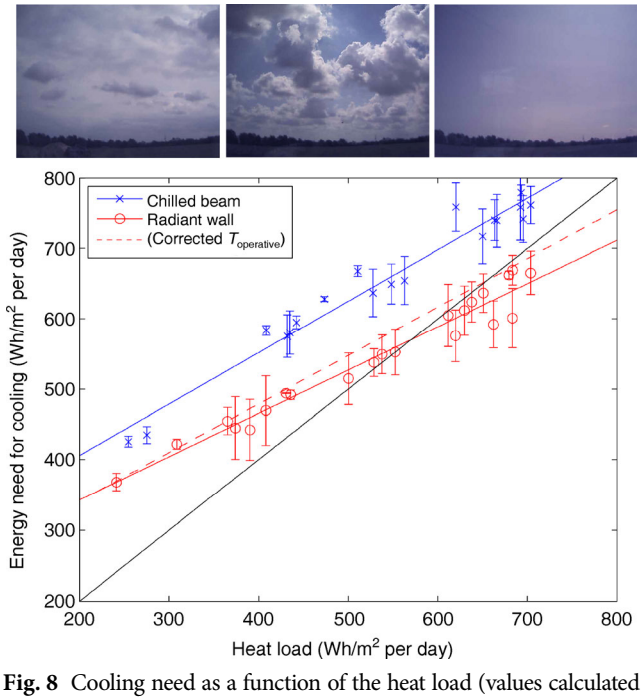

Fig. 8 Cooling need as a function of the heat load (values calculated over 24 hours, starting from 1:30 a.m.). The pictures of the sky shown above are on an indicative basis

4.3 Discussion

From both the steady-state and the dynamic simulations, similar behaviour has been observed: the radiant wall has better energy effectiveness than the active chilled beam. As described theoretically by Le Dréau and Heiselberg (2014), the lower cooling need can be explained by differences in the ventilation losses. The heat losses through ventilation are higher with the radiant wall than with the active chilled beam due to a higher outlet temperature, which can be caused by different factors: a temperature difference between the air and the surfaces ($\Delta T_{\text{air occ.zone}-\text{radiant}}$), an air temperature gradient ($\Delta T_{\text{outlet level}-\text{air occ.zone}}$) and/or a short-circuit between the inlet and the outlet ($\Delta T_{\text{outlet}-\text{outlet level}}$). By analysing these parameters, it is possible to prescribe correction factors on the ventilation heat balance depending on the type of terminal (Eq. (4)). This method is similar to the one proposed in the European standard EN 15316: in this standard, an equivalent internal temperature is defined to account for temperature stratification and control variations (EN 15316-2-1 2007). Equation (4) can be used directly in simplified calculation tools, which do not differentiate the air temperature from the surface temperature and do not have advanced models for terminals. This method can also be used in more advanced Building Energy Simulation (BES) tools to specify the homogeneity of air distribution (in this case, $\Delta T_{\text{air occ.zone}-\text{radiant}}$ does not need to be included if terminals are properly simulated). In the following part, the additional terms of Eq. (4) will be studied separately to isolate the effect of the different physical phenomena. In order to account for differences in the comfort level (dynamic case), the analysis will be conducted by comparing the terminals based on the cooling need, instead of the heat load.

$$Q_{\text{vent}} = \dot{m} C_{\text{p air}} \left(T_{\text{inlet}} - T_{\text{operative}} - \frac{\Delta T_{\text{air occ.zone}-\text{radiant}}}{2} - \Delta T_{\text{outlet level}-\text{air occ.zone}} - \Delta T_{\text{outlet}-\text{outlet level}} \right) \quad (4)$$

In the experiments with the electric carpet simulating the solar load, the air temperature in the test room is around 0.5 – 1 K higher with the radiant wall than with the active chilled beam. As this difference increases with the cooling need, the effectiveness of radiant terminals also increases. Similar values of asymmetry between air and surfaces temperatures have been observed in the second set of experiments (Fig. 9).

Additionally, a temperature gradient is achieved in the room when the radiant wall is activated. This temperature

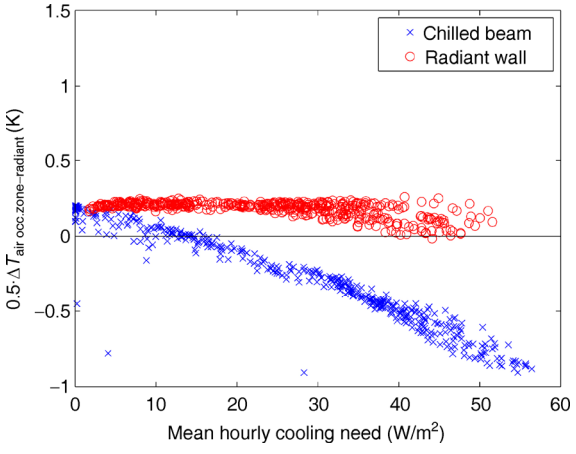

Fig. 9 Difference between the air temperature in the occupied zone and the radiant temperature depending on the cooling need (hourly values, dynamic experiments)

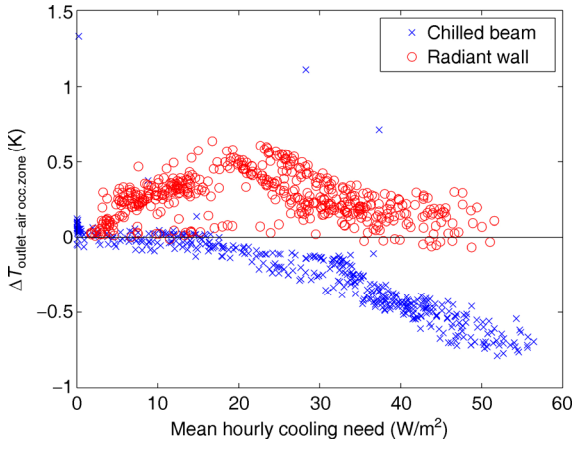

Fig. 11 Difference between outlet temperature and the air temperature in the occupied zone depending on the cooling need (hourly values, dynamic experiments)

gradient increases the outlet temperature and thus the ventilation losses. This temperature gradient is highly dependent on the power and location of the heat load. For the steady-state experiments, the difference between the outlet and the mean air temperature in the occupied zone increases from 0.2 up to 1.3 K when the cooling need rises from 25 W/m² up to 40 W/m² (Fig. 10). But when solar radiation is the main heat source, the temperature gradient with the radiant wall is not higher than 0.5 K (Fig. 11). In fact, the direct solar radiation absorbed by the floor tends to homogenise the room air temperature, thereby decreasing the vertical temperature gradient.

From Fig. 11, it can also be observed that the difference between the outlet and the air temperature is negative for the active chilled beam. This is due to a short-circuit between part of the inlet air and the outlet.

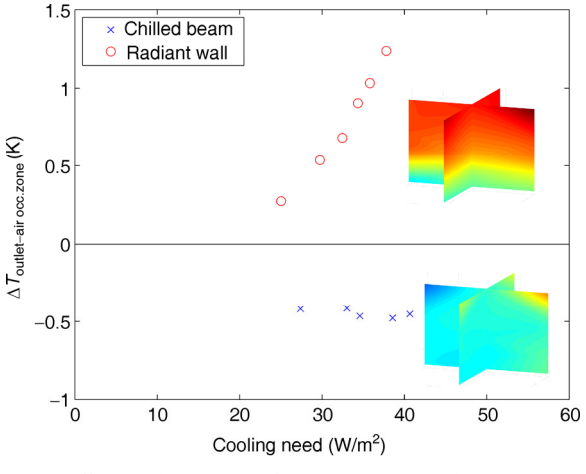

Fig. 10 Difference between outlet temperature and air temperature in the occupied zone (steady-state experiments). The temperature field in the room is shown on the right on an indicative basis

By quantifying these different temperature differences ($\Delta T_{\text{air occ.zone}-\text{radiant}}$, $\Delta T_{\text{outlet level}-\text{air occ.zone}}$ and $\Delta T_{\text{outlet}-\text{outlet level}}$), it is possible to get a detailed explanation of the better energy effectiveness of the radiant wall compared to the active chilled beam (grey areas in Fig. 6).

5 Comparison of the level of comfort

The comfort level achieved in the test room has been evaluated by combining the results of both steady-state and dynamic experiments, as the results are similar. The analysis is performed on an hourly basis and during the working hours (i.e. from 8:30 a.m. till 5:30 p.m.).

The radiant asymmetry and the vertical air temperature difference have been calculated for the different experiments, but no discomfort has been identified. Therefore, only the results about the draught rate and the local equivalent temperature will be presented in this paper.

5.1 Draught rate

The risk of draught has been evaluated in two critical locations: in the middle of the test room (down the inlet) and down the radiant wall. The risk of draught is calculated from the air temperature and the velocity measurements, assuming a constant turbulence intensity of 40% (EN ISO 7730 2005).

The risk of draught in the middle of the test room is evaluated by selecting the highest value from the measurements performed at 0.1 m, 0.6 m, 1.1 m and 1.7 m (Fig. 12). Due to the higher air temperature, the risk of draught decreases when the cooling need increases. The risk of draught for the two cooling terminals is below 20%, which corresponds to the limit of category II (normal level of

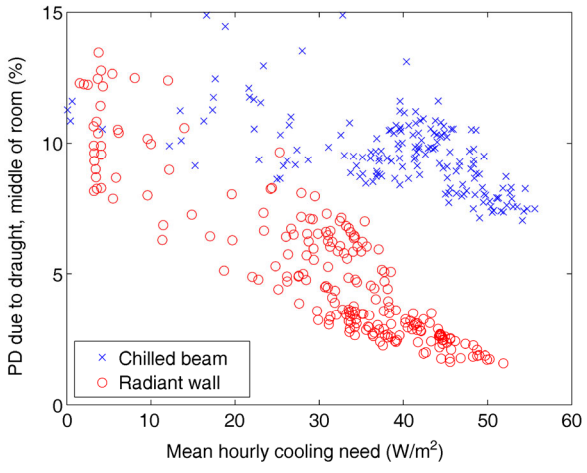

Fig. 12 Risk of draught in the middle of the room as a function of the cooling need

expectation). The risk of draught with the active chilled beam is higher due to the increased air velocity (around 0.12 m/s as compared to 0.07 m/s for the cooled wall), but this increased air velocity is too small to have a large impact on the global comfort (EN ISO 7730 2005).

The minimum surface temperature reached by the radiant wall is equal to 18℃, which is higher than the due-point. This cold surface creates a down-draught, which can cause discomfort in the occupied zone. Therefore, the maximum velocity at the floor level, close to the radiant wall, has been measured in three different positions, and the Percentage Dissatisfied (PD) due to the down-draught has been calculated (Fig. 13). The PD is below 14% for all the experimental cases, even though the velocity down the wall rises up to 0.2 m/s. A similar relationship as Heiselberg (1994) has been found between the air velocity and the temperature difference between the air and the surface.

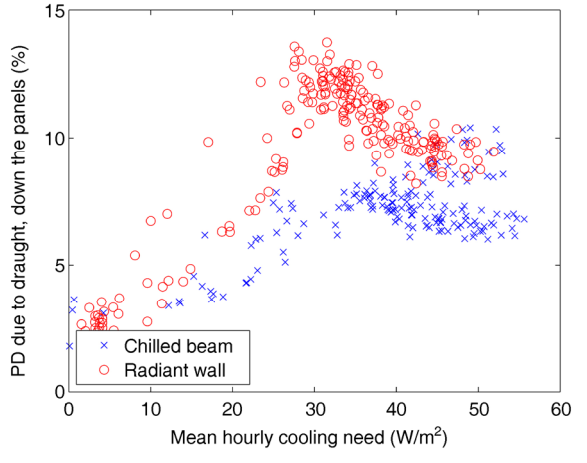

Fig. 13 Risk of draught down the radiant wall as a function of the cooling need

5.2 Local comfort evaluation with the thermal manikin

The local comfort has been evaluated using the thermal manikin, which was running at a constant skin temperature of 34℃. The heat flux required to maintain isothermal conditions has then been used to evaluate the comfort of the 17 body segments. Figure 14 characterizes the comfort conditions achieved with the two terminals for a cooling need of 40 W/m². With the active chilled beam, the head, the chest, the left hand and forearm show a slightly lower equivalent temperature due to the cold jet flowing close to these body segments. With the radiant wall activated, the top of the head and the back of the thermal manikin are slightly colder due to the radiation from the cold wall. But the decrease of temperature (lower than 2 K) is not significant enough to sense any local discomfort (Nilsson 2007).

Besides the local cooling effect of some body segments, a comfort asymmetry between the left and the right part of the thermal manikin can be observed due to the solar radiation warming up the window surface (Fig. 14).

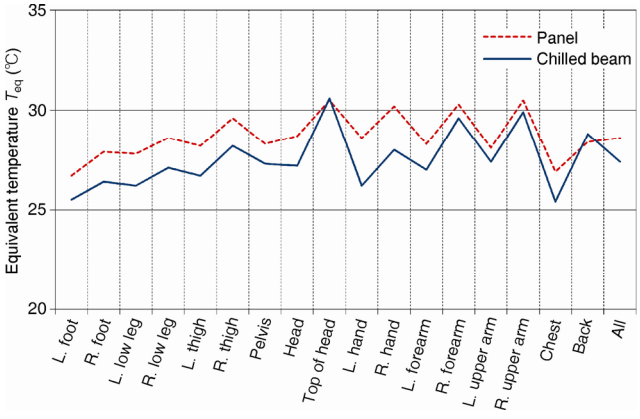

Fig. 14 Local equivalent temperature for the different body parts of the manikin and for the whole body (cooling need ≈40 W/m² at 11 a.m.)

6 Conclusion

The two experimental set-ups are characterised by differences in the boundary conditions (steady-state vs. dynamic) and also in the level and type of heat load. The first set-up corresponds to the case of a room equipped with internal solar shadings, which stop most of the solar radiation. It results in a heat load concentrated at the window level. The second set-up highlights the effect of direct solar radiation on the cooling performance as no shading device was placed at the window level.

Despite these differences, similar conclusions can be drawn out of these two sets of experiments. The radiant wall is more energy-efficient for cooling down a space than the

active chilled beam. The energy savings (in term of delivered energy) can be estimated to around 10%, due to higher ventilation losses. A detailed analysis of the ventilation heat balance has been performed in order to isolate the effect of individual parameters, such as the asymmetry between air and radiant temperature, the air temperature gradient and the possible short-circuit between inlet and outlet. These three elements are the key parameters to characterise the effectiveness of emitters and can be used in standards and BES tools to differentiate the emitters (Eq. (4)).

In these experiments, the three parameters mentioned above play an equally important role in decreasing the cooling need of the radiant wall compared to the active chilled beam. It has been observed that the asymmetry between air and radiant temperature increases with the cooling need and leads to a lower air temperature for the active chilled beam. For a cooling need around 30 W/m^2, the air temperature achieved with the radiant terminal is around 1 K higher than with the active chilled beam. Additionally, the cooled wall creates stratification in the test room, which increases the outlet temperature of around 0.5 K. This temperature gradient varies as a function of the intensity and type of heat load. In the case of a heat load concentrated at the window level, the increase of outlet temperature can even be up to 1.3 K. Finally, direct losses between the inlet and outlet have been observed. This short-circuit decreases by around 0.5 K for the outlet temperature of the active chilled beam compared to the radiant wall.

Regarding comfort, both terminals met the general requirements, except at high solar heat gains. Overheating was observed due to the absence of solar shading and due to the limited cooling capacity of the terminals. The local comfort conditions (radiant asymmetry, vertical air temperature gradient, risk of draught) were also evaluated and the measured parameters were within the comfort range. In addition to the classic local comfort parameters, a thermal manikin was used to evaluate the discomfort in individual body parts. Even though a decrease of some segment temperatures was observed, this decrease was not large enough to create local discomfort.

Acknowledgements

This work is collectively sponsored by the Danish Agency for Science, Technology and Innovation and the Ministry of Science and Technology of P.R. China in the Sino-Danish collaborated research project: "Activating the Building Construction for Building Environment Control" (Danish International DSF project no. 09-71598, Chinese international collaboration project no. 2010DFA62410).

References

Babiak J, Olesen BW, Petras D (2007). Low temperature heating and high temperature cooling, REHVA Guidebook Nbr. 7.

Causone F, Baldin F, Olesen BW, Corgnati SP (2010). Floor heating and cooling combined with displacement ventilation: Possibilities and limitations. *Energy and Buildings*, 42: 2338-2352.

EN 12524 (2000). Building Materials and Products—Hygrothermal Properties, Tabulated Design Values.

EN 1264-3 (2009). Water Based Surface Embedded Heating and Cooling Systems—Part 3: Dimensioning.

EN 15251 (2007). Indoor Environmental Input Parameters for Design and Assessment of Energy Performance of Buildings Addressing Indoor Air Quality, Thermal Environment, Lighting and Acoustics.

EN 15316-2-1 (2007). Heating Systems in Buildings—Method for Calculation of System Energy Requirements and System Efficiencies—Part 2-1: Space Heating Emission Systems.

EN 673 (2011). Glass in Building—Determination of Thermal Transmittance (U value)—Calculation Method.

EN ISO 13786 (2007). Thermal Performance of Building Components—Dynamic Thermal Characteristics—Calculation Methods.

EN ISO 15099 (2003). Thermal Performance of Windows, Doors and Shading Devices—Detailed Calculations.

EN ISO 7726 (2001). Ergonomics of the Thermal Environment—Instruments for Measuring Physical Quantities.

EN ISO 7730 (2005). Ergonomics of the Thermal Environment—Analytical Determination of Thermal Comfort by Using Calculations of the PMV and PPD Indices and Local Thermal Comfort Criteria.

Fabrizio E, Corgnati SP, Causone F, Filippi M (2012). Numerical comparison between energy and comfort performances of radiant heating and cooling systems versus air systems. *HVAC&R Research*, 18: 692–708.

Feng J, Schiavon S, Bauman F (2013). Cooling load differences between radiant and air systems. *Energy and Buildings*, 65: 310–321.

Hannay J, Laret L, Lebrun J, Marret D, Nusgens P (1978). Thermal comfort and energy consumption in winter conditions. A new experimental approach. *ASHRAE Transactions*, 84(1): 150–175.

Heiselberg P (1994). Draught risk from cold vertical surfaces. *Building and Environment*, 29: 297–301.

Imanari T, Omori T, Bogaki K (1999). Thermal comfort and energy consumption of the radiant ceiling panel system: Comparison with the conventional all-air system. *Energy and Buildings*, 30: 167–175.

Kalyanova O (2008). Double-skin façade. PhD Thesis, Department of Civil Engineering, Aalborg University, Denmark.

Lawrence Berkeley Laboratory (LBL) (2012a). WINDOW 6.3, A PC Program for Analyzing Window Thermal Performance in Accordance with Standard NFRC Procedures.

Lawrence Berkeley Laboratory (LBL) (2012b). THERM 6.3, A PC Program for Analyzing the Two-Dimensional Heat Transfer Through Building Products.

Le Dréau J, Heiselberg P (2014). Sensitivity analysis of the thermal performance of radiant and convective terminals for cooling buildings. *Energy and Buildings*, doi: 10.1016/j.enbuild.2014.07.002.

Le Dréau J, Heiselberg P, Jensen RL (2014a). Experimental Data from a Full-scale facility investigating radiant and convective terminals: Uncertainty and sensitivity analysis, Description of the experimental data. DCE Technical Report No. 168, Department of Civil Engineering, Aalborg University. Available: http://vbn.aau.dk/files/197208203/Experimental_data_from_a_full_scale_facility_investigating_radiant_and_convective_terminals.pdf.

Le Dréau J, Heiselberg P, Jensen RL (2014b). Experimental investigation of the influence of the air jet trajectory on convective heat transfer in buildings equipped with air-based and radiant cooling systems. *Journal of Building Performance Simulation*, doi: 10.1080/19401493.2014.938121.

Lehmann B, Dorer V, Koschenz M (2007). Application range of thermally activated building systems tabs. *Energy and Buildings*, 39: 593–598.

Myhren JA, Holmberg S (2008). Flow patterns and thermal comfort in a room with panel, floor and wall heating. *Energy and Buildings*, 40: 524–536.

Nilsson HO, Holmér I (2003). Comfort climate evaluation with thermal manikin methods and computer simulation models. *Indoor Air,* 13: 28–37.

Nilsson HO (2007). Thermal comfort evaluation with virtual manikin methods. *Building and Environment*, 42: 4000–4005.

Olesen BW, Mortensen E, Thorshauge J (1980). Thermal comfort in a room heated by different methods. *ASHRAE Transactions*, 86(1): 34–48.

Patankar SV (1980). Numerical Heat Transfer and Fluid Flow. New York: Taylor & Francis.

PT Teknik (1999). Comfortina. Available: http://Pt-Teknik.Dk/.

Roth K, Dieckmann J, Zogg R, Brodrick J (2007). Chilled beam cooling. *ASHRAE Journal*, 49(9): 84–86.

Schellen L, Loomans MGLC, Kingma BRM, de Wit MH, Frijns AJH, van Marken Lichtenbelt WD (2013). The use of a thermophysiological model in the built environment to predict thermal sensation: Coupling with the indoor environment and thermal sensation. *Building and Environment*, 59: 10–22.

Tanabe S, Arens EA, Bauman F, Zhang H, Madsen T (1994). Evaluating thermal environments by using a thermal manikin with controlled skin surface temperature. *ASHRAE Transactions*, 100(1): 39–48.

Tomasi R, Krajčík M, Simone A, Olesen BW (2013). Experimental evaluation of air distribution in mechanically ventilated residential rooms: Thermal comfort and ventilation effectiveness. *Energy and Buildings*, 60: 28–37.

Vandaele L, Wouters P (1994). The PASSYS Services: Summary Report. Belgian Building Research Institute for the European Commission.

Winther FV (2013). Intelligent Glazed Facades. PhD Thesis, Department of Civil Engineering, Aalborg University, Denmark.

Paper 5

Experimental investigation of convective heat transfer during night cooling with different ventilation systems and surface emissivities

Energy and Buildings 61 (2013) 308–317

Contents lists available at SciVerse ScienceDirect

Energy and Buildings

journal homepage: www.elsevier.com/locate/enbuild

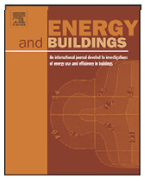

Experimental investigation of convective heat transfer during night cooling with different ventilation systems and surface emissivities

J. Le Dréau*, P. Heiselberg, R.L. Jensen

Department of Civil Engineering, Aalborg University, Sohngaardsholmsvej 57, DK-9000 Aalborg, Denmark

ARTICLE INFO

Article history:
Received 20 May 2012
Received in revised form 7 February 2013
Accepted 8 February 2013

Keywords:
Night-time ventilation
Full-scale experiments
Mixing ventilation
Displacement ventilation
Low-emissivity
Radiation pattern
Convective heat transfer coefficient
Mixed convection
Correlations
Local CHTC

ABSTRACT

Night-time ventilation is a promising approach to reduce the energy needed for cooling buildings without reducing thermal comfort. Nevertheless actual building simulation tools have showed their limits in predicting accurately the efficiency of night-time ventilation, mainly due to inappropriate models for convection. In a full-scale test room, the heat transfer was investigated during 12 h of discharge by night-time ventilation. A total of 34 experiments have been performed, with different ventilation types (mixing and displacement), air change rates, temperature differences between the inlet air and the room, and floor emissivities. This extensive experimental study enabled a detailed analysis of the convective and radiative flow at the different surfaces of the room. The experimentally derived convective heat transfer coefficients (CHTC) have been compared to existing correlations. For mixing ventilation, existing correlations did not predict accurately the convective heat transfer at the ceiling due to differences in the experimental conditions. But the use of local parameters of the air flow showed interesting results to obtain more adaptive CHTC correlations. For displacement ventilation, the convective heat transfer was well predicted by existing correlations. Nevertheless the change of floor emissivity influenced the CHTC at the surface of interest.

DOI: http://doi.org/10.1016/j.enbuild.2013.02.021

Paper 6

Experimental investigation of the influence of the air jet trajectory on convective heat transfer with air-based and radiant cooling systems

Journal of Building Performance Simulation, 2014
http://dx.doi.org/10.1080/19401493.2014.938121

Taylor & Francis
Taylor & Francis Group

Experimental investigation of the influence of the air jet trajectory on convective heat transfer in buildings equipped with air-based and radiant cooling systems

J. Le Dréau*, P. Heiselberg and R.L. Jensen

Department of Civil Engineering, Aalborg University, Sohngaardsholmsvej 57, DK-9000 Aalborg, Denmark

(*Received 9 January 2014; accepted 20 June 2014*)

The complexity and diversity of airflow in buildings make the accurate definition of convective heat transfer coefficients (CHTCs) difficult. In a full-scale test facility, the convective heat transfer of two cooling systems (active chilled beam and radiant wall) has been investigated under steady-state and dynamic conditions. With the air-based cooling system, a dependency of the convective heat transfer on the air jet trajectory has been observed. New correlations have been developed, introducing a modified Archimedes number to account for the air flow pattern. The accuracy of the new correlations has been evaluated to ±15%. Besides the study with an air-based cooling system, the convective heat transfer with a radiant cooling system has also been investigated. The convective flow at the activated surface is mainly driven by natural convection. For other surfaces, the complexity of the flow and the large uncertainty on the CHTCs make the validation of existing correlations difficult.

Keywords: convective heat transfer coefficient; cooling; radiant wall; active chilled beam; air jet trajectory; Archimedes number

DOI: http://doi.org/10.1080/19401493.2014.938121

ISSN 1901-7294
DCE Thesis No. 57